Cleavage of Carbon-Carbon Bonds in Aldehydes and Ketones

Mazziotta, Andrea

Publication date:
2017

Document Version
Publisher's PDF, also known as Version of record

Cleavage of Carbon-Carbon Bonds in Aldehydes and Ketones

Ph.D. Thesis

Department of Chemistry

Technical University of Denmark

Andrea Mazziotta

Kgs. Lyngby

November 2017

"Unless you expect the unexpected you will never find truth,

For it is hard to discover and hard to attain"

-Heraclitus

PREFACE

This dissertation presents the work conducted during my Ph.D. studies in the Department of Chemistry at the Technical University of Denmark (DTU) from September 2013. During this time, I have been working on two distinctive projects aiming at the development of technologies and the understanding of defunctionalization of organic molecules.

These years have been very intense and sprinkled with moments of joy and frustration, which eventually delivered great rewards.

In this period I have been supported by numerous persons which deserve to be credited.

First and foremost, I would like to thank my supervisor Prof. Robert Madsen, who gave me the opportunity to join his group and move to Denmark. His advice, guidance and support were essential for my work, and his care about my personal growth and his work ethic, make him a great supervisor. I hope I was able to repay the trust you gave me in the first place.

I also acknowledge Associate Professor Peter Fristrup for the consultancy concerning the first project, and the DFT-calculations.

Thanks to former and current members of Madsen group whom I came across for making my experience so enjoyable.

In particular, I need to thank Ilya Makarov, who also contributed with the DFT-calculations present in this work, in addition of being a mentor when I arrived at DTU; my former lab mate, former office mate, current friend Maximilian Boehm for his support and for all the stimulating conversations. To the fabulous Clotilde d'Errico and Enzo Mancuso, remembering the good times we shared

in the lab, I owe a special thanks for giving me your precious feedback on the thesis.

Thanks also to the older and new members of the crew: Andreas, Bo, Giuseppe, Dennis, Emilie, Enzo, Fabrizio, Fabrizio, and Simone, the chat and coffees with you were a real relief during the hardest moments.

My gratitude goes also to whom who oil the gears of this machine making the department running efficiently, the technicians and members of the building center and IT department in particular Anne Hector, Lars Egede Bruhn, John Madsen, Brian Dideriksen, Brian Ekman-Gregersen, and Charlie Johansen.

Thanks to the people that were close to me when I needed them and that will be: Giuseppe, Luca, Enzo and Fabrizio.

I am grateful to my mom and dad, my brothers Daniele and Adriano for their love and support, even in the toughest moments.

Finally, thanks to my beloved extraordinary wife, talented chemist and loving mother, Carola. I cannot think someone more understanding, patient, and helpful than you. Thanks to the little big loves of mine, my daughters Beatrice and Teresa. Although so small, you taught me the lessons that no book can contain and no scientist can explain.

This thesis is dedicated to you.

Andrea Mazziotta,

November 2017.

ABSTRACT

The disconnection of carbon-carbon bonds has a relevant role in organic chemistry in the same way as the formation of these bonds and is probably even more challenging. An interesting and sometimes overlooked transformation involves the hydroxide-mediated cleavage of carbon-carbon bonds in aldehydes and ketones which has been known for more than a century. The generated fragments are the carboxylate and various neutral residues, such as ketones, nitroalkanes, sulphonyl alkanes, trihaloalkanes (haloform reaction)[1] and other moieties. The neutral residues are all very weak acids with pK_a values between 10 and 40. We have discovered by serendipity that toluene residues with a pK_a of about 41 can also be cleaved from ketones with hydroxide in generally good yields.

Herein, we present studies of the cleavage of different substituted benzylic ketones and aldehydes promoted by hydroxide sources in various solvent systems with the aim to investigate the scope of the reaction and clarify the mechanism. Kinetic data resulting from Hammett correlation plots were investigated and compared with theoretical values from density functional theory (DFT) calculations. DFT calculations were also conducted to determine the relative free energies of possible intermediates and transition states.

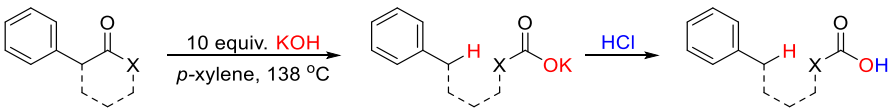

Dehydrogenative decarbonylation of alcohols is an attractive reaction based on two individual processes: the acceptorless dehydrogenation of an alcohol and the decarbonylation of the resulting aldehyde. In this transformation, valuable

products are formed, such as the unfunctionalized organic residue and two gases, hydrogen and carbon monoxide, respectively. The gaseous mixture is also known as synthesis gas (*SynGas*) and has many applications ranging from energy production to chemical manufacture.

Homogeneous catalysis has previously been investigated to mediate this process with the aid of metal species based on rhodium and iridium complexes. However, both metals showed limitations in the scope and affordability.

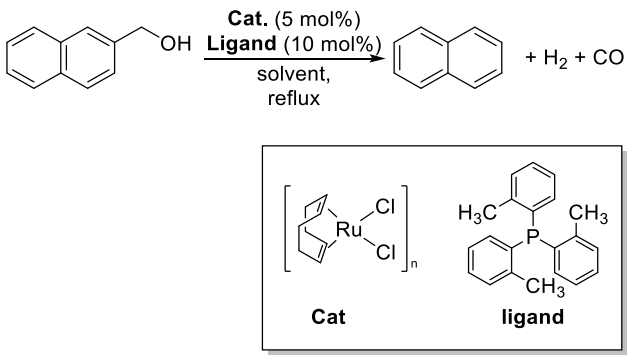

In this work, a cheaper alternative is presented, based on the system $Ru(COD)Cl_2$ and the phosphine P(*o*-tolyl)$_3$ for the dehydrogenative decarbonylation of alcohols.

The reaction was applied to both benzylic and long chain linear aliphatic alcohols. The intermediate aldehyde can be observed during the transformation, which is therefore believed to proceed through two separate catalytic cycles involving first dehydrogenation of the alcohol, followed by decarbonylation of the resulting aldehyde.

RESUMÈ

Brydningen af carbon-carbon bindinger har en relevant rolle i organisk kemi på samme måde som dannelsen af disse bindinger har og førstnævnte er tilmed formentligt mere udfordrende. En interessant og sommetider overset omdannelse involverer hydroxid-formidlet brydning af carbon-carbon bindinger i aldehyder og ketoner, hvilket har været kendt i mere end et århundrede. De dannede fragmenter er carboxylat og forskellige neutrale forbindelser såsom ketoner, nitroalkaner, sulfonylalkaner, trihaloalkaner (haloform reaktion) og andre specier. Alle de neutrale forbindelser er meget svage syrer med pK_a værdier mellem 10 og 40. Ved et lykketræf har vi opdaget, at også toluenforbindelser med en pK_a værdi på omkring 41 kan kløves fra ketoner ved behandling med hydroxid i generelt høje udbytter.

Heri præsenterer vi studier af kløvningen af forskelligt substituerede benzyl ketoner og -aldehyder formidlet af hydroxidkilder i forskellige solventsystemer med det formål at undersøge anvendelsen af reaktionen og afklare mekanismen. Kinetiske data fra Hammett korrelationskurver blev undersøgt og sammenlignet med teoretiske værdier fra *Density Functional Theory* (DFT) beregninger. DFT beregninger blev også udført for at bestemme de relative frie energier af de mulige intermediater og *transition states*.

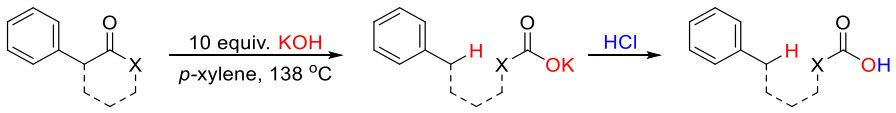

X = H, CH_3, $(CH_2)_n$

Dehydrogenativ decarbonylering af alkoholer er en attraktiv reaktion baseret på to individuelle processer: acceptorfri dehydrogenering af en alkohol og

decarbonylering af det resulterende aldehyd. I denne omdannelse dannes værdifulde produkter såsom den ikke-funktionaliserede organiske forbindelse samt to gasser, henholdsvis hydrogen og carbonmonooxid. Gasblandingen kendes også som syntesegas (SynGas) og har mange anvendelser spændende fra energiproduktion til kemisk fremstilling.

Homogen katalyse har tidligere vist sig at formidle denne proces ved brug af metalforbindelser baseret på rhodium- og iridiumkomplekser. Desværre møder begge metaller begrænsning i anvendelse og prisbillighed.

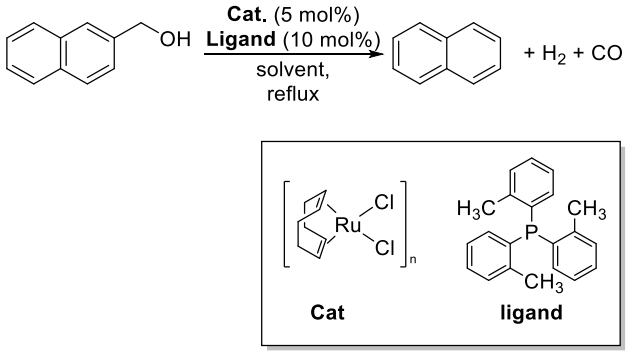

I dette projekt præsenteres et billigere alternativ til dehydrogenativ decarbonylering af alkoholer baseret på systemet $Ru(COD)Cl_2$ og phosphinen P(*o*-tolyl)$_3$.

Reaktionen blev anvendt på både aromatiske og langkædede, lineære, alifatiske alkoholer. Intermediat aldehydet kan observeres under omdannelsen, hvilken derfor menes at forløbe igennem to separate katalytiske cyklusser bestående af en indledende dehydrogenering af alkoholen efterfulgt af decarbonylering af det resulterende aldehyd.

LIST OF ABBREVIATIONS

Ac	Acetyl
acac	Acetylacetonate
Ar	Aryl
Atm	Atmosphere
BIPHEP	Bis(diphenylphosphino)-1,1'-biphenyl
Bn	Benzyl
Bu	Butyl
Cat.	Catalyst
Cy	Cyclohexyl
Cp	Cyclopentadienyl
Cp*	Pentamethylcyclopentadienyl
COD	Cyclooctadiene
d	Doublet
DCM	Dichloromethane
DavePhos	2-Dicyclohexylphosphino-2'-(N,N-dimethylamino)biphenyl
DFT	Density Functional Theory
DMF	Dimethylformamide
DMSO	Dimethylsulfoxide
DPEPhos	(Oxydi-2,1-phenylene)bis(diphenylphosphine)
Dppe	1,2-Bis(diphenylphosphino)ethane
Dppp	1,3-Bis(diphenylphosphino)propane
EDG	Electron donating group

equiv.	Equivalent(s)
ESI	Electrospray ionization
Et	Ethyl
Eq	Equivalent
EWG	Electron withdrawing group
GC-MS	Gas Chromatography Mass Spectrometer(metry)
HMF	5-(hydroxymethyl)furfural
HRMS	High Resolution Mass Spectrometry
I^{i}Pr	1,3-Diisopropylimidazol-2-ylidene
^{i}Pr	*iso*-Propyl
L	Ligand
KIE	Kinetic isotope effect
m	Meta
M	Metal
Me	Methyl
^{n}Bu	*normal*-Butyl
NHC	N-Heterocyclic carbene
NMR	Nuclear magnetic resonance
o	Ortho
p	Para
Ph	Phenyl
ppm	Parts per million
q	Quartet
S_N1	Unimolecular nucleophilic substitution
S_N2	Bimolecular nucleophilic substitution
^{t}Bu	*tert*-Butyl
t	Triplet
Tf	Trifluoromethanesulfonyl (triflyl)
THF	Tetrahydrofuran

TLC	Thin layer chromatography
TOF	Turn-over frequency/ Time of flight
TON	Turn-over number
TO^M	Tris(4,4-dimethyl-2-oxazolinyl)borate
Xantophos	4,5-Bis(diphenylphosphino)-9,9-dimethylxanthene
Å	Ångström

TABLE OF CONTENTS

1 INTRODUCTION

This thesis is divided in two sections, the *hydroxide mediated cleavage of ketones and aldehydes* (chapter 2) and the *Ruthenium catalyzed dehydrodecarbonylation of primary alcohols* (Chapter 3). Both of these reactions, albeit with important variations, try to achieve defunctionalization of oxygenated functionalities to eventually generate carbon-hydrogen bonds in place of carbon-carbon bonds (Scheme 1.1).

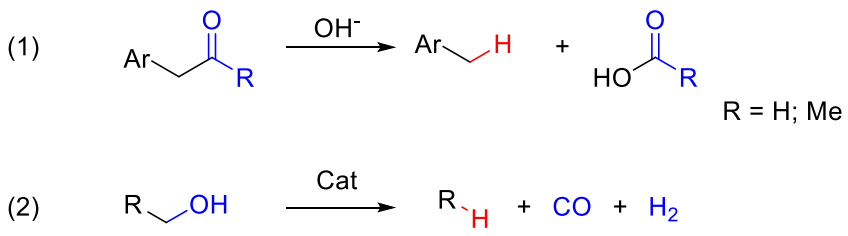

Scheme 1.1: General scheme for reactions introducing hydrogen instead of oxygenated groups.

As first, the behavior of benzylic ketones and aldehydes towards a hydroxide base was studied. In these conditions, the formyl or acyl group is cleaved resulting in the corresponding formate or carboxylate and the bare tolyl derivative remains.

The attention shifted towards the development of a catalytic system able to promote dehydroxymethylation of alcohols. Also in this case a hydrocarbon is formed, but the oxygenated group is released as two small gaseous molecules, hydrogen and carbon monoxide.

The attempt to break down organic molecules in more simple pieces can be considered unusual in the current panorama of reactions aiming to form carbon-carbon bonds starting from simple building blocks to some more complex molecules. The next chapter is focused on understanding the importance and possible applications for this methodology.

1.1 DEFUNCTIONALIZATION REACTIONS

The disconnection of carbon-carbon bonds has a relevant role in organic chemistry as well as their formation. This former process can be considered even more challenging. The dissociation energy of carbon-carbon single bonds is very high (83-85 Kcal mol^{-1}).[2] Moreover, these bonds obviously show a very low polarization that makes a heterolysis very difficult to occur. In order to promote the breakage, transition metals are often useful. However, unlike carbon hydrogen activation, carbon-carbon breakage is still very arduous. This process is favored only when the departing carbon is activated by a functional group or is part of a very strained rings.[3,4] The projects that have been carried out during my doctorate deal with reactions involving carbon-carbon bond breakage and replacement with carbon-hydrogen bond. Defunctionalization reactions like these are particularly important both from a synthetical point of view and as a tool for biomass degradation. For instance, in

synthesis, functional group elimination has shown importance for natural building block modification.[5–8] A good example of a defunctionalization of a natural molecule for the synthesis of a useful target is the preparation of L-threose from D-glucose catalyzed by a rhodium dppp complex, published by Madsen and Monrad.[9] In Scheme 1.2 is reported the key step of the aldose intermediate undergoing the elimination of the carbonyl functionality in order to obtain the corresponding tetrose, shortened by one carbon atom and carbon monoxide.

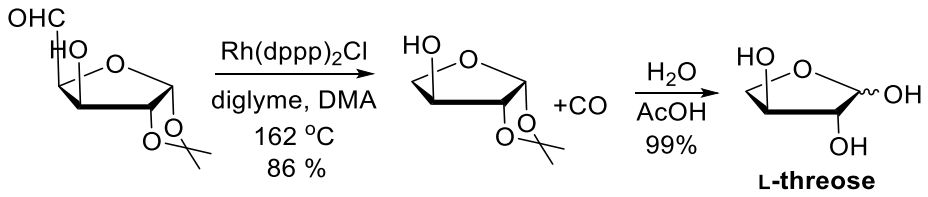

Scheme 1.2: Synthesis of L-threose through catalytic decarbonylation.

A common strategy in organic synthesis is the use of certain functional groups that can help to direct or enhance the reactivity of reaction substrates. These groups are not necessarily present in the final target molecule and so it is useful that the groups can be cleaved after completing their function.[10,11] Additionally carbon-based directing groups are utilized, such as the ones shown in Scheme 1.3.

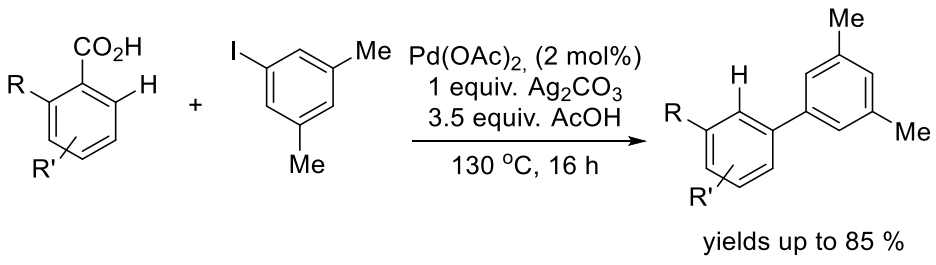

Scheme 1.3: Coupling between aryl halides and benzoic acid derivatives.

In this benzoic acid derivative, the carboxylic acid function directs the activation of the *ortho* hydrogen by coordination with the palladium catalyst and thus allowing the coupling with the aryl halide. The carboxylic acid is then removed by a silver salt, leaving the bare *meta*-substituted biaryl compounds.[12] This methodology was later implemented by Larrosa *et al.* to achieve the *meta*-arylation of phenols Scheme 1.4.[13] In this work a general phenol is *ortho*-functionalized with a carboxylate group by addition of CO_2. Subsequently the carboxylate promotes a palladium mediated arylation, and at last the carboxylic function is removed, similarly to the previous example.

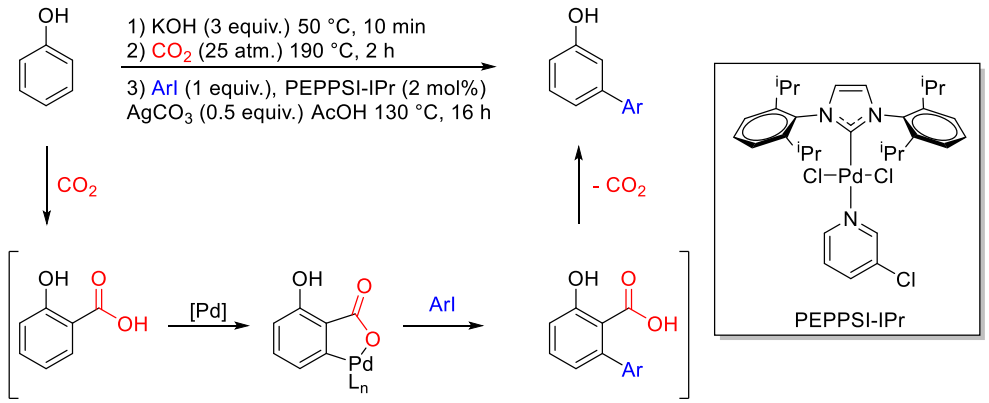

Scheme 1.4: Direct *meta*-arylation of phenols.

All those steps occurred in a one pot sequence with an overall *meta* selectivity. This procedure has been also employed as key step towards the synthesis of the γ-secretase inhibitor in Scheme 1.5. [13]

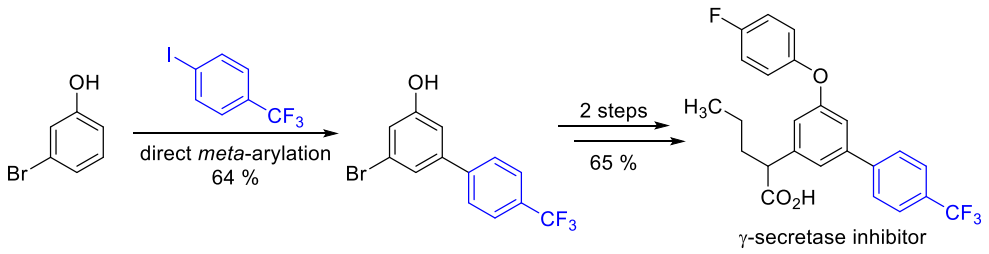

Scheme 1.5: Synthesis of γ-secretase inhibitor.

As previously mentioned, particularly strained bonds are more susceptible to metal-mediated cleavage. For instance, Bart and Chirik reported that the catalyst $(PPh_3)_3RhCl$ can easily react with a cyclopropane derivative in order to form a rhodacyclobutane, that can eventually produce the acyclic process.[14] The reaction can be conducted either in the presence or absence of hydrogen gas giving rise to the corresponding saturated and unsaturated compound (Scheme 1.6).

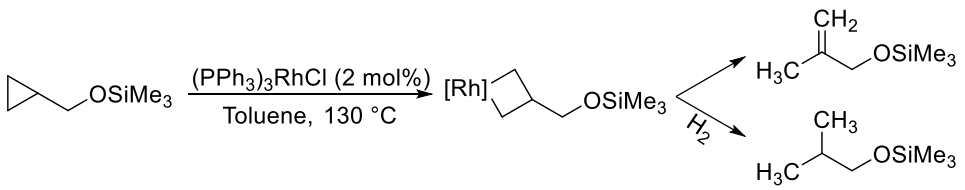

Scheme 1.6: Rhodium mediated cyclopropane ring-opening.

Carreira *et al.*[15] showed that defunctionalization, in this case of an aldehyde decarbonylation, can be considered a potent tool for the obtainment of optically active 1,1-diarylethanes. In this reaction, easily accessible enantiomeric pure β,β-diarylpropionaldehydes[16] are converted by a rhodium catalyst with retention of the stereogenic center.

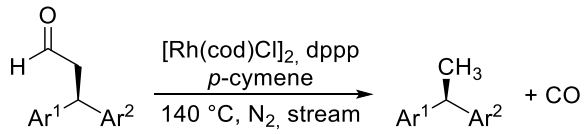

Scheme 1.7: Decarbonylation of optically active aldehydes proposed by Carreira *et al.*[15]

In the previous examples, the removed functionalities are carbonyl moieties or strained bonds and are catalyzed by transition metal species. This approach has been also applied to the breakdown of complex molecules, in particular, oxo-defunctionalization is widely important and is gaining increasing attention for degradation of biomass and naturally abundant chemicals in order to achieve liquid fuels and chemical building blocks.[17–19]

For example, various hexoses like glucose and fructose are converted to 5-(hydroxymethyl)furfural or 5-HMF or just HMF on an industrial scale. In turn, it can be defunctionalized for the preparation of fuels, moreover, chemicals like levulinic acid (LevH), 5-hydroxy-4-keto-2-pentenoic acid (HKPA) and γ-valerolactone (GVL) are produced (Scheme 1.8).[19,20]

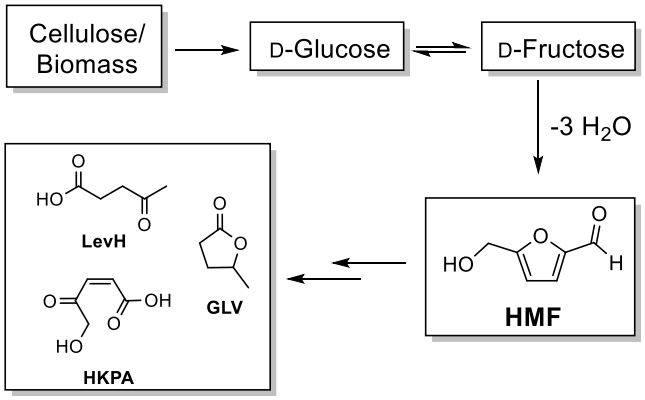

Scheme 1.8: Production and uses of HMF.

Nowadays, new methodologies allow HMF manipulation for the obtainment of furfuryl alcohol (FFA) in a chemospecific fashion.

For instance, the treatment of HMF with a palladium-based heterogeneous catalyst at 130 °C, allow the formation of the product in 12 hours (Scheme 1.9 a).[21]

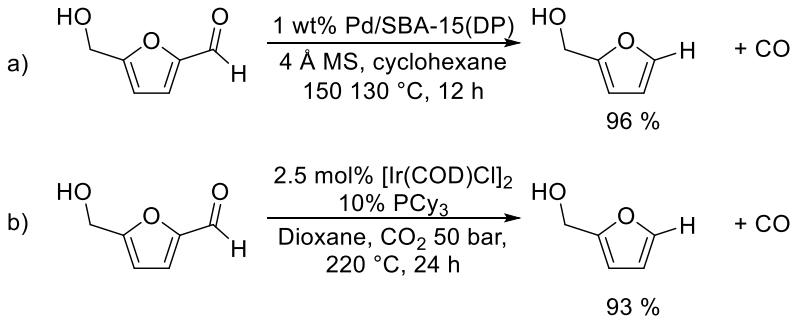

Scheme 1.9: Decarbonylation of HMF to form FFA.[21,22]

Decarbonylation of HMF is also possible with homogenous catalysis (Scheme 1.9 b).[22] The reaction occurs in a so called CO_2-expanded solvent phase and employing an iridium/phosphine catalyst.

So far we have seen processes that involve the degradation of oxo-functionalities through the cleavage of carbon-carbon bonds. Catalysis is sometimes required but it is not always needed. In the next chapter, we are going deeper into the first project, an uncatalysed disconnection of carbon-carbon bonds in ketones and aldehydes in basic media.

2 HYDROXIDE-MEDIATED CLEAVAGE OF CARBON-CARBON BONDS IN KETONES AND ALDEHYDES

2.1 BACKGROUND

Basic hydrolysis of acid derivatives, such as esters and amides, is a very well established pillar of mechanistic organic chemistry. Cleavage of aldehydes or ketones in which a carbon-carbon bond or a carbon-hydrogen bond are broken by a formal addition of water, is maybe less well known, even though it has been investigated profoundly during the years.[23] All these reactions can be included in the group of nucleophilic acyl substitution by the hydroxide ion. In this chapter, we will address these types of reactions looking for analogies and differences between the cleavage of different departing groups.

2.1.1 Hydrolytic cleavage of esters and amides

Ester alkaline hydrolysis is the formal reaction of an ester with a hydroxide ion to produce an alcohol and a carboxylate salt. The reaction has been widely investigated from a mechanistic point of view.[24] The feasible routes for ester hydrolysis are classified according to the overall order of the reaction and the position of the carbon-oxygen bond cleavage. This can be next to the acylic residue (Ac) or to the alkylic residue (Al).[24] In principle 4 possible mechanisms could arise from the combination of monomolecular/bimolecular kinetic (1 or 2) and oxo-acylic or oxo-alkylic fission (Scheme 2.1). This type of classification can be also applied to the hydrolysis in acidic media although this pathway is not examined in this dissertation.

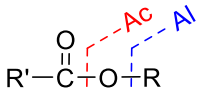

	Monomolecular	Bimolecular
Ac	Unknown	Main mechanism
Al	Few examples in diluted bases	$Ph_3CCO_2CH_3$

Scheme 2.1: Scheme of possible hydrolysis mechanisms in basic means.

Esters generally undergo hydrolysis through a BAc_2 mechanism (Scheme 2.2) in which the hydroxide ion attacks the unsaturated carbon leading to a tetrahedral intermediate (1) with subsequent expulsion of alkoxide ion (2). These steps are reversible nevertheless, step (3), the acid-base reaction to form the carboxylate and the alcohol from the acid, is irreversible and it is the driving force of the reaction.

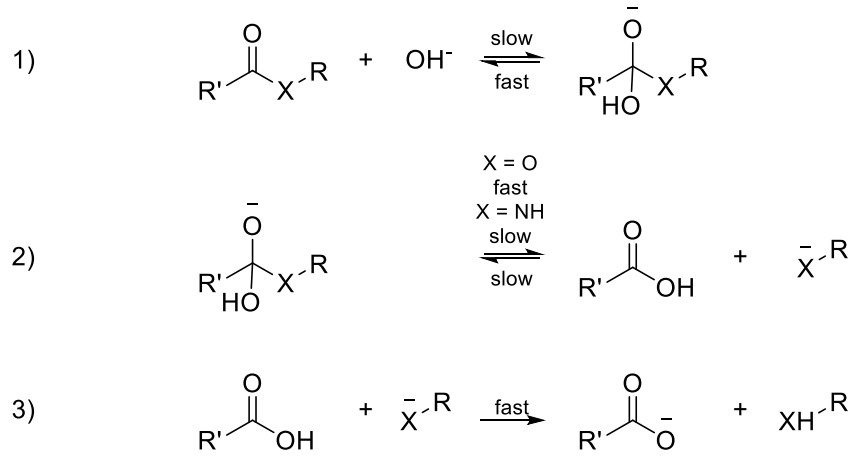

Scheme 2.2: BAc_2 mechanism for hydrolysis of esters and amides.

The BAc_2 mechanism is the most frequent pathway, but certain compounds react according to other mechanisms. In fact, oxy-fixation to the alkyl group can occur. In hydrolysis of methyl triphenylacetate for instance, the BAl_2 mechanism competes with the most prevalent BAc_2.[25] The corresponding monomolecular process (BAl_1) needs the prior ionization of the ester into a carboxylate and an alkyl carbocation. This can occur for the hydrolysis of some hindered esters of allylic, benzylic or tertiary alcohols but only with very weak basic conditions. The kinetic behavior was proven by racemization of the generated alcohol in optically active substrates.[26,27]

On the contrary, a monomolecular mechanism with acyl fixation has not been observed yet. Amide hydrolysis sees an analogous mechanism.[28] The only difference seems that in this case the amide expulsion is the rate-determining step, as the amide anion is much more basic.

It is important to note that in all the mentioned mechanisms, no matter of how unlikely the detachment of the residue can be, the final carboxylate deprotonation is the irreversible step that drives the transformation to completion.

2.1.2 Cleavage of aldehydes and ketones

Esters and ketones are not the only carbonyl compounds that can undergo cleavage reaction with alkali hydroxides. Stanislao Cannizzaro in 1853 observed at first that benzaldehydes disproportionate to yield benzoic acid and benzylalcohol by reaction with a hydroxide base.[29] Following studies explained the scope and the mechanism of the reaction.[30] The reaction involves nucleophilic acyl substitution in which (in absence of more suitable leaving groups) a hydride is donated to another acceptor aldehyde according to Scheme 2.3:.

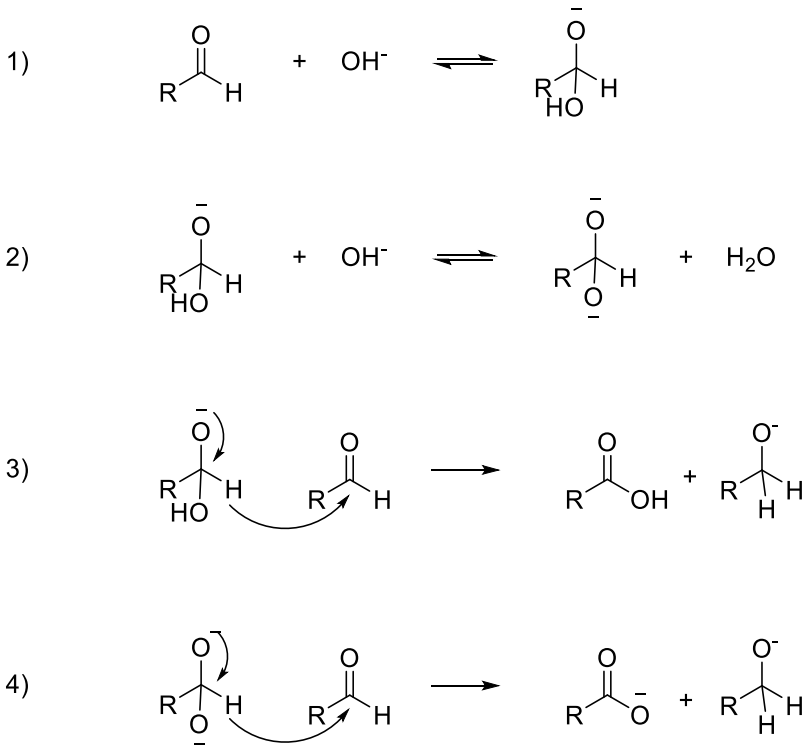

Scheme 2.3: Two possible alternatives for the Cannizzaro reaction mechanism.

The hydride ion is a weak leaving group and the transformation is proposed to go through different mechanisms. At low concentration of the base, the tetrahedral intermediate collapses to produce the acid and the alkoxide (step 3 in Scheme 2.3). At higher concentration, the reaction is believed to go through a much unstable, doubly charged intermediate (step 4, same scheme). This fact seems confirmed from the dependence of the rate of the reaction with respect to hydroxide ion that appears to be $k[RCHO]^2[OH^-]$ at low hydroxide concentration. The mechanism that goes through the dianion needs another equivalent of base and therefore the reaction rate behaves like $k[RCHO]^2[OH^-]^2$ at higher concentration.

Beside hydrides, also carbon substituents can be released from aldehydes or ketones under basic aqueous conditions.[23] One of the best known examples is the haloform reaction.[1,31,32] In the presence of a base and a halonium ion source, a methyl ketone is transformed into the corresponding trihalomethyl ketone. In the same basic environment, a cleavage occurs readily in order to yield a carboxylate and a haloform molecule (chloroform, bromoform, iodoform). The reaction is so straightforward that for instance an iodoform test is also used as a common analytical essay for methylketones. Trihalomethane is a fairly strong acid (pK_a for CHX_3 = 18-21)[33] and this justifies the stability of the released anion.

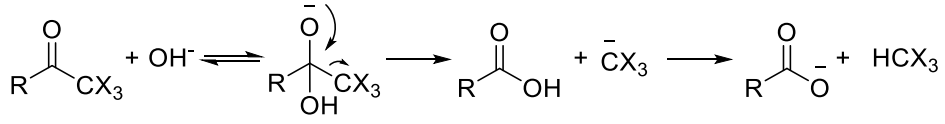

Scheme 2.4: Key steps of the haloform reaction.

However, the cleavage of alpha carbons in aldehydes and ketones is more than an exception. Another example is represented by the hydrolysis of acetoacetic esters or β-diketones,[34–36] the so called retro-Claisen condensation. What these reactions have

in common is that they are all driven by the formation of a stabilized enolate anion (pK_a for ketones = 19-20, for esters ~25). The mechanism was investigated in case of acetylacetones and their close derivatives.[36] The authors of the study observed that, unlike trihalomethylketones, acetylacetone is enolizable and has a very low pK_a (pK_a for acetyl acetone = 9) and this suggests that in alkaline media the compound is totally dissociated according to equation (2.1). Moreover, it has been observed that the corresponding 3,3-dimethyl acetylacetone, that has the enolizable position blocked, is cleaved much more readily.[36] This suggests that the anionic form **A**$^-$ is not the reactive species but, on the contrary, is a resting state that subtracts the reactive substrate and slows down the reaction. The reaction follows a pseudo first-order kinetics, compatible with a fast titration of the diketone HA with the base, and then a second equivalent of base that promotes the reaction. When the reaction is performed in a solution of sodium ethoxide in ethanol, it shows pseudo zero-order kinetics in base.[37] This can suggest a dioxy anionic intermediate **II** and a pathway like the one shown in equations 2.1-2.4. That cannot be achieved by a hemiacetal anion obtained after addition of ethoxide.

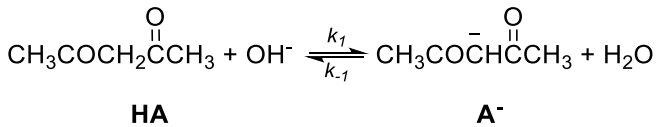

(2.1)

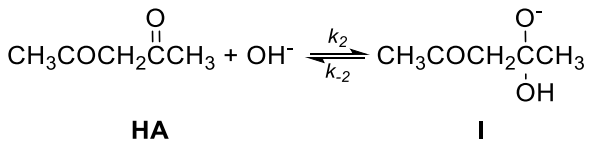

(2.2)

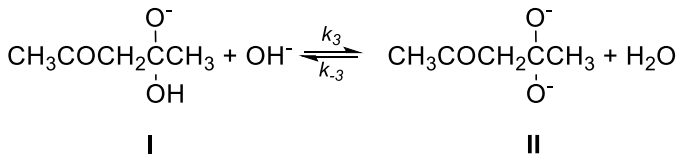

(2.3)

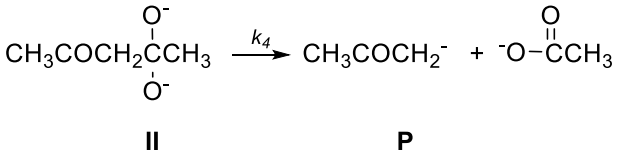

II **P** (2.4)

The two cited reactions define two types of mechanisms. It is reasonable to think that the monooxy anion **I**, can collapse in order to release the carbon residue only if this residue is sufficiently nucleofugal. Less nucleofugal groups need to go through a doubly charged intermediate (**II**) that is much more unstable. The nucleofugacity takes into account the stability of the released carbanion, and for this reason it mirrors to a certain degree the trend in pK_a of the conjugate acid of the leaving groups.[38–40]

This seems to be confirmed if we look at the following examples. The 1,1-bis(carbalkoxy)alkyl group[41] and a cyano group[42] are hydrolyzed in water even under very mild basic conditions. Kinetic evidences support the formation of a singly charged intermediate. That is due to the fact that both cyanide and malonic enolates are very stable carbon anions (Scheme 2.5 a).

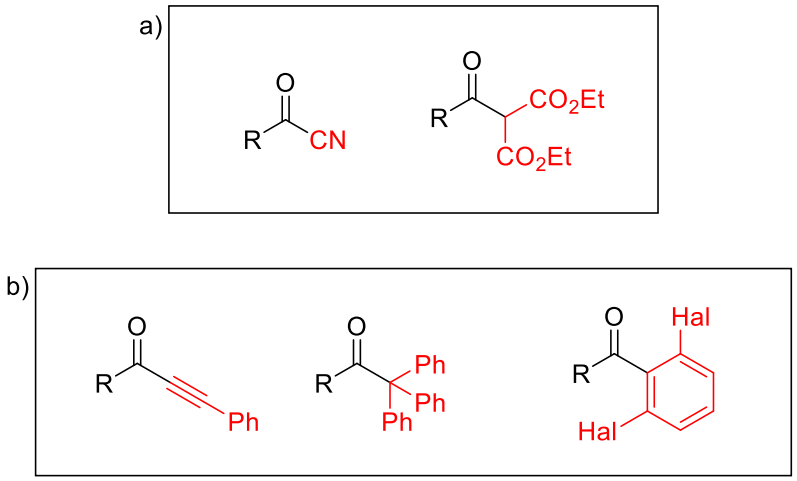

Scheme 2.5: Some substrates can undergo cleavage of carbon-based substituents in aqueous solution a) by a monoanion mechanism; b) through a dianion.

In other cases, also less stable carbon groups are released in alkaline aqueous solution, like when the cleaved anions are acetylenes,[43] triphenylmethanes[44,45] and 2,6-dihalobenzenes (Scheme 2.5 b).[46,47] The conjugate acids of these groups have a pK_a ranging between 20 and 40. In all the examples, it appears that a di-charged intermediate is involved. Furthermore, the kinetics described in many of the previous works reports a reaction order in the hydroxide of one, even with a dianionic mechanism.[36,43,47]

Other reactions only occur under much more severe conditions, like high temperatures and the use of organic solvents. This is the case of non-enolizable ketones, like benzophenones, in the reaction to form benzenes and benzoic acids.[48] The reaction occurs by mixing neat benzophenone and potassium hydroxide and followed by heating with a direct flame.

2.1.3 The Haller-Bauer reaction

The cleavage reaction of ketones with metal hydroxides is closely related with an older reaction, the so called Haller-Bauer reaction.[49] This reaction consists of the cleavage of benzophenones with sodium or potassium amide in ammonia or with an aromatic solvent.[49,50] In case of asymmetric benzophenones like the one in Scheme 2.6 the most electron-poor ring tends to be the most nucleofugal. Examples show the following reactivity order for the departing aromatic ring: 2-Cl or 2-OMe > 3-Cl > 2-CO_2^- > 2-Me > 4-Cl > 3-MeO > 4-Ph > H > 4-MeO or 4-Me > 3-Me > 4-CO_2^-.[51] This correlation shows a good match to what we expect to be the ability of an aryl group to host a negative charge.

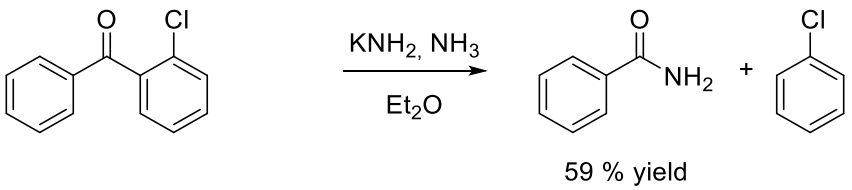

Scheme 2.6: Haller-Bauer reaction on an asymmetric benzophenone.

In recent years, the Haller-Bauer reaction has found some interesting synthetic applications in more complex structures.[52,53] For instance, the cyclobutanone derivative in Scheme 2.7 can be solvolyzed in liquid ammonia to afford a densely decorated cyclopentane ring.[54]

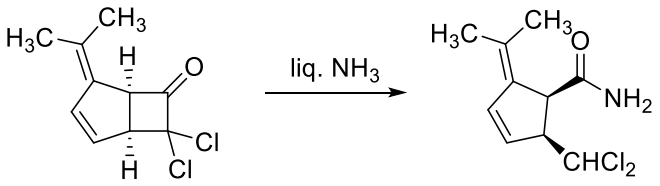

Scheme 2.7: Haller-Bauer reaction of an α,α-dichloro cyclobutanone.[54]

2.2 RESULTS AND DISCUSSION

2.2.1 Preliminary studies

The cleavage of carbon-carbon bonds in aldehydes was first discovered by serendipity during the catalyzed oxidation of primary alcohols into carboxylic acids with liberation of molecular hydrogen. This experiment was conducted in our laboratories by a fellow Ph.D. student. The reaction successfully achieved its goal with several benzylic and alkylic substrates, employing 1% of [$RuCl_2I$*i*Pr(*p*-cymene)], 1% of $PCy_3{\cdot}HBF_4$, and a slight excess of potassium hydroxide in refluxing toluene.[55] Scheme 2.8.a shows the reaction of 2-phenylethanol (**1**) that was converted into phenylacetic acid (**2**) in a 75% yield.

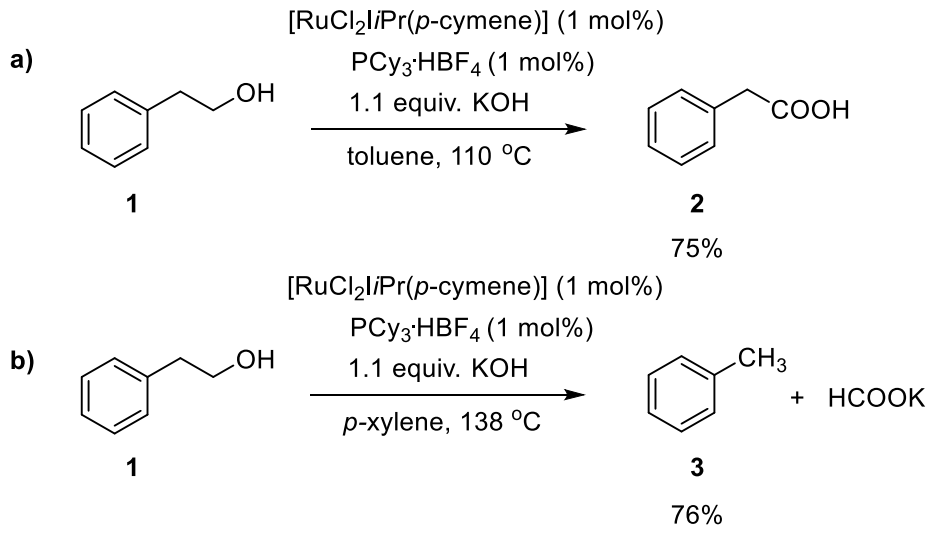

Scheme 2.8: Scheme for a) the formation of carboxylic acids from primary alcohols catalyzed by ruthenium and b) the formation of the unexpected cleavage product.

The modest yield was attributed to the formation of a side product that, at first, was not possible to identify. However, raising the reaction temperature from 110 °C to 138 °C, by the use of *p*-xylene as solvent, gave rise to the side product as the predominant species and it could now be identified. In this second case, 76% of toluene (GC-calculated yield) was found. Toluene was assumed to be the same byproduct observed at lower temperatures. However, it was not detected due to the choice of toluene itself as the solvent. Further NMR analysis of the crude mixture obtained after evaporation of the solvent revealed that potassium formate was also formed.

2.2.2 Reaction identification

After the first results, it was interesting to understand how the carbon-carbon bond could possibly break, and which conditions were important for the reaction outcome.

One of the first hypotheses was that the salt of phenylacetic acid (**2**) could fragment to form toluene and formate. In order to verify this theory, compound **2** was let to react with the catalytic system and in presence of 5.0 equivalents of potassium hydroxide. Under the described conditions the acid was stable and no reaction occurred. In the same way, it was observed that 2-phenylacetaldehyde (**4**) afforded the condensation product **5** that was identified by GC-MS and its structure was determined by NMR. Besides compound **5**, the reaction of substrate **4** with KOH afforded the corresponding cleavage products, both with and without the catalyst, although in low amounts. Finally, as anticipated, the alcohol **1** afforded the cleavage product with the best yield, although only in presence of the catalytic system. Since hydrogen was released during the reaction, the products bore a higher oxidation state than the starting material. We speculated that the ruthenium catalyst was only responsible for the dehydrogenation of 2-phenylethanol to aldehyde **4**. The latter was formed in sufficient low concentration so that the bimolecular reaction leading to

product **5** was avoided and a monomolecular pathway was preferred. In fact, in the latter case, the attack of the hydroxide took place to afford toluene and formate. When the aldehyde **4** was reacting at a higher concentration, like when employed as a starting material, two molecules of the substrate would have a higher chance to react with each other. In turn, they could afford the alkene **5** through formation of an intermediate aldol product, followed by eliminative aldehyde cleavage (Scheme 2.9), similarly to what has been proposed in the literature.[56]

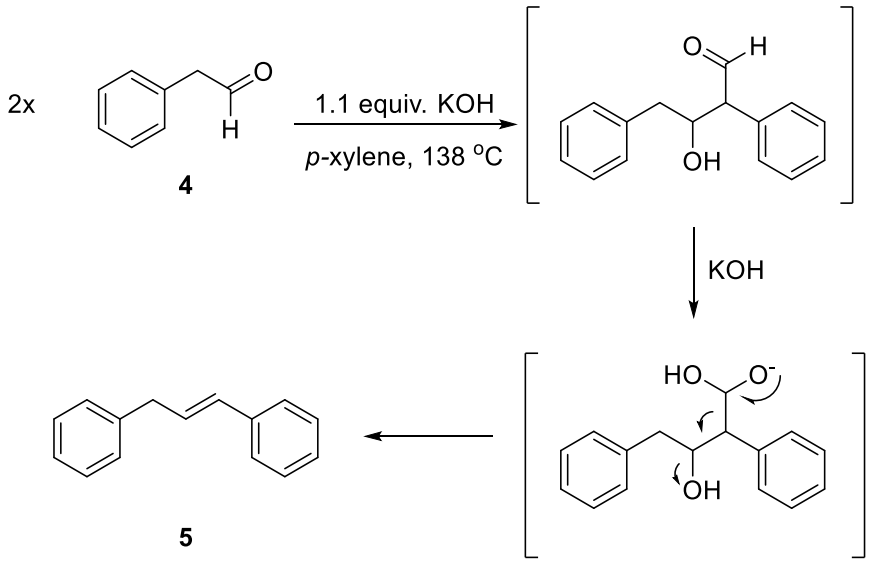

Scheme 2.9: Hypothesis for the formation of alkene **5** from phenylacetaldehyde.

2.2.3 Reaction optimization

In the previous section, it was observed that the starting aldehyde **4** can be transformed into toluene in the presence of 1.1 equivalent of KOH in refluxing *p*-xylene. However, when the concentration of the starting material was the one employed so far (0.5 M, Table 2.1 entry 1) the product was obtained only with poor yield. The yield was determined by GC-MS by comparison with a known amount of

n-nonane used as internal standard. This result, together with the reactions discussed in paragraph 2.2.2, suggested that the aldehyde could lose a carbonyl group in the form of potassium formate but only if the reaction conditions allowed for a low concentration of the reactant.

Table 2.1: Preliminary reaction studies for the cleavage of phenylacetaldehyde (**4**)[a]

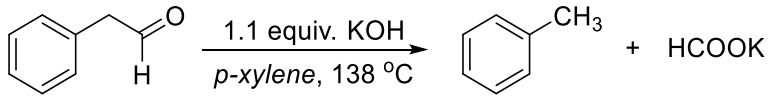

4 **3**

Entry	Conc. [**4**] (M)	Solvent	Yield (**3**)%[b]
1	0.5	*p*-xylene	11
2[c]	0.5	*p*-xylene	89
3	0.05	*p*-xylene	85
4[d]	0.05	*p*-xylene	-
5[e]	0.05	*p*-xylene	20
6	0.05	DMSO	-
7	0.05	H_2O	-

[a] Reaction conditions: Phenyl acetaldehyde (2.5 mmol), KOH (50 mmol), solvent, reflux temperature under nitrogen stream. Analyzed after full conversion; [b] GC yield; [c] ***4*** *added over 2 hours; [d] T = 80 °C; [e] NaOH used instead of KOH.*

To confirm this assumption, it was attempted to have a low concentration of the aldehyde in solution by adding it into a preheated suspension of the base in *p*-xylene over two hours by means of a syringe pump. This reaction afforded toluene in 89% yield determined by gas chromatography (Table 2.1 entry 2). Product **5** was not observed in the reaction mixture.

A similar result was obtained upon diluting 10-fold the aldehyde in *p*-xylene (from 0.5 M to 0.05 M). In this case, the reaction yielded the product in good yield (85%, entry 3).

It should be noted that while decreasing the aldehyde concentration, the concentration of the base was kept roughly constant by adding 50 mmol (20 equivalents) of KOH to the solution. Lowering the temperature to 80 °C was detrimental for the outcome of the reaction. No toluene was detected and instead product **5** was identified as the main product by GC-MS. This could be explained by the entropic factor that depends on the temperature, which may favor the monomolecular reaction at high temperature and the bimolecular one at lower temperature. The use of sodium hydroxide caused a severe drop in the yield to 20 % (entry 5). This result demonstrated the great influence of potassium as a counter ion since, due to its larger radius, it increases the solubility of the base in the organic solvent and formed a less tight ionic couple with the anionic species. Attempts to change the solvent were unsuccessful, as the reaction occurred only in aromatic solvents like toluene and xylene.

Water and DMSO, at the corresponding refluxing temperatures, led to a poor conversion and the formation of side products (entries 6 and 7). Therefore, in entry 3, with a substrate concentration of 0.05 M in *p*-xylene was considered the best result and, despite it showed a slightly lower yield as compared to entry b, it was believed to be more convenient than by prolonging the addition over two hours.

2.2.4 Scope and reaction limitations

The developed conditions were employed on different substrates to clarify the scope and the limitations of the reaction (Table 2.2). The reactions were monitored by GC-MS and the yields were determined either by GC-MS, by comparison with nonane as internal standard, or by isolation of the products from the crude mixture by chromatography. Notably, the reaction with the ketone phenylacetone proceeded smoothly and toluene was obtained in 91% yield (Table 2.2 entry 1).

Table 2.2: Reactions for cleavage of ketones and aldehydes[a]

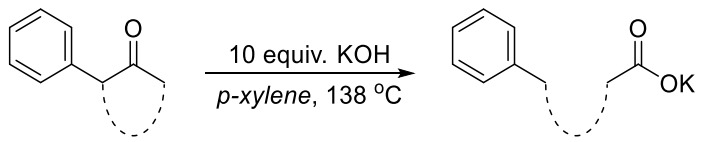

Entry	Substrate		Product		Yield %
1	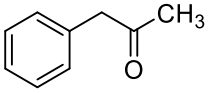	**6**	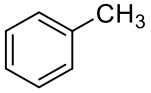	**3**	91[b]
2	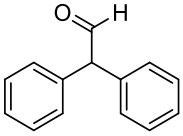	**7**	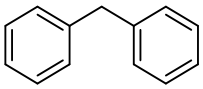	**8**	21[b]
3	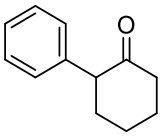	**9**	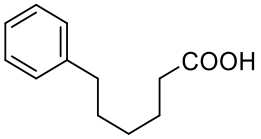	**10**	78[c]
4	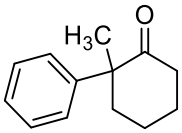	**11**	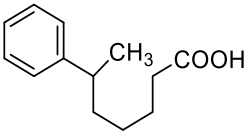	**12**	40[c]

Entry	Substrate		Product		Yield %[b]
5	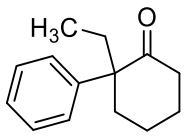	**13**	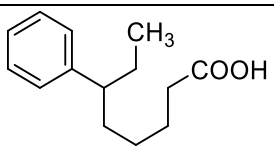	**14**	65[c]
6	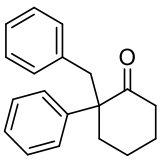	**15**	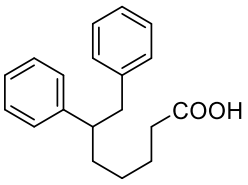	**16**	76[c]
7	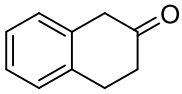	**17**	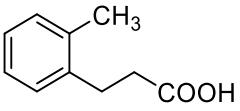	**18**	18[c]
8	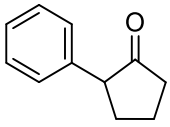	**19**	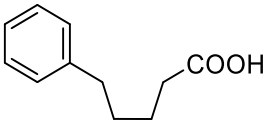	**20**	64[c]
9	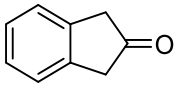	**21**	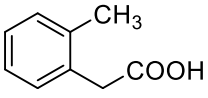	**22**	90[c]
10	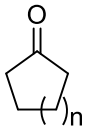 n = 0; 1; 2	n = 0; **23a** n = 1; **23b** n = 2; **23c**	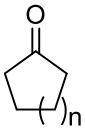 n = 0; 1; 2	n = 0; **24a** n = 1; **24b** n = 2; **24c**	- - -
11	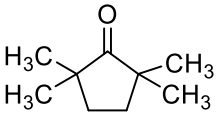	**25**	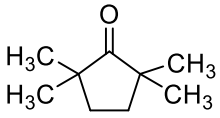	**26**	-

Entry	Substrate		Product		Yield %
12	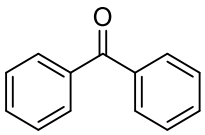	**27**		**28**	82[b]

[a] Reaction conditions: Aldehyde/ketone (2.5 mmol), KOH (50 mmol), p-xylene (50 mL), 138 °C, nitrogen stream. Analyzed after full conversion; [b] GC yield; [c] Isolated yield.

Diphenylacetaldehyde, on the other hand, afforded diphenylmethane in only 21% yield together with several high molecular products which were not further identified (entry 2).

The cleavage of cyclic ketones was considered particularly interesting for the possibility to afford long chain carboxylic acids, as a new synthetic route to these compounds.

The fragmentation occurred nicely with 2-phenylcyclohexanone that gave 6-phenylhexanoic acid in 78% isolated yield (entry 3). A slightly lower yield was obtained when an additional substituent at the 2-position was present on the cyclohexanone scaffold, presumably due to the increased steric hindrance (entries 4-6). In these last cases ω-substituted long chain acids were obtained. β-Tetralone afforded 3-(*o*-tolyl)propanoic acid in a regioselective fashion, highlighting the reactivity of the benzylic residue over the aliphatic moiety. Unfortunately, the product was only produced in a low yield of the carboxylic acid (entry 7). Five-membered ketones could also undergo the cleavage as shown with 2-phenylpentanone and 2-indanone. This experiment afforded the carboxylic acids in 64 and 90% yield, respectively (entries 8 and 9). Alkyl ketones, such as the series of homologous cyclic ketones (entry 10), were poorly converted into a mixture of high molecular mass product and no carboxylic acids were observed. 2,2,5,5-Tetramethylcyclopentanone did not react at all upon

refluxing the reaction mixture at 138 °C. Furthermore the same outcome was observed by setting the reaction temperature to 160 °C in a closed vessel.

Benzophenone was investigated in the past by running the reaction at 260 °C with KOH.[57] In this study, this substrate afforded benzene in good yield (entry 12).

2.2.5 Base studies for evaluation of the mechanism

Along with the synthetic outlook from this kind of disconnections, it would also be very interesting to clarify the reaction mechanism, especially regarding the differences and the analogies with the already known protocols.

For studying different kinetic parameters in the hydrolysis reaction of carbonyl compounds, 1-phenylacetone (**6**) was chosen as the model substrate since it gave the best results in terms of yield. Additionally it was judged to be quite representative of all of the substrates that were previously tested.

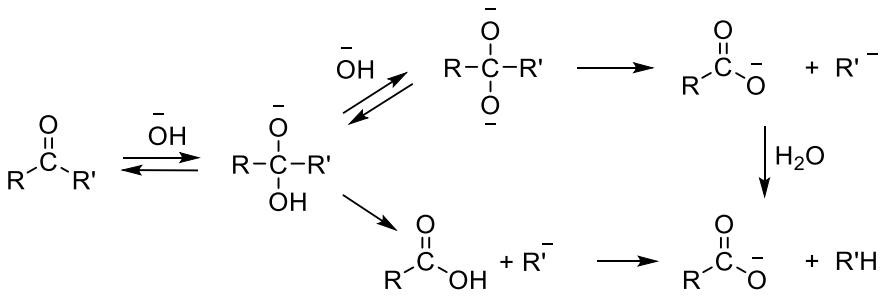

Scheme 2.10: Reported mechanistic pathways for the cleavage of aldehydes and ketones with bases

As briefly explained in paragraph 2.2 and vastly reported in the literature,[31,32,34,35,43,46,47] the class of reactions constituted by the cleavage of carbonyl compounds in the presence of a base usually occurs with two main mechanisms, as displayed in Scheme 2.10. The first one involves the immediate cleavage of the compound after acetal monooxyanion formation, while the other needs the formation of a dianion.

When the monooxyanion intermediate is formed, two outcomes are possible: 1) if the departing residue R' is sufficiently stabilized as a carboanion, it can be readily expelled to reestablish the planarity of the carbonyl carbon; 2) if otherwise, the residue is less nucleofugal, a larger activation energy is required and most likely an extremely reactive dianion is thus formed. The dianion can collapse to form two differently charged species, the R'^{-} residue and the carboxylate. The dioxyanion is only formed by the addition of a base containing an extractable hydrogen, like hydroxide and amide. Alkoxides, for instance, despite having a similar pK_b compared to hydroxides, have no further proton to be extracted. This implies that only the reaction occurring through the monoanion mechanism could progress with these bases, eventually affording esters instead of acids.

By treating the 1-phenyl-2-propanone (**6**) with sodium methoxide and potassium *t*-butoxide only a poor conversion into toluene was observed (yield 14% and 5% respectively). Nevertheless, by carrying out the same experiment with potassium *t*-butoxide, followed by addition of 3 equivalents of water, toluene was afforded as a product in a commensurate yield (77%). Moreover, in all the cases neither the methyl ester nor the *t*-butyl ester were recovered from the reaction mixture. This result suggested that hydroxide had a role in the reaction mechanism beyond its function as a general nucleophile, and it might promote the step where the dianion is formed.

The reaction order, with respect to the base, was determined for 1-phenylacetone in a range of KOH concentrations between 0.2 M and 0.5 M. The plot of initial rates as a function of the KOH concentrations showed a linear dependence for values below 0.4 M. After that point, the reaction rate dropped moderately (Figure 2.1).

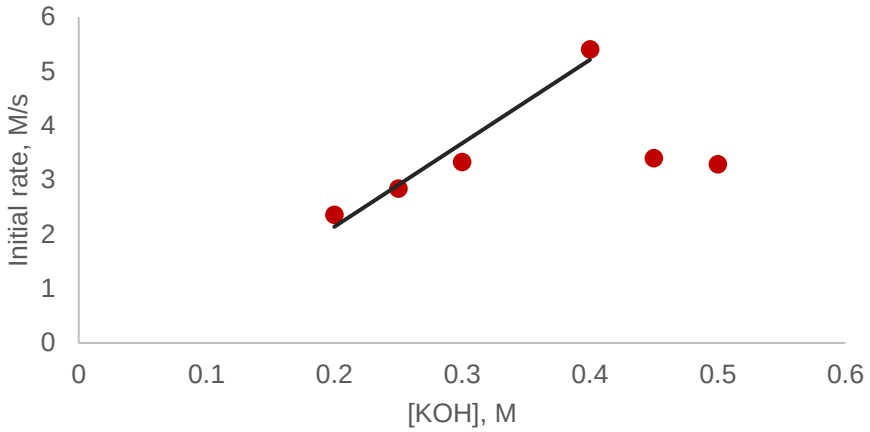

Figure 2.1: Reaction rate dependence on base concentration

The linear correlation suggested that the reaction has first order dependence on KOH. This is an important breakthrough, even if it is not conclusive in terms of identifying the mechanism. A pseudo-first order kinetic pathway can be observed also when the substrate has ionizable protons that can be accepted by the base.[36]

With regard to the deviation of the last part of the curve it might be due to the saturation of the solution with the base that is not fully soluble in the solvent. Another explanation might be the effect of the formation of hydrogen-bonded species[58] that can lead to a lower active concentration of hydroxide ions.

2.2.6 Hammett studies

A negative charge is developed in the molecule and it is eventually left behind on the aromatic residue during the cleavage of ketones and aldehydes. For this reason,

evaluating the effect of the substituents on the aromatic ring, based on their electronic effects, can be, in principle, very helpful.

Different *p*-substituted phenyl acetones (**29 a-d**) were allowed to react in a competitive reaction with the unsubstituted compound **6**. Samples of the reactions were taken and the formation of the two different toluene derivatives **3** and **30 a-d** was evaluated by GC-MS.

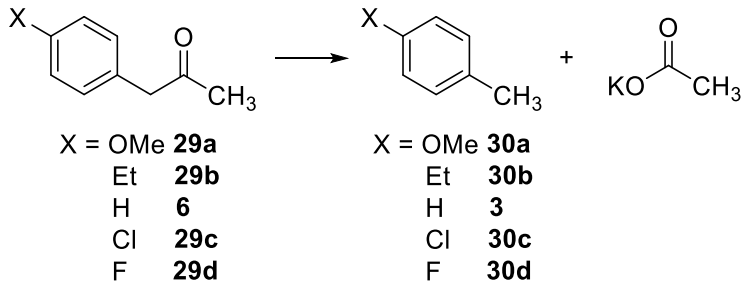

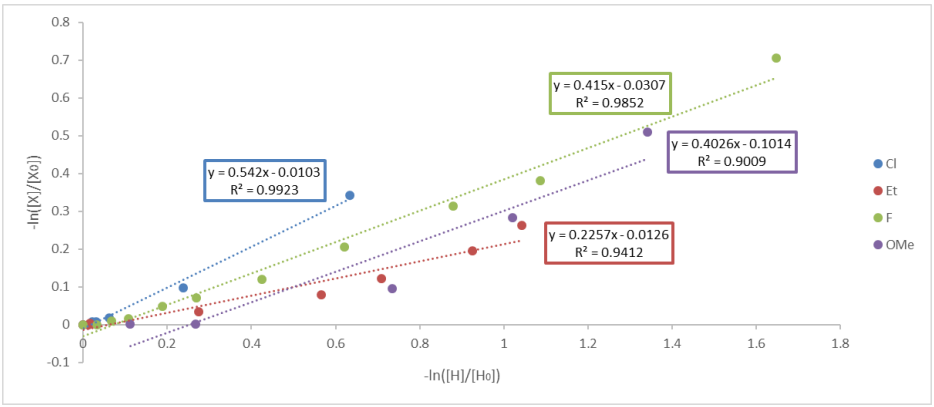

Figure 2.2: Relative reaction rates of different *p*-substituted phenylacetones

Figure 2.3 shows the Hammett plot which consists in the graph of the logarithm of relative rates as a function of the substituent constant σ^-. As evident from the figure, the data do not seem to have a correlation, and the reaction of the unsubstituted

substrate seems to have the fastest rate. Similar plots were also made with with the other Hammett substituent constant *i.e.* σ, σ^+ or $\sigma^\cdot$ (for radical reaction). Nevertheless all of them portrayed a similar scattered plot.

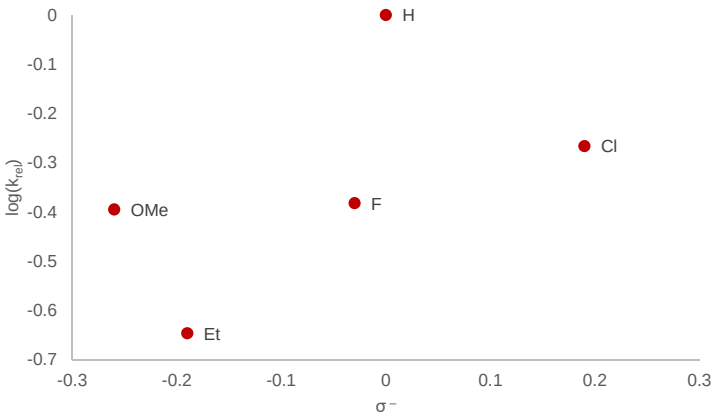

Figure 2.3: Hammett plot for different *p*-substituted phenylacetones

This apparently unpredictable behavior can be explained by considering that the base could also mediate the substrate deprotonation of the α-position of the ketone. In particular, the ketone that bears the aryl group is more prone to deprotonation. The acid-base reaction subtracts active substrates from the solution, and most likely inhibits the attack of a second hydroxide on the carbonyl moiety.

As we can speculate, the pK_a decreases when electron-withdrawing substituents are in place, unlike the substituent effect σ that increases with the substituent electron withdrawing effect.

In order to determine this effect, it is important to determine the kinetic profile of the reaction. The transformations promoted in a competitive experiment are displayed in the equations below.

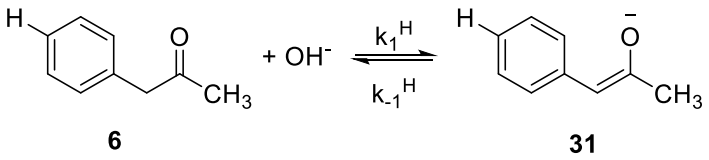

6 **31**

$$K_1^H = \frac{k_1^H}{k_{-1}^H} = \frac{[\mathbf{31}]}{[\mathbf{6}][OH^-]} = \frac{K_a^H}{K_w} \qquad 2.5$$

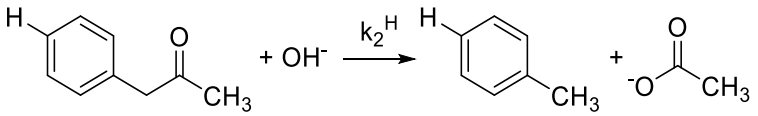

6 **3** 2.6

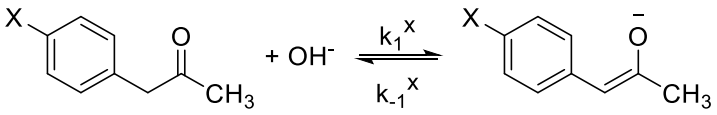

29 **32**

$$K_1^X = \frac{k_1^X}{k_{-1}^X} = \frac{[\mathbf{32}]}{[\mathbf{29}][OH^-]} = \frac{K_a^X}{K_w} \qquad 2.7$$

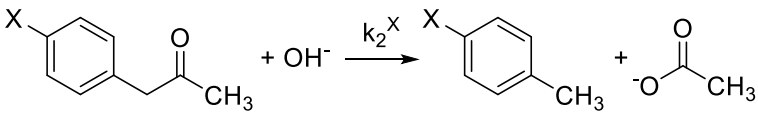

29 **30** 2.8

For simplicity, the derivation of only one substrate (X) will be calculated and then the same equation will be used for the resulting expression for the second substrate (H).

The rate of the reaction is determined by equation 2.8, hence:

$$rate_X = \frac{d[\mathbf{30}]}{dt} = k_2^X[\mathbf{29}][OH^-] \quad 2.9$$

The concentration of the ketone **29** in solution is the initial concentration, net of the ketone converted into the product **30**, and the deprotonated one (**32**), which in turn can be expressed through equation 2.10.

$$[\mathbf{29}] = [\mathbf{29}]_o - [\mathbf{30}] - [\mathbf{32}] = [\mathbf{29}]_o - [\mathbf{30}] - \frac{K_a^X}{K_w}[\mathbf{29}][OH^-] \quad 2.10$$

$$\longrightarrow [\mathbf{29}] = \frac{[\mathbf{29}]_o - [\mathbf{30}]}{1 + \frac{K_a^X}{K_w}[OH^-]} \quad 2.11$$

Now, we can substitute [**29**] in equation 2.9 with the expression from above:

$$\frac{d[30]}{dt} = k_2^X \frac{([\mathbf{29}]_o - [\mathbf{30}])K_w}{K_a^X[OH] + K_w}[OH^-] \quad 2.12$$

$$\frac{d[\mathbf{30}]}{([\mathbf{29}]_o - [\mathbf{30}])} = k_2^X \frac{K_w[OH^-]}{K_a^X[OH] + K_w}dt \quad 2.13$$

Considering [OH-] in great excess, and so constant at the beginning of the reaction, when the rate is measured constant, integrating the equation 2.13 from **30** = 0 at t = 0 to **30** at the time t = t,

$$\ln\left(\frac{[\mathbf{29}]_o - [\mathbf{30}]}{[\mathbf{29}]_o}\right) = -k_2^X \frac{K_w[OH]}{K_a^X[OH^-] + K_w} t \qquad 2.14$$

And considering $K_a^X[OH^-] \gg K_w$ at the beginning of the reaction, the expression is reduced to:

$$\ln\left(\frac{[\mathbf{29}]_o - [\mathbf{30}]}{[\mathbf{29}]_o}\right) = -k_2^X \frac{K_w}{K_a^X} t \qquad 2.15$$

As we can see from equation **2.15**, the conversion depends on the acid dissociation constant for the ketone (K_{aX}).

After dividing the equation obtained earlier for the one that can be written for the X = H, we obtain the following equation, which derives the Hammett correlation.

$$\frac{\ln\left(\frac{[\mathbf{29}]_o - [\mathbf{30}]}{[\mathbf{29}]_o}\right)}{\ln\left(\frac{[\mathbf{6}]_o - [\mathbf{3}]}{[\mathbf{6}]_o}\right)} = \frac{-k_2^X \frac{K_w}{K_a^X}}{-k_2^H \frac{K_w}{K_a^H}} \qquad 2.16$$

That becomes:

$$\ln\left(\frac{[\mathbf{29}]_o - [\mathbf{30}]}{[\mathbf{29}]_o}\right) = \frac{k_2^X}{k_2^H}\frac{K_a^H}{K_a^X} \ln\left(\frac{[\mathbf{6}]_o - [\mathbf{3}]}{[\mathbf{6}]_o}\right) \qquad 2.17$$

By plotting $\ln\left(\frac{[\mathbf{29}]_o-[\mathbf{30}]}{[\mathbf{29}]_o}\right)$ versus $\ln\left(\frac{[\mathbf{6}]_o-[\mathbf{3}]}{[\mathbf{6}]_o}\right)$, that represents the logarithms of the conversion of the products, the slope $\frac{k_2^X}{k_2^H}\frac{K_a^H}{K_a^X}$ is obtained.

Now, it is possible to use this ratio in the Hammett equation in order to isolate the contribution from the reaction of cleavage over the deprotonation equilibrium:

$$\log\frac{k_X}{k_H} = \sigma^{-}\rho \Rightarrow \log\left(k_{rel}\frac{K_a^X}{K_a^H}\right) = \sigma^{-}\rho \Rightarrow \log(k_{rel}) + \log\frac{K_a^X}{K_a^H} = \sigma^{-}\rho \qquad 2.18$$

The ratio $\log\frac{K_a^X}{K_a^H}$ can be rewritten in terms of pK_a as follows:

$$\log\frac{K_a^X}{K_a^H} = \log(K_a^X) - \log(K_a^H) = -pK_a^X + pK_a^H \qquad 2.19$$

Thus, the resulting Hammett equation is:

$$\log(k_{rel}) - pK_a^X + pK_a^H = \sigma^{-}\rho \qquad 2.20$$

By plotting $(\log(k_{rel}) - pK_a^X + pK_a^H)$ versus σ^{-}, the reaction constant ϱ can be obtained. For the specific case, it resulted in a value of 6.7.

The equation assumed that the cleavage step follows a first order kinetic profile in hydroxide, but the same results can be achieved by considering a second order kinetic pathway in hydroxide. The pK_a values of the 2-aryl acetones were calculated in-silico in DMSO.

Table 2.3: Initial and corrected parameters for Hammett studies

Entry	X	pK_a [a]	σ^-	log(k_{rel})	log(k_{rel}) – pK_a^X + pK_a^H
a	OMe	22.5	-0.26	-0.395	-2.195
b	Et	21.5	-0.19	-0.646	-1.446
c	H	20.7	0	0	0
d	F	20.7	-0.03	-0.382	-0.382
e	Cl	19.6	0.19	-0.266	0.834

[a] pK_a *in DMSO calculated: Jaguar, version 7.8. Schrodinger, LLC, New York, NY, 2010.*

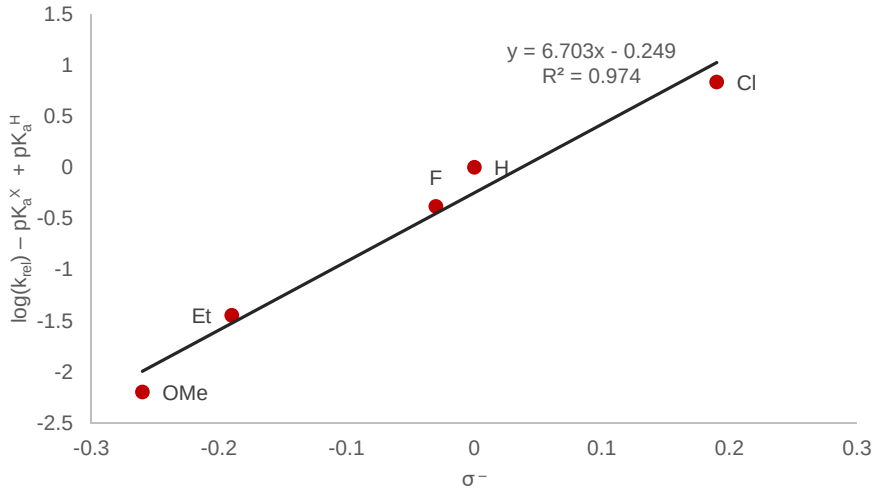

Figure 2.4: Corrected Hammett plot for different *p*-substituted phenylacetones

The equation correlated best using σ^- over σ, σ^+ or $\sigma^\cdot$. This indicated that a direct conjugation between the substituent and the negative charge took place. Moreover, the high value of ρ of 6.7 suggested that almost a full negative charge was developed on the benzylic residue. These results highlighted that the rate-determining step was the carbon-carbon bond breakage reaction and that the process had a late transition state.

2.2.7 In-silico studies

Density functional theory (DFT) in silico calculations were conducted in collaboration with Dr. Ilya Makarov for a conclusive understanding of the reaction mechanism.

In order to obtain a reliable outcome, and select the right basis set, the cleavage of 2,6 dichlorobenzaldehyde with NaOH in aqueous media, previously reported by Bunnett and coworkers in 1961[47] was examined. The reaction was selected as a reference since the mechanism has previously been studied in detail by kinetic measurements and all the necessary activation parameters have been established.[47] Moreover, 2,6-dichlorobenzaldehyde is relatively small and does not have many conformational degrees of freedom, which facilitates the optimization and the search for the transition states. Finally, 2,6 dichlorobenzaldehyde, as well as benzylic aldehydes and ketones taken into account in this study, do not contain any heavy atoms and therefore the same basis sets can be used in both cases.

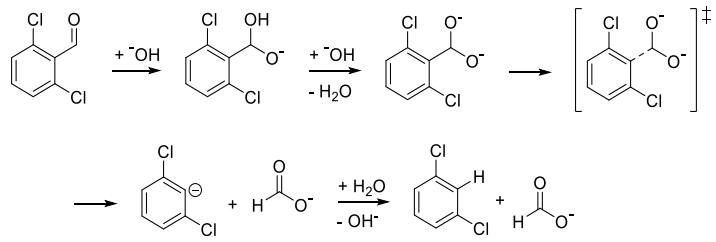

Scheme 2.11: Scheme of the reaction described by Bunnett

The authors proposed the involvement of a dianionic intermediate and experimentally measured the activation Gibbs free energy as $\Delta G^{\neq} = 108.8$ kJ·mol^{-1} at 58 °C, i.e. the temperature corresponding to the reaction conditions.[47]

By means of DFT calculations, it was possible to obtain a value of the activation energy of 113.7 kJ·mol^{-1}, only 4.9 kJ·mol^{-1} higher than the measured value. The elaborated method saw the negative charge of the reactant and the hydroxide coordinated with three explicit water molecules each, and the combination of the 6-311++G** basis set and the M06-2X functional proved to be ideal. By all means, all the structures were optimized in water.

The optimized parameters for the basis set were employed for the study of a reaction reported in this work: the cleavage of 2-phenylacetaldehyde. This substrate was selected since the cleavage reaction was originally discovered on this specific molecule, and because the aldehyde of interest is structurally close to 2,6 dichlorobenzaldehyde.

The coordination water for hydroxide ions, as well as the intermediate anions, were taken into account to fit the data because, although water was not explicitly added to the reaction, solid KOH contains up to 15 % of water in weight. We could estimate the presence of almost 4.7 equivalents of H_2O since KOH was used in 10-fold excess in this transformation.

The two plausible pathways are shown in Scheme 2.12. They involve the formation of the dioxyanion in pathway A and the direct fragmentation of the monooxyanion in pathway B.

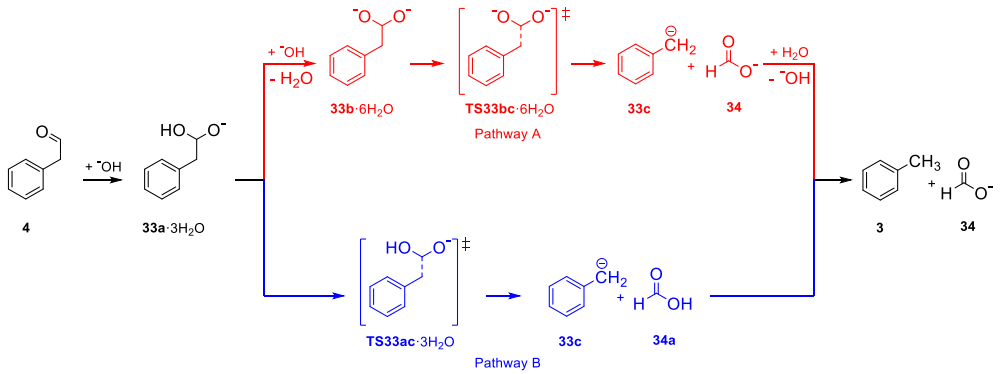

Scheme 2.12: Two possible pathways for cleavage of 2-phenylacetaldehyde

For both mechanisms, the energetic pathways were calculated. It showed that pathway B is more favorable than pathway A by almost 100 kJ·mol^{-1}, starting from the common intermediate, the monooxianion **33a**·3H_2O.

Even though the barrier for the fragmentation step is lower for pathway A ($\Delta G^{\neq}$ (A) = 40.5 kJ·mol–1) than for pathway B ($\Delta G^{\neq}$ (B) = 117.1 kJ·mol^{-1}), the preceding deprotonation step led to a high lying dianion **33b**·6H_2O (ΔG(**33b**·6H_2O) – ΔG(**33a**·3H_2O) = 173.3 kJ·mol^{-1}) which rendered pathway A less favorable overall.

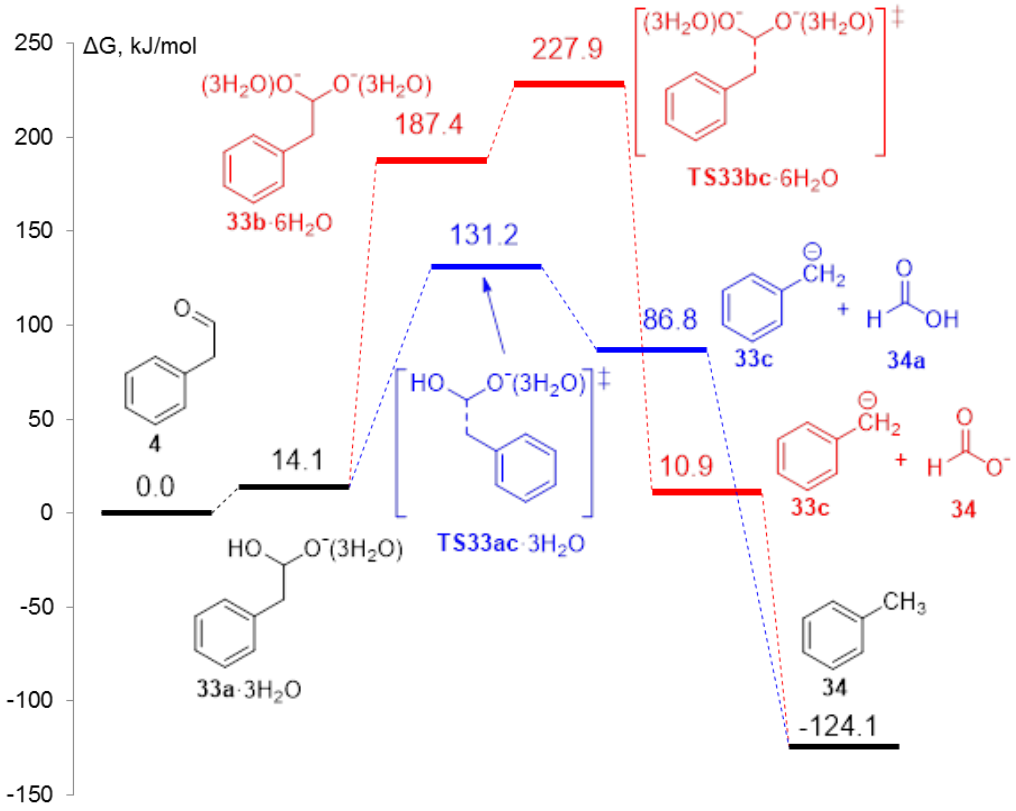

Figure 2.5: Energy diagram for the feasible reaction patway

Moreover, the transition states corresponding to the rate limiting steps are displayed in Figure 2.6. In this picture it is possible to note that the distance between the departing carbon belonging to the formate and the tolyl residue is much larger in the case of the **TS33ac** (2.614 Å), showing a late transition state, as compared to **TS33bc** in which the distance is only 2.086Å.

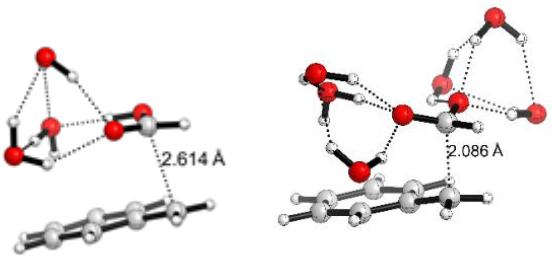

b) **TS33ac** a) **TS33bc**

Figure 2.6: Portrayal of putative transition states for a) monoanionic and b) dianionic mechanisms

The different mechanistic behavior of the two studied reactions can be ascribed to the solvent effect. Previously, the fragmentation of aldehydes and ketones were carried out in water as the solvent, and in these cases the dianionic intermediate was invoked,[1,31,32,34,46] including the one reported by Bunnett and coworkers.[47]

On the other hand, the use of an aromatic solvent as *p*-xylene determined a poor solvation of the ionic species. As a result the dioxyanion formation became more unfavorable and led to the fragmentation through the monooxy anion mechanism.

2.2.8 Final remarks about the mechanism

The DFT calculations outlined a monooxy anion pathway as the preferred route for the cleavage of the 2-phenylacetaldehyde. The fact that the reaction did not proceed using alckoxide ions was considered a clue in favor of a dianionic pathway. However, the calculation supported the hypothesis that the formation of oxyanionic species in organic solvent needed the solvation of protic species, such as hydroxide or water. This effect is responsible for the stabilization of the charged species and the consequent conversion of the substrate. In addition, Hammett studies were consistent with the defined mechanism. In fact, the high reaction constant (ϱ = 6.7),

characteristic of a full charge developed in the benzylic position in the rate-determining step, suggested a very late transition state, where the departing group is very distant from the rest of the molecule. The calculated structure marked a C-C distance of 2.614 Å for the examined case, corresponding to almost no interaction between the groups, and a product-like transition state. Compared to that, the dioxo-anionic path involved a transition state in which the two carbon groups are much closer (distance 2.06 Å).

2.2.9 Conclusions

In conclusion, the substrate scope of the potassium hydroxide-mediated carbon-carbon cleavage reaction was extended to various benzyl carbonyl compounds. Acyclic compounds afforded the alkane shortened by one carbon, while the cyclic substrates afforded interesting ω-mono and disubstituted long chain carboxylic acids. Moreover, the mechanism for the reaction was investigated with both experimental and theoretical methods. By using *p*-xylene as solvent, it was found that the reaction proceeded through a monooxy-anion intermediate, in contrast to the expectations and the previous reports in the literature for the scission of poorly stabilized aldehydes and ketones in aqueous media. The results showed that DFT calculations can be employed to distinguish between the two reaction pathways. Finally the good agreement between experiment and theory opens up for the possibility of in-silico substrate screening.

2.3 EXPERIMENTAL SECTION

2.3.1 General informations

All solvents were of HPLC grade and were not further purified and all chemicals were purchased from Sigma Aldrich. Column chromatography separations were performed on silica gel (220 - 440 mesh). Thin layer chromatography (TLC) was performed on aluminum sheets precoated with silica gel (Merck 25, 20 × 20 cm, C-60 F254). The plates were visualized under UV-light. Reactions were monitored by gas chromatography on a Shimadzu GC-MS-QP2012S instrument equipped with an Equity-5, 30mm × 0.25mm × 0.25μm column. Nonane was used as the internal standard and GC yields were determined with the following equations:

$$y(\%) = k_X \cdot \frac{A_X}{A_0} \cdot \frac{m_X}{MW_0} \cdot \frac{MW_s}{m_s} \cdot 100$$

$$\frac{n_X}{n_0} = k_X \cdot \frac{A_X}{A_0}$$

Where A_X = product peak's area, A_0 = standard peak's area, m_0 = mass (mg) of the internal standard in the reaction mixture, MW_0 = molecular weight of the internal standard, m_s = mass (mg) of the initial substrate, MWs = molecular weight of the initial substrate, k = value extrapolated from the product's calibration curve determined plotting n_X/n_0 as function of A_X/A_0 where n_X and n_0 are number of moles of compound X and standard.

NMR spectra were recorded on a Bruker Ascend 400 spectrometer. Chemical shifts were measured relative to the signals of residual $CHCl_3$ (δ_H = 7.26 ppm) and $CDCl_3$ (δ_c = 77.16 ppm). Multiplicity are reported as s = singlet, d = doublet, t = triplet, q = quartet, dd = double doublet, dt = double triplet, dq = double quartet, ddt = double double triplet, m = multiplet, br. s = broad singlet, while coupling constants are shown in Hz. HRMS measurements were made using ESI with TOF detection.

Phenylacetones,[59] 2-phenylcyclopentanone[60] and 2-phenylcyclohexanone[61] were prepared according to literature procedures.

2.3.2 Characterization of the starting materials

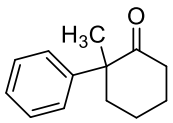

2-Methyl-2-phenylcyclohexanone (**11**):[62] Following a literature procedure[62] 2-phenylcyclohexanone (1.0 g, 5.74 mmol) in *tert*-butanol (10 mL) was treated with potassium *tert*-butoxide (673 mg, 6.00 mmol) for 45 min followed by addition of methyl iodide (0.7 mL, 11.2 mmol). The mixture was stirred at room temperature for 2.5 h and worked up by addition of water and extraction with EtOAc. Purification by flash chromatography (heptane/EtOAc 95/5) gave 950 mg (88%) of the product as a colorless oil. ^{1}H NMR (400 MHz, $CDCl_3$) δ 7.35 (t, J = 7.6 Hz, 2H), 7.24 (t, J = 7.4 Hz, 1H), 7.20–7.18 (m, 2H), 2.71–2.68 (m, 1H), 2.45–2.25 (m, 2H), 1.76–1.65 (m, 4H), 2.02–1.92 (m, 1H), 1.27 (s, 3H). ^{13}C NMR (100 MHz, $CDCl_3$) δ 214.3, 143.4, 129.1, 126.7, 126.2, 54.5, 40.1, 38.3, 28.6, 28.6, 22.0.

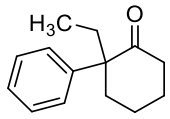

2-Ethyl-2-phenylcyclohexanone (**13**):[63] Prepared in 81% yield (940 mg) as a colorless oil from 2-phenylcyclohexanone and ethyl iodide as described above for 2-methyl-2-phenylcyclohexanone. ^{1}H NMR (400 MHz, $CDCl_3$) δ 7.34 (t, J = 7.6 Hz, 2H), 7.23 (t, J = 7.3 Hz, 1H), 7.15 (d, J = 7.3 Hz, 2H), 2.74–2.70 (m, 1H), 2.40–2.10 (m, 2H), 1.94 (ddd, J = 2.9, 5.9, 12.0 Hz, 1H), 1.88–1.59 (m, 6H), 0.61 (t, J = 7.5 Hz, 3H). ^{13}C NMR

(100 MHz, $CDCl_3$) δ 214.1, 140.9, 128.8, 127.2, 126.7, 57.7, 40.4, 34.5, 32.6, 28.5, 21.8, 8.2.

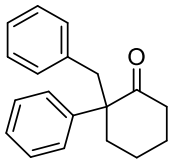

2-Benzyl-2-phenylcyclohexanone (**15**):[64] Prepared in 90% yield (1.4 g) as a white solid from 2-phenylcyclohexanone and benzyl bromide as described above for 2-methyl-2-phenylcyclohexanone. ^{1}H NMR (400 MHz, $CDCl_3$) δ 7.32–7.21 (m, 3H), 7.13–7.02 (m, 3H), 6.96–6.94 (m, 2H), 6.57–6.54 (m, 2H), 3.12 (d, J = 13.5 Hz, 1H), 2.98 (d, J = 13.5 Hz, 1H), 2.48–2.46 (m, 1H), 2.36–2.33 (m, 2H), 1.96–1.92 (m, 1H), 1.74–1.64 (m, 4H). ^{13}C NMR (100 MHz, $CDCl_3$) δ 213.4, 140.0, 137.4, 130.9, 128.8, 127.5, 127.4, 126.9, 126.1, 58.1, 46.4, 40.3, 34.8, 28.4, 21.5.

2.3.3 General procedure for cleavage of ketones

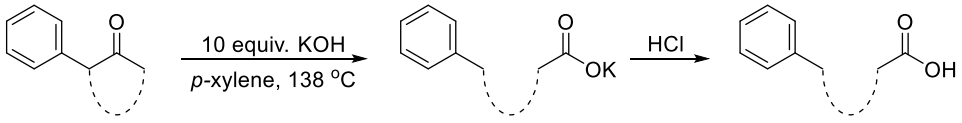

A suspension of KOH (1.4 g, 25 mmol) in *p*-xylene (50 mL) was heated to reflux followed by dropwise addition of a solution of the ketone (2.5 mmol) in *p*-xylene (1 mL) over 10 min (for reactions where the GC yield was determined 150 mg of nonane was also added as an internal standard). The reaction was stirred at reflux for an additional 1 h. The mixture was cooled to room temperature and extracted with water (3 x 50 mL). The combined aqueous phases were carefully acidified with 6 M hydrochloric acid to pH 2 and then extracted with ethyl acetate (3 x 60 mL). The combined organic layers were washed with brine, dried over Na_2SO_4 and

concentrated in vacuo. The residue was purified by flash column chromatography (pentane/ethyl acetate 95/5 → 80/20) to afford the carboxylic acid.

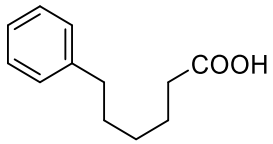

6-Phenylhexanoic acid (**10**):[65] Isolated as a colorless oil in 78% yield (374 mg). ^{1}H NMR (400 MHz, $CDCl_3$) δ 11.04 (bs, 1H), 7.26–7.30 (m, 2H), 7.16–7.20 (m, 3H), 2.62 (t, *J* = 7.7 Hz, 2H), 2.36 (t, *J* = 7.5 Hz, 2H), 1.61–1.72 (m, 4H), 1.36–1.44 (m, 2H). ^{13}C NMR (100 MHz, $CDCl_3$) δ 179.8, 142.6, 128.5, 128.4, 125.8, 35.8, 34.0, 31.2, 28.8, 24.7.

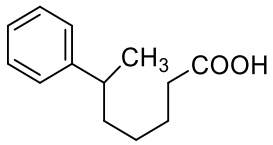

6-Phenylheptanoic acid (**12**):[66] Isolated as a colorless oil in 40% yield (206 mg). ^{1}H NMR (400 MHz, $CDCl_3$) δ 11.57 (bs, 1H), 7.52 (t, *J* = 7.5 Hz, 2H), 7.27–7.24 (m, 3H), 2.79–2.74 (m, 1H), 2.38 (t, *J* = 7.6 Hz, 2H), 1.75–1.63 (m, 4H), 1.38–1.19 (m, 5H). ^{13}C NMR (100 MHz, $CDCl_3$) δ 180.5, 147.6, 128.5, 127.1, 126.0, 39.9, 38.1, 34.1, 27.3, 24.8, 22.5.

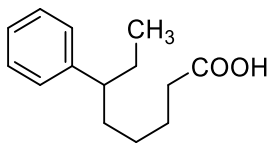

6-Phenyloctanoic acid (**14**): Isolated as a colorless oil in 65% yield (374 mg). ^{1}H NMR (400 MHz, $CDCl_3$) δ 10.66 (bs, 1H), 7.27 (t, *J* = 7.6 Hz, 2H), 7.18 (t, *J* = 7.5 Hz, 1H), 7.13 (d, *J* = 7.5 Hz, 2H), 2.44–2.36 (m, 1H), 2.30–2.26 (m, 2H), 1.72–1.42 (m, 6H), 1.29–1.13 (m, 2H), 0.76 (t, *J* = 7.4 Hz, 3H). ^{13}C NMR (100 MHz, $CDCl_3$) δ 180.2,

145.7, 128.4, 127.8, 126.0, 47.8, 36.2, 34.1, 29.9, 27.2, 24.9, 12.3. HRMS: m/z calcd for $C_{14}H_{20}O_2Na$ 243.1356 $[M + Na]^+$, found 243.1348.

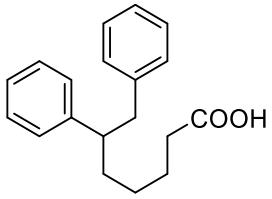

6,7-Diphenylheptanoic acid (**16**): Isolated as a yellowish solid in 76% yield (534 mg). Mp: 77 – 80 °C (ethanol). ^{1}H NMR (400 MHz, $CDCl_3$) δ 10.94 (bs, 1H), 7.28–7.21 (m, 2H), 7.21–7.12 (m, 4H), 7.10 (d, *J* = 6.9 Hz, 2H), 7.01 (d, *J* = 7.0 Hz, 2H), 2.89–2.87 (m, 2H), 2.84–2.77 (m, 1H), 2.26–2.21 (m, 2H), 1.74–1.46 (m, 4H), 1.22–1.15 (m, 2H). ^{13}C NMR (100 MHz, $CDCl_3$) δ 180.3, 145.0, 140.7, 129.3, 128.4, 128.2, 127.8, 126.2, 125.9, 48.0, 44.0, 35.2, 33.9, 27.1, 24.8. HRMS: m/z calcd for $C_{19}H_{22}O_2Na$ 305.1512 $[M + Na]^+$, found 305.1512.

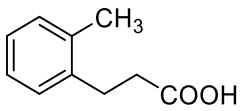

3-(*o*-Tolyl)propanoic acid (**18**):[67] Isolated as a colorless oil in 18% yield (74 mg). ^{1}H NMR (400 MHz, $CDCl_3$) δ 7.18–7.12 (m, 4H), 2.98–2.94 (m, 2H), 2.67–2.63 (m, 2H), 2.33 (s, 3H). ^{13}C NMR (100 MHz, $CDCl_3$) δ 178.8, 138.3, 136.1, 130.5, 128.5, 126.6, 126.3, 34.4, 28.1, 19.4.

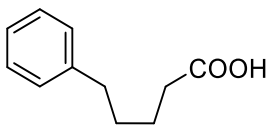

5-Phenylpentanoic acid (**20**):[65] Isolated as a colorless oil in 64% yield (285 mg). ^{1}H NMR (400 MHz, $CDCl_3$) δ 11.8 (bs, 1H), 7.30–7.26 (m, 2H), 7.20–7.17 (m, 3H), 2.66–

2.62 (m, 2H), 2.40–2.36 (m, 2H), 1.70–1.67 (m, 4H). ^{13}C NMR (100 MHz, $CDCl_3$) δ 179.5, 142.1, 128.5, 128.5, 126.0, 35.7, 33.9, 30.9, 24.4.

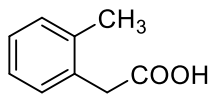

2-(*o*-Tolyl)acetic acid (**22**):[68] Isolated as a white solid in 90% yield (338 mg). ^{1}H NMR (400 MHz, $CDCl_3$) δ 7.21–7.17 (m, 4H), 3.67 (s, 3H), 2.33 (s, 2H). ^{13}C NMR (100 MHz, $CDCl_3$) δ 177.3, 137.0, 132.0, 130.4, 130.3, 127.7, 126.2, 38.8, 19.6.

2.3.4 Computational details.

All calculations were performed in Jaguar (Jaguar, version 9.0; Schrodinger, Inc.: New York, NY, 2015.) by using the Maestro graphical interface.[69] All the structures were optimized in the gas phase and the single-point solvation energy was calculated for the optimized structures by using a standard Poisson–Boltzmann solver with suitable parameters for water or xylene as the solvent. Default dielectric constant and probe radius were used for solvation with water while for xylene the following parameters were employed: dielectric constant ε = 2.2, probe radius r = 2.9 Å. Gibbs free energies were obtained from the vibrational-frequency calculations for the gas-phase geometries at 298 K and 311 K or 411 K. All the transition states were characterized by the presence of one negative vibrational frequency. Graphical representation of the calculated structures was made in CYLview.(Legault, C. Y.CYLview, version 1.0b; Université de Sherbrooke, 2009.)

2.3.5 Experimental procedure for determening hydroxide dependence on reaction rate

A suspension of KOH in xylene (49 mL) was heated to reflux followed by quick addition of an accurately measured solution (1 mL) of phenylacetone (335 mg, 2.5 mmol) and nonane (150 mg, internal standard) in xylene. The reaction was stirred at reflux and samples were collected over one hour. The samples were cooled to room temperature, diluted with dichloromethane and filtered through a syringe filter. GC yields were determined by comparison between the signal of nonane and the signal of toluene.

2.3.6 Experimental procedure for Hammett studies

A suspension of KOH (1.4 g, 25 mmol) in xylene (49 mL) was heated to reflux followed by quick addition of a solution (1 mL) of phenylacetone (1.25 mmol), the 4-substitued phenylacetone (1.25 mmol) and nonane (75 mg, internal standard) in xylene. The reaction was stirred at reflux and samples were collected over two hours. The samples were cooled to room temperature, diluted with dichloromethane and filtered through a syringe filter. GC yields were determined by comparison between the signal of toluene, the 4-substitued toluene and nonane.

3 RUTHENIUM-MEDIATED DEHYDROGENATIVE DECARBONYLATION OF PRIMARY ALCOHOLS

3.1 BACKGROUND

3.1.1 Transition metal catalysis in organic transformations

Organic chemistry is the chemistry of carbon based compounds, in which carbon atoms can bind most frequently other carbon atoms and hydrogen, but also a variety of metals and nonmetal elements, with different electronegativity and features. Hence a wide versatility of carbon atoms bonded with heteroelements arises.

In particular, organometallic compounds are a valid tool to promote organic chemistry reactions. The work of François Auguste Victor Grignard on organomagnesium halides carried out in 1900 is one of the earliest examples. He discovered that these compounds can add to ketones yielding tertiary alcohols. Hereafter, organomagnesium halides were called Grignard reagents and the whole process a Grignard reaction. The enormous impact of his discoveries was recognized with a Nobel prize in 1912. After that moment, various organometallic compounds

were exploited, such as organolithium compounds in 1930 and lithium diorganocuprates, better known as Gilman reagents, in 1952.[70]

Transition metals incredibly widened the landscape of organic chemistry due to the new reactivity of the energy accessible *d*-orbitals. *d*-Block metals found a larger employment as catalysts rather than stoichiometric reagents. For this reason, they represent a great improvement in the field and brought to life the concept of green chemistry.[71]

One of the first chemical processes employing a metal catalyst in an homogeneous solution was in fact the hydroformylation reaction introduced by Otto Roelen in 1938.[72] In this transformation, an alkene is converted into an aldehyde in the presence of a mixture of hydrogen, carbon monoxide and a cobalt catalyst. However, the importance of *d*-block metals in catalysis became more relevant only during the 60's and the 70's.

In 1965, Nobel laureate Sir Geoffrey Wilkinson introduced chloridotris(triphenylphosphane)rhodium(I) for the hydrogenation of alkenes.[73] This 16-e$^-$ planar complex pre-dissociates into a 14-e$^-$ catalyst releasing a phosphine ligand (Scheme 3.1) and allowing the binding of a molecule of hydrogen. Wilkinson catalyst was one of the first phosphine metal complexes and it pushed forward the understanding of metal catalysis, metal complexes structure and it helped to develop ^{31}P-NMR techniques.

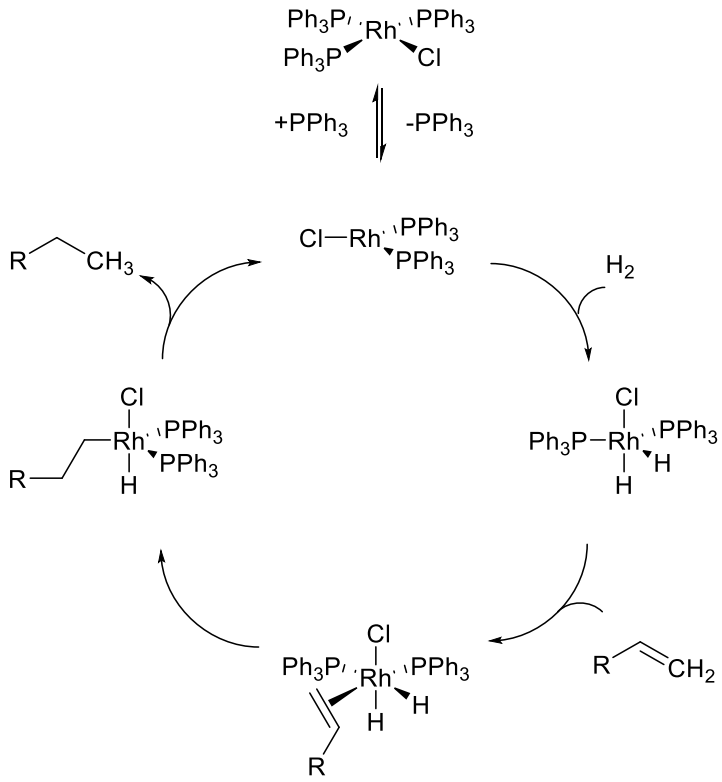

Scheme 3.1: Catalytic cycle of the olefin hydrogenation by using Wilkinson's catalyst.

Another milestone in transition metal catalyzed transformations is olefin metathesis. Initially, this transformation was casually discovered when it was found that propene led to ethylene and 2-butenes after being heated over a molybdenum catalyst.[74] At the beginning of the 70's, Yves Chauvin advanced the first rationalization about its mechanism involving metallocycles.[75] However, it was the long and extensive work of Robert H. Grubbs and Richard R. Schrock on the development of efficient catalysts that led to the process that we know.[76] These efforts eventually culminated with the recognition of the Nobel Prize for the three chemists in 2005.

Another fundamental family of metal catalyzed processes is represented by the cross coupling reaction. In this type of transformation main group organometals are reacted with an electrophilic partner and a transition metal catalyst, most prominently palladium, which binds the single components on its center and promote the formation of a new carbon-carbon single bond.[77] Palladium-catalyzed cross coupling reactions have been mostly disclosed thanks to the contribution of Richard F. Heck, Ei-ichi Negishi, and Akira Suzuki awarded with Nobel prize after more than 30 years from their initial research discoveries.

Undeniably the possibility to make important industrial processes feasible thanks to transition metal catalysis was a great discovery and many research groups, resources and efforts were involved in this field. The reactivity of transition metals is very diverse, despite that some general features are recurring and we will explore them in the next paragraph.

3.1.2 Structure and properties of transition metal coordination complexes

Coordination complexes are compounds constituted by a metal core in its oxidation state which act as Lewis acids binding Lewis bases called ligands. Even though this model suggests an ionic nature of the metal-ligand bond, it is more often presented with a high degree of covalent character, sometimes even very nonpolar, or it can happen that the metal is the negative pole of the molecule. The number of atoms directly bound to the metal is the coordination number and their disposition is the geometry of the complex.[78,79]

3.1.2.1 Ligand-metal interaction

Different formalisms can be found to describe the bond between a metal and a ligand. In particular, ligands can be classified in two groups according to their nature. A neutral ligand, which shares a lone pair in order to obtain a metal-ligand σ bond, takes the name of *dative ligand* or type *L* ligand or even *neutral ligand*. Contrarily, if a ligand in its neutral form contributes with a single electron or it has to bear a negative charge in order to share a lone pair, it is defined as a *covalent ligand* or type *X* ligand or *charged ligand*. Sometimes ligands are a combination of the first and the second type classification, which can happen when more than one atom binds to the metal.

A further classification arises when we are talking about ligands coordinating to the metal with multiple atoms. Specifically if these atoms are contiguous we have a polyhapto ligand and we refer to it with the Greek letter η (eta) followed by the number of atoms bound to the metal. Different from hapticity is denticity or chelation, defined as the aptness of a molecule to bind the metal with two or more non-contiguous atoms. Ligands bearing this characteristic are identified with a composed name containing the Greek prefix indicating the number of coordinating atoms with the suffix *–dentate* (e.g. bidentate, tridentate, tetradentate,…) or with the Greek character ϰ (kappa) followed by the same number. A latter case involves specific ligands that can bridge to metal cores through the formation of chemical bonds. This type of ligands is designated with the letter μ (mu).

3.1.2.2 Electron count

The behavior of metal complexes depends also on the number of electrons in the valence shell. A metal has 9 valence orbitals: 5 (n)*d*-orbitals, three (n+1)*p*-orbitals and one (n+1)*s*-orbital. Hence, it may contain at most 18 electrons according to the so called 18 electron rule. Complexes having a closed shell are particularly stable, but also 16 e^- complexes are rather common.

It is possible to calculate the overall number of valence shell electrons easily through the formula:

Total valence electrons = *metal group + no. of anionic ligands +2 no. of dative ligands - total charge on the complex*

Besides estimating the stability and estimating the electronic properties, the electron count is a tool for predicting the geometry of transition metal complexes.

3.1.2.3 Geometries

Transition metals complexes can arrange in different geometries as shown in Figure 3.1. In analogy to main group elements, the disposition of the substituent depends in most of the cases on steric effects. In fact metal substituents arrange in order to minimize steric interactions. However electronic effects often override this behavior. In this case, a potent tool to explain and predict the structure of a complex is the *crystal field theory*.

As illustrated in Figure 3.1, the five valence *d*-orbitals loose degeneration due to the effect of the charges that surround the metal. The array of surrounding ligands affects the energy level of the existing *d*-orbitals.

Therefore the most favorable geometry is the one that allows the electrons to minimize the energy according to these diagrams. For example, four coordinate complexes according to steric argument should arrange in a tetrahedral fashion. However it is well established that d^8 complexes of second and third-row metals very frequently show a square planar geometry. This is because these eight electrons have much higher gain in terms of energy. In complexes of the first row metals this difference in energy is not very important and therefore steric factors can take over.

Besides the metal nature, also the charge and the nature of ligand influence the splitting diagram.

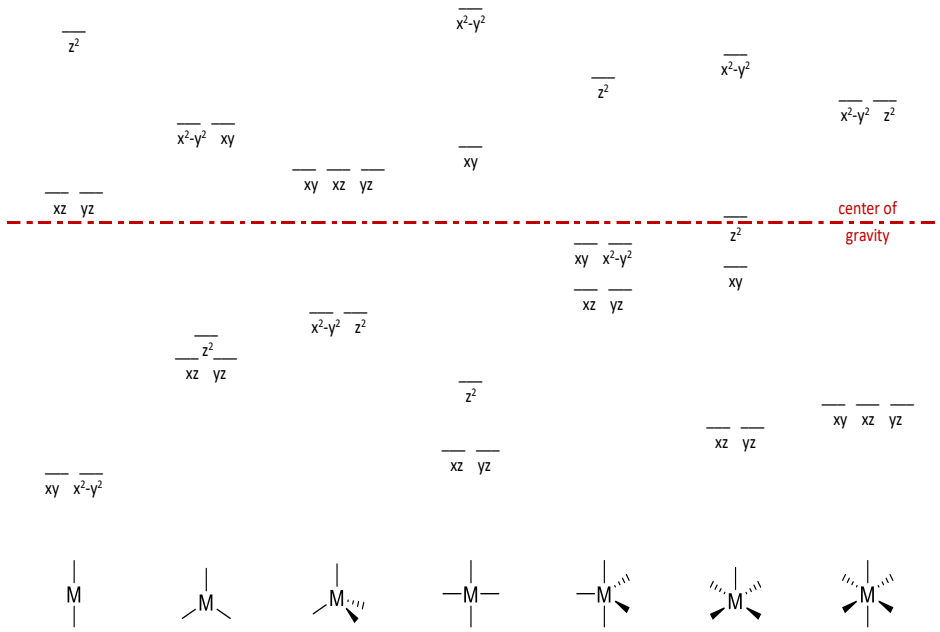

Figure 3.1: Orbital energies of different metal complexes

3.1.3 Transition metal complexes in organic transformations

The power of coordination complexes is the possibility to undergo or catalyze a variety of reactions precluded to main group elements. These transformations were unexplored since the '60s but, in the recent years, organic chemists learned how to master these processes. The following part will explain the basic reactions which a complex can undergo. [78,79]

a) *Ligand exchange*

A ligand exchange reaction is the replacement of a coordinated ligand with a free ligand. The substitution can occur with two mechanisms: dissociative, typical of octahedral complexes and for complexes with 18 electrons, and associative, typical of square planar complexes with 16 or 17 electrons. These mechanisms show analogy with the S_N1 and S_N2 mechanisms, respectively, for what it concerns order of reactivity, electronic effect and steric effect on both the nucleophile and the metal.

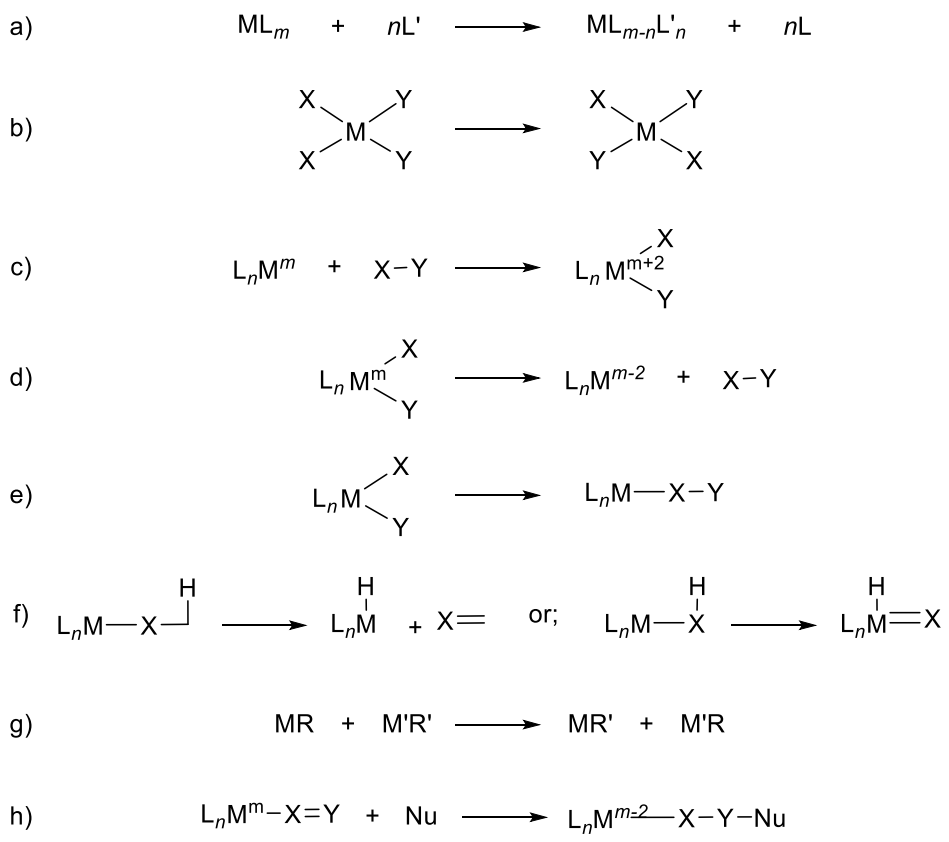

Scheme 3.2: Feasible reactions for transition metals *M* in organic chemistry transformations

b) Cis-trans isomerization

As we have already seen, metal complexes with mixed ligands can have different stereochemistry according to the arrangement of the ligands on the metal core. The ligand can also migrate from one coordination site to another. This could occur through different mechanisms: dissociative, associative and twist. The first two can be considered inner substitutions and follow the same path as for ligand exchange. In fact, an associative mechanism occurs when a certain ligand binds the metal, followed by the release of a ligand of the same type, causing an apparent migration of the ligand. On the other hand, a dissociative mechanism takes place when a ligand, already present on the metal, leaves the complex only for being attached in a different position, forming a geometrical isomeric complex. Complexes can also scramble ligands and the mechanism depends on the nature of these ligands (twist). [80]

c) Oxidative addition

Oxidative addition reaction occurs when a metal with generally low oxidation state cleaves a bond in a non-metal reagent. The formal oxidation state of the metal increases by two by this process and the metal center gains two additional ligands consisting of the two fragments of the reagent. The reaction can be concerted and in this case, the addition occurs with *cis* selectivity, or it can be stepwise, without specified stereochemistry of the addition.

d) Reductive elimination

Reductive elimination is the reverse of the oxidative addition. Two groups bound to the metal are coupled together and, as a consequence, the metal oxidation number is formally reduced by two. Electron poor complexes, with bulky substituents and few ligands, generally react faster. The elimination of two groups placed *cis* to each other

is more common. Nevertheless also *trans* substituents can eliminate with a stepwise mechanism.

e) Migratory insertion

Migratory insertion is a reaction in which one group bound to a metal atom is transferred to an adjacent unsaturated group like CO, olefins or carbenes generating a new bond. The vacant site is now generally replaced by another ligand.

f) Elimination

Elimination or de-insertion is the reverse of insertion and it occurs when a substituent, most commonly hydrogen, migrates from the ligand to the metal itself. We can find two types of elimination. When the migrating substituent sits on the atom directly attached to the metal core, it is called alpha elimination, otherwise, if it is attached to the neighboring atom, it is a beta elimination.

g) Transmetallation

Transmetallation is the reaction in which a group bound to a metal is transferred to a different metal core. This represents one of the basic steps of the cross coupling reaction. In fact the formation of organic complexes of transition metal catalysts rely on the ability of main group metals, but also of different transition metal compounds, to transfer an organic group to replace an anionic ligand on the metal complex.

b) Nucleophilic attack on coordinated ligand

Typically the metal core of a complex constitutes the electrophilic portion of the complex, thus it can pull electron density from its ligands. Unsaturated ligands such as olefins or carbonyls bound to some metals are then becoming very electrophilic and allowing to accept the attack of a nucleophile. After the process the new group stays attached to the metal decreasing the oxidation state of the metal by two.

3.1.4 Dehydrogenation of alcohols

The oxidation of an alcohol has always been achieved *via* strong stoichiometric oxidants such as chromium-based reagents, hypervalent iodine, activated DMSO, just to cite few. However in more recent years the use of transition metal catalysts has allowed to use weaker hydrogen acceptors like carbonyl compounds, imines, olefins, alkynes or O_2, or even liberating molecular hydrogen from the molecule in the so-called acceptorless dehydrogenations (AD).

The first work that explored the activity of metals, in this case aluminum, in catalyzing an hydrogen transfer from a substrate to an acceptor is the Oppenauer reaction (Scheme 3.3).[81]

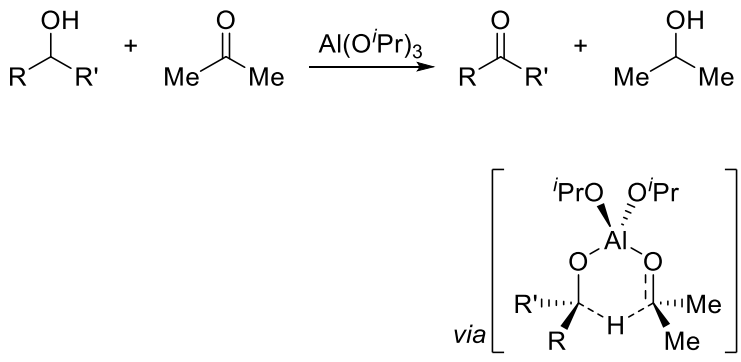

Scheme 3.3: Oppenauer reaction by mutual oxidation-reduction of alcohols and ketones

In this transformation, a secondary alcohol is oxidized to a ketone in the presence of a sacrificial ketone, often acetone, which is the acceptor of the hydrogen molecule by action of $Al(O^iPr)_3$.

In contrast to this approach the acceptorless dehydrogenation asserted itself. These methods turned the drawback of using a stoichiometric oxidant, the production of large quantities of often toxic chemical waste, into the opportunity to have a valuable byproduct such as hydrogen.

Earliest examples of dehydrogenations were carried out on secondary alcohols, and employed ruthenium and rhodium in the presence of an acid able to combine a proton with the hydride ion.[82–85] The reaction was later improved by Milstein by using PNP-pincer ligands which allowed to decrease the loading of the ruthenium catalyst[86] and the use of neutral conditions (Scheme 3.4).[87]

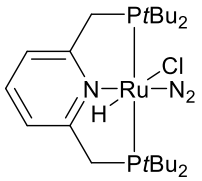

Scheme 3.4: Milstein pincer complex for dehydrogenation of alcohols. [87]

In recent years, iridium[88,89] showed a similar activity to ruthenium and some other cheaper metals, such as cobalt[90] and iron[91] have emerged. Dehydrogenation of primary alcohols are often precluded due to the insertion reaction of the ruthenium complexes to form ruthenium carbonyl species that deactivate the catalyst. Yamaguchi reported that the use of phenyl pyridone as ligand for an iridium complex

avoided this problem with consequent formation of aldehydes from primary alcohols (Scheme 3.5) as well as ketones from secondary alcohols.[91]

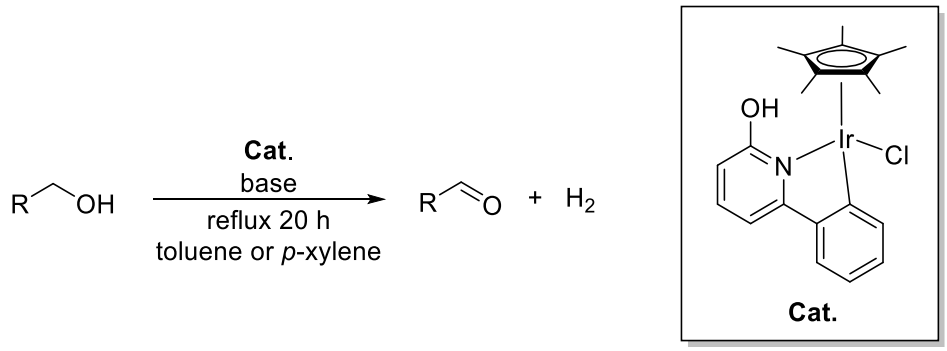

Scheme 3.5: Yamauchi dehydrogenation of primary alcohols.[91]

The AD methodology is a class of reactions rather than one single process. In fact, it includes all the chemical reactions that allow a primary alcohol to be converted to different functionalities with an overall oxidation of the molecule and loss of dihydrogen. Our research group was particularly active in this field by developing the complex $RuCl_2(I^iPr)(p\text{-cymene})$ that was employed as catalyst for the formation of esters, amides, imines and carboxylic acids starting from alcohols.[55,92–95] Various pincer ligands were also employed for the synthesis of esters and amides.[96]

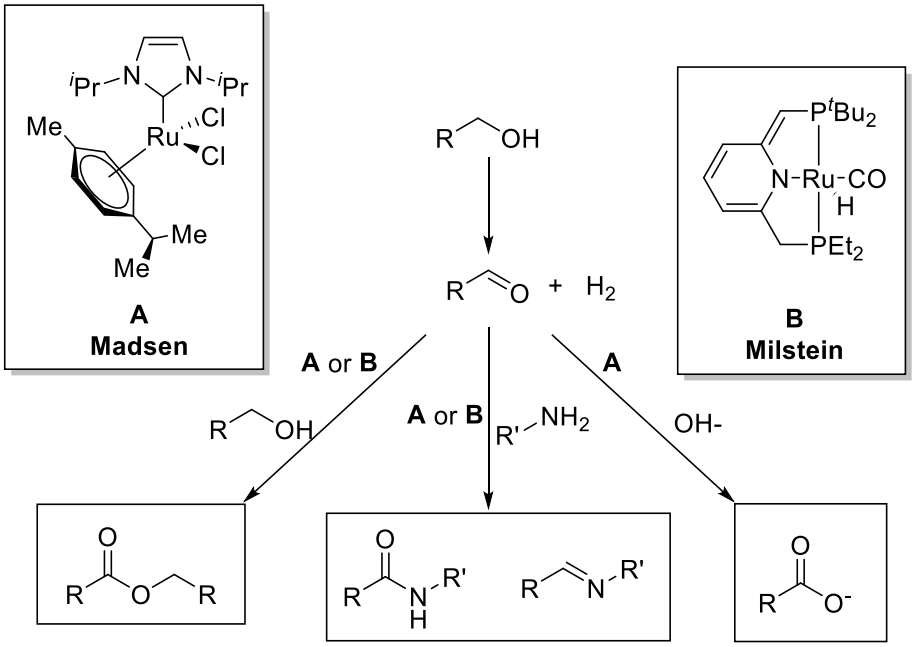

Scheme 3.6: Madsen and Milstein catalysts for the oxidative heterocoupling of primary alcohols.[55,92–96]

Generally the mechanism for the dehydrogenation with late transition metals involves the formation of a dihydride species which, through reductive elimination, releases a dihydrogen molecule (Scheme 3.7 a). Particularly, the ruthenium complexes have been investigated with DFT techniques.[97,98] Other mechanisms like monohydride formation, in which the hydrogen is taken from the alcohol with a base and then released to the hydride on the metal, can take place in some cases, especially with an outer sphere mechanism like the one using Shvo's catalyst (Scheme 3.7 b).[91]

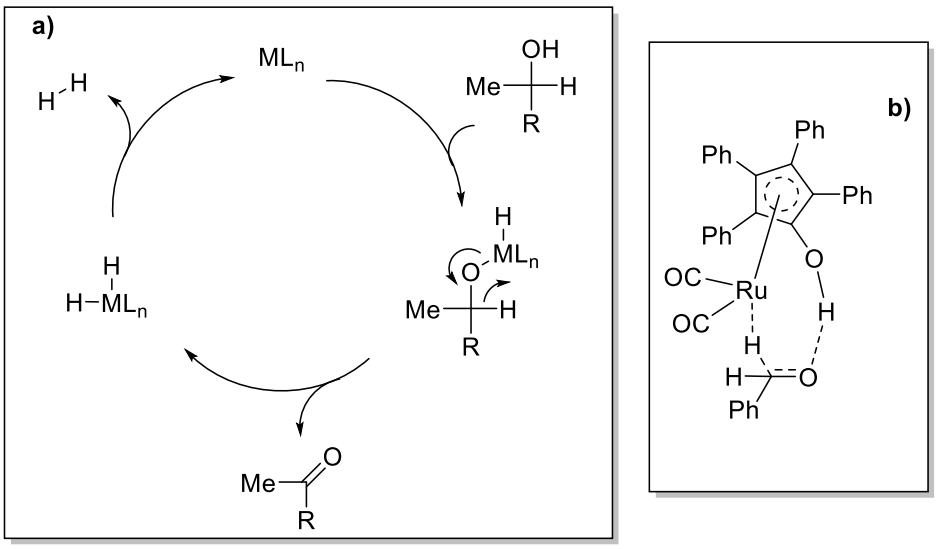

Scheme 3.7: Generally accepted key steps for the dehydrogenation of an alcohol a) through dihydride species b) with Shvo's catalyst in a ligand assisted mechanism

3.1.5 Decarbonylation of aldehydes

In the previous section we saw that it is common for late transition metals complexes to react with aldehydes, and this fact precluded in many cases the dehydrogenations on primary alcohols. These metals, in fact, can go through oxidative addition of aldehydes to afford acyl-hydrido complexes. Decarbonylative complexes are able to promote the de-insertion of CO, allowing the formation of a carbonylated species of the metal that is considered in many cases the driving force of the process.[99] Decarbonylation of aldehydes to obtain unsubstituted hydrocarbons can be achieved by stoichiometric metals like Wilkinson's catalyst $RhCl(PPh_3)_3$ that forms in solution the species $RhCOCl(PPh_3)_2$.[100] As a consequence of the high energy bond between CO and the metal center, desorption of carbon monoxide needs high energy to restore the catalyst and permit the catalytic cycle to occur, that in the earliest examples was obtained by using refluxing high boiling solvents. For instance, Wilkinson's

catalyst needs temperatures above 200 °C.[101] The first efficient catalytic decarbonylation of aldehydes with a transition metal was observed already in 1959 by using $Pd(OH)_2$ on $BaSO_4$ for the cleavage of myrtenal led by Eschinazi.[102] Complexation with polydentate phosphines like triphos[103] and dppp[104] increases the catalytic activity of rhodium. The mechanism involving the latter complex was investigated both experimentally and with computational methods by Fristrup and Madsen[105] suggesting CO extrusion as the rate limiting step (Figure 3.2).

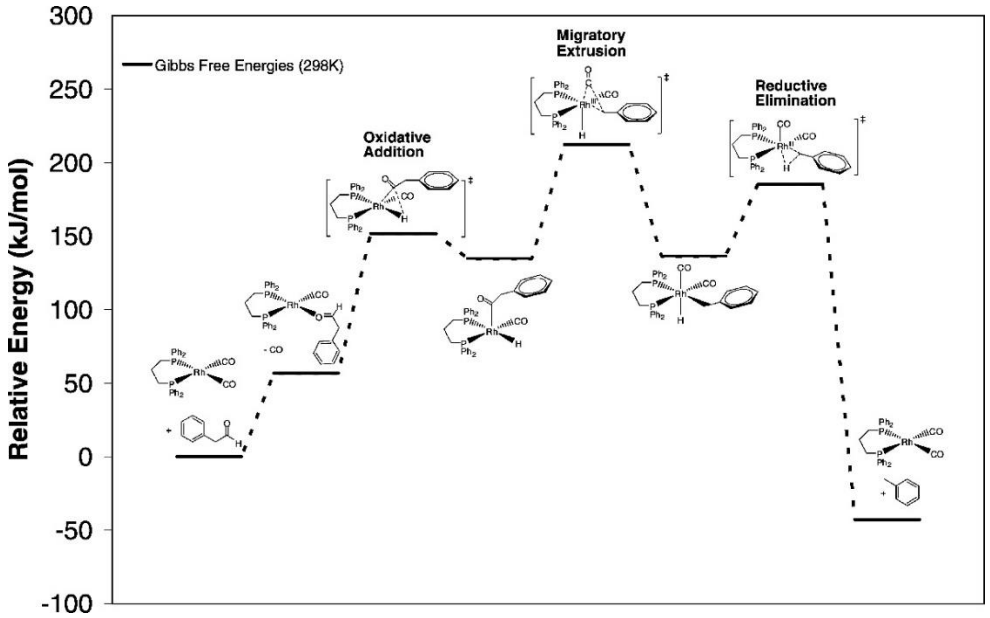

Figure 3.2: Energy profile for the decarbonylation of phenyl acetaldehyde[105]

Also Iridium is active towards decarbonylation of aldehydes, and in fact $[IrCl(cod)]_2$ in presence of PPh_3 proved to be an efficient system to promote the reaction of vinyl aldehydes and benzaldehyde substrates under mild conditions (Scheme 3.8).[106]

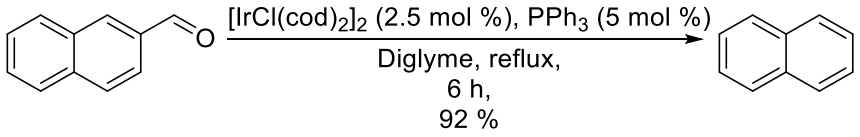

Scheme 3.8: Tsuji decarbonylation of naphtaldehyde

Porphyrin metal complexes with ruthenium[107] and iron[108] were employed to decarbonylate aromatic aldehydes at low temperatures (Scheme 3.9). In the first case, carbon monoxide dissociates by effect of visible radiation at room temperature. On the other hand, a purge of argon is needed and a radical pathway was proposed when iron is used.

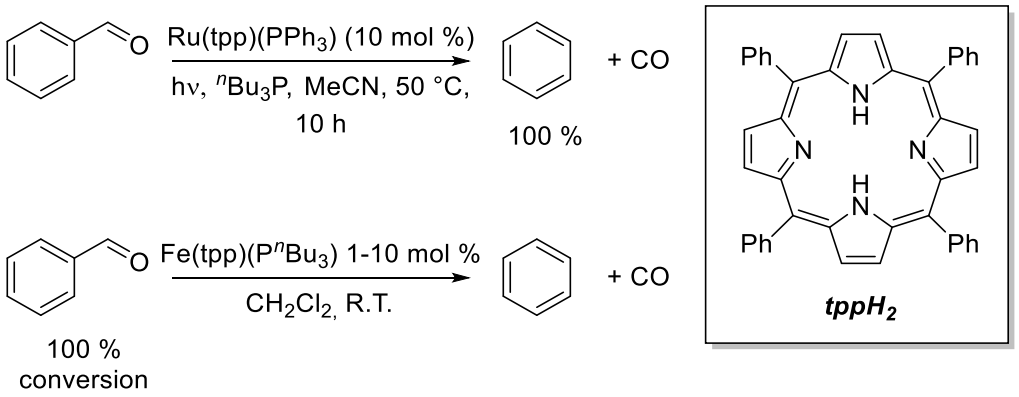

Scheme 3.9: Ruthenium and iron based decarbonylation of benzaldehyde

Evidences of aldehyde decarbonylation are found in the study of hydroacylation of olefins with aldehydes in presence of ruthenium carbonyl complex ($Ru_3(CO)_{12}$)(Scheme 3.10).[109]

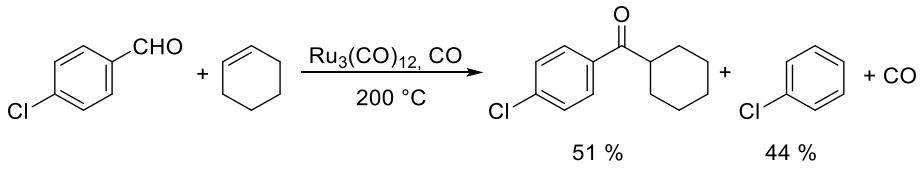

Scheme 3.10: Ruthenium mediated hydroacylation.

Allowing to react 4-chloro benzaldehyde with cyclohexene in carbon monoxide atmosphere, the expected ketone was formed in 51 % yield. As side product chlorobenzene was also observed in comparable amount. It was also noticed that when the atmosphere of carbon monoxide was replaced by nitrogen or argon, the yield in ketone dropped considerably. This fact was explained thanks to experiments with isotope labelled substrate on the carbonyl carbon. When ^{13}C labelled aldehydes reacted, the obtained ketone showed the incorporation of ^{12}C, pointing out a scrambling of this position with the atmospheric carbon monoxide and, illustrating that some of the steps in the decarbonylation of aldehydes are reversible.

Few years later, Green and coworkers attempted to convert cinnammaldehyde into 3-phenylpropionic acid using a homogenous ruthenium catalyst.[110] By applying known conditions for the conversion of crotonaldehyde to butyric acid to the cinnamaldehyde substrate they could observe the formation of styrene as the major product, together with side products from polymerization.[111]

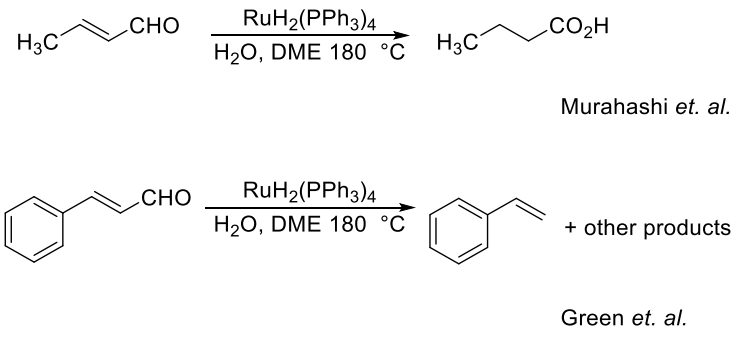

Scheme 3.11: Reaction of aldehydes with $RuH_2(PPh_3)_4$.[110,111]

These reactions proved that ruthenium can be a decarbonylative catalyst, albeit with a still limited scope.

3.1.6 Reaction of dehydrogenative decarbonylation of primary alcohols

Dehydrogenative decarbonylation of alcohols is based on two individual processes: the acceptorless dehydrogenation of an alcohol and the decarbonylation of the resulting aldehyde. In this transformation, valuable products are formed, such as the unfunctionalized organic residue and two gases, hydrogen and carbon monoxide. The starting material is a primary alcohol, a cheap and readily available feedstock. Moreover, the released gases constitute the so-called synthesis gas or SynGas. Despite its appeal, this reaction is still much underinvestigated because of some inherent difficulties in the process.

With respect to the thermodynamics of the reaction, it can be immediately noticed that dehydrogenations, as well as decarbonylations, are *endothermic* reactions (Scheme 3.12).[112]

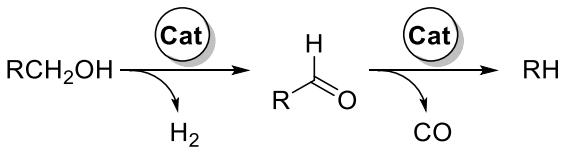

	dehydrogenation	decarbonylation	total
R = H	ΔH_{rxn} = 354 kJmol^{-1}	ΔH_{rxn} = -227 kJmol^{-1}	ΔH_{rxn} = 128 kJmol^{-1}
R = Me	ΔH_{rxn} = 81 kJmol^{-1}	ΔH_{rxn} = 11 kJmol^{-1}	ΔH_{rxn} = 92 kJmol^{-1}
R = Ph	ΔH_{rxn} = 68 kJmol^{-1}	ΔH_{rxn} = 25 kJmol^{-1}	ΔH_{rxn} = 93 kJmol^{-1}

Scheme 3.12: Energies for dehydrogenation of alcohols and decarbonylation of aldehydes

Entropy factors, like the formation of gas molecules, can drive the reaction to the product formation in the absence of stoichiometric hydrogen or CO acceptors that can promote the reaction. Moreover, transition metals show high affinity for carbon monoxide, as seen in the previous section, which can poison the catalyst, thus blocking the catalytic cycle. The ideal catalyst for this transformation should be able to promote the two independent reactions under the same reaction conditions and, at the same time, being stable in the presence of hydrogen and carbon monoxide.

One of the first attempts to defunctionalize a primary alcohol with this approach was reported by Obora and Ishii (Scheme 3.13).[113] Their work, described that the primary alcohols obtained thanks to a Guerbet reaction catalyzed by $[Cp^*IrCl_2]_2$, underwent a dehydrodecarbonylation reaction, achieved using a combination of two different iridium complexes $[Cp^*IrCl_2]_2$ and $[IrCl(cod)]_2$/dppe, presumably involving two independent catalytic cycles, one for the dehydrogenation and one for the decarbonylation.

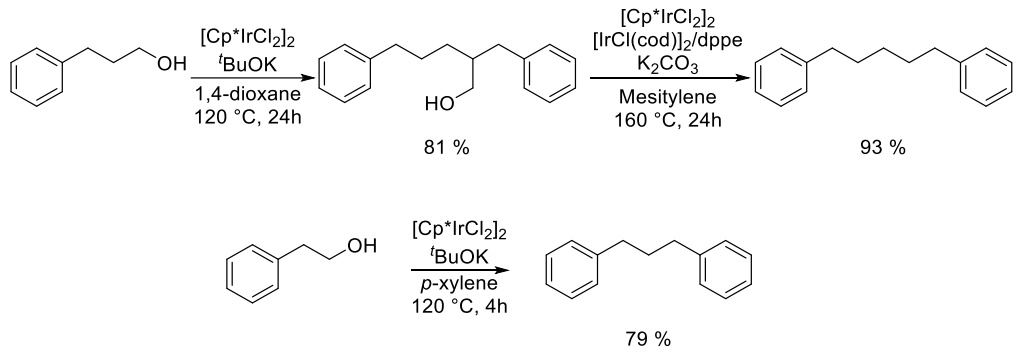

Scheme 3.13: Reaction investigated by Obora and Ishii[113]

In the same work, 2-phenylethanol derivatives in the presence of the single $[Cp^*IrCl_2]_2$ complex furnished, in a single step, the cleaved dimer. In the light of the previous considerations on cleavage of aldehydes in presence of bases, it can be hypothesized that the role of the iridium catalyst here is the mere dehydrogenation of the substrate to phenylacetaldehyde and the final hydrogenation of the product, while the carbon-carbon cleavage could be the product of the reaction studied in chapter 2.

In 2006, Madsen *et al.* invented a very efficient method for tandem dehydrogenation and decarbonylation. For this transformation, $RhCl_3 \cdot 3H_2O$ and dppp were used for the decarbonylation of an aldehyde generated *in situ* by the Oppenahuer catalyst $Al(O^tBu)_3$, and even better results were achieved by using $[Cp^*IrCl_2]_2$ /K_2CO_3.[104]

In 2012 Sadow *et al.* utilized rhodium to achieve the reaction of dehydrogenation and decarbonylation with a single catalytic system.[112] In particular, rhodium complexes with tris(4,4-dimethyl-2-oxazolinyl)phenylborate (TO^M), like $[TO^MRh(CO)_2]$, is active at room temperature for the photolysis of a broad range of substrates. The use of UV radiation was needed for the reaction outcome (Scheme 3.14).

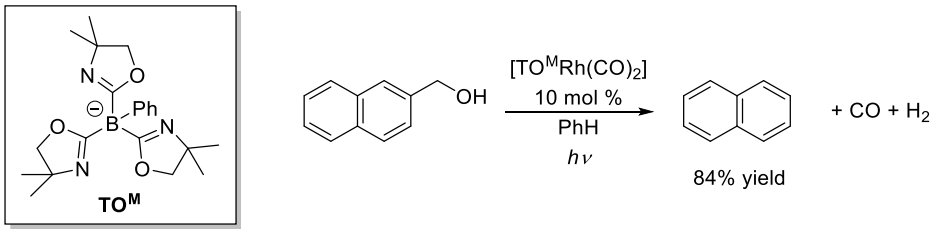

Scheme 3.14: Dehydrogenative decarbonylation by Sadow *et al.*[112]

It was found that the photo-promoted step of the reaction is the dissociation of a molecule of CO from the catalyst to form the complex [To^{M}Rh(CO)] necessary for the dehydrogenation step.

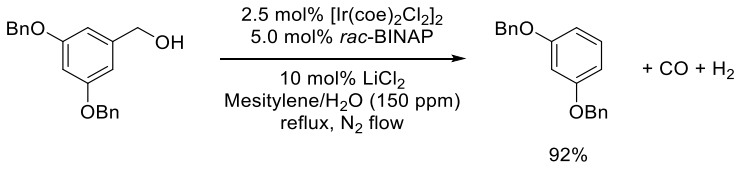

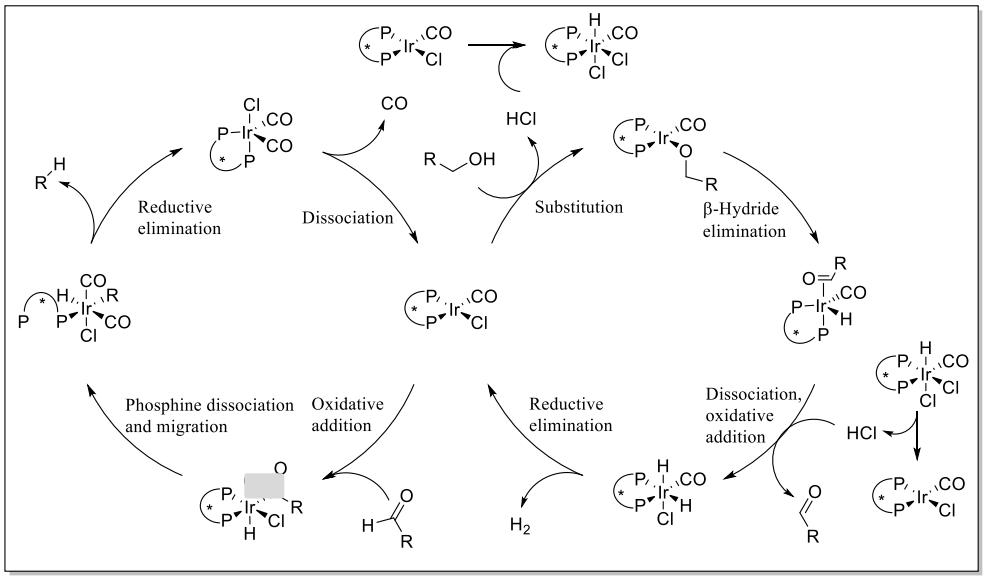

Scheme 3.15: Reaction scheme and proposed mechanism for dehydrogenative decarbonylation of alcohols with iridium[114]

After the discoveries of Obora and Ishii about the possibility to use iridium as both decarbonylative and dehydrogenative catalyst, the Madsen research group speculated about the possibility to find an appropriate iridium catalyst able to promote both reactions. In 2012, they succeeded and developed the catalytic system $[Ir(coe)_2Cl_2]$/*rac*-BINAP, forming the iridium-phosphine complex *in situ* (Scheme 3.15).[114]

Best conditions for the reaction involves the use of a high boiling solvent, such as mesitylene in the presence of water and LiCl.

Later in 2015, the mechanism of the iridium−BINAP catalyzed dehydrogenative-decarbonylation of primary alcohols was elucidated thanks to mechanistic experiments and DFT calculations.[115]

The observation that the catalyst was able to decarbonylate aldehydes under the same conditions, without any activation needed by the alcohol, suggested two separate catalytic cycles (Scheme 3.15). Moreover, the two kinetic isotopic effects (KIE) were investigated, both for the overall reaction and for the decarbonylation alone. The former resulted in a 1.42 ± 0.07 KIE value, which can be ascribed entirely to the dehydrogenation step. In fact, the decarbonylation was found to be kinetically unaffected by a hydrogen/deuterium replacement on the substrate (KIE 1.0 ± 0.05).

All the experiments and computational data contributed to define the mechanism. The rate determining step for the dehydrogenation should be the β-hydride elimination and, for the decarbonylation, the CO extrusion.

This methodology has immediately interested academics, especially for the possibility to obtain syngas for hydroformylation reactions since H_2 and CO are produced in the optimal ratio of 1:1 at low pressure. In this way, the use of an external source of this explosive and toxic mixture can be avoided.

Andersson[116] extended the scope of the reaction with iridium−BINAP to different polyols and then Madsen[117] utilized the obtained syngas to make a reductive carbonylation of styrene in the presence of $Rh(H)(CO)(PPh_3)_3$.

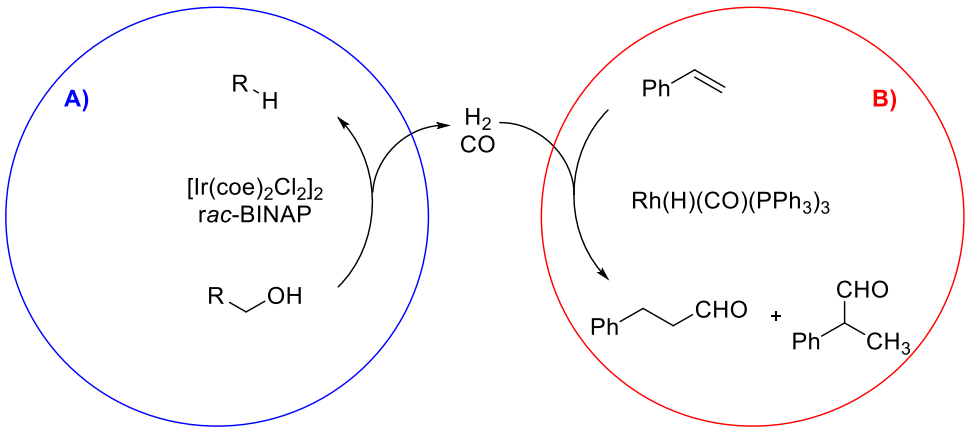

Scheme 3.16: Andersson[116] and Madsen[117] reaction scheme

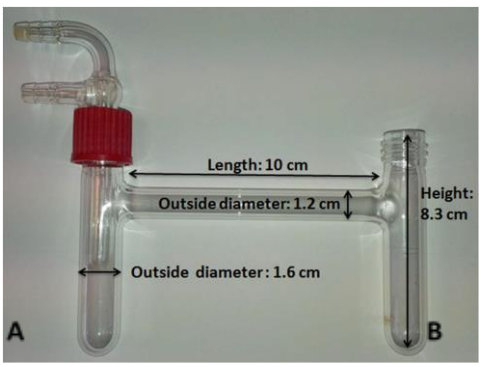

Figure 3.3: Picture of syngas production and *in situ* hydroformylation as seen in Madsen *et al.*[117,118]

The reaction occurs in a two-chamber apparatus in which every reaction independently proceed with only migration of syngas from chamber A to chamber B, like the one shown in Figure 3.3.[117,118]

3.1.7 Syngas: occurrence and application

Syngas is the acronym for synthesis gas, which is a versatile source for the production of chemicals and fuels. It is constituted by molecular hydrogen and carbon monoxide in a variable ratio and often mixed with carbon dioxide.

Currently, the syngas production mainly consists of a process in which natural gas and light hydrocarbons are converted into syngas through a reaction with steam, the so called *steam reforming reaction* (3.1). Having a lower ratio of H_2/CO is often desirable and, in order to achieve that, dry reforming is utilized. In this process, water is replaced by CO_2 (3.1-3.3). These processes are promoted by supported nickel catalysts.

$$CH_4 + H_2O \rightarrow CO + 3H_2 \qquad \text{steam reforming} \qquad (3.1)$$

$$C_nH_m + nH_2O \rightarrow nCO + \frac{m}{2}\left(n+\frac{m}{2}\right) \qquad (3.2)$$

$$CH_4 + CO_2 \rightarrow 2CO + 2H_2 \qquad \text{dry reforming} \qquad (3.3)$$

$$CH_4 + \frac{1}{2}O_2 \rightarrow CO + 2H_2 \qquad \text{partial oxidation} \qquad (3.4)$$

$$CO + H_2O \rightarrow CO_2 + H_2 \qquad \text{Water-gas shift} \qquad (3.5)$$

Oxygen can also convert methane into syngas with *partial oxidation* (eq. 3.4).[119] Unlike steam reforming, partial oxidation is exothermic. Next to the described methodologies, coal and biomass are also showing an emergent role for the production of syngas.[120]

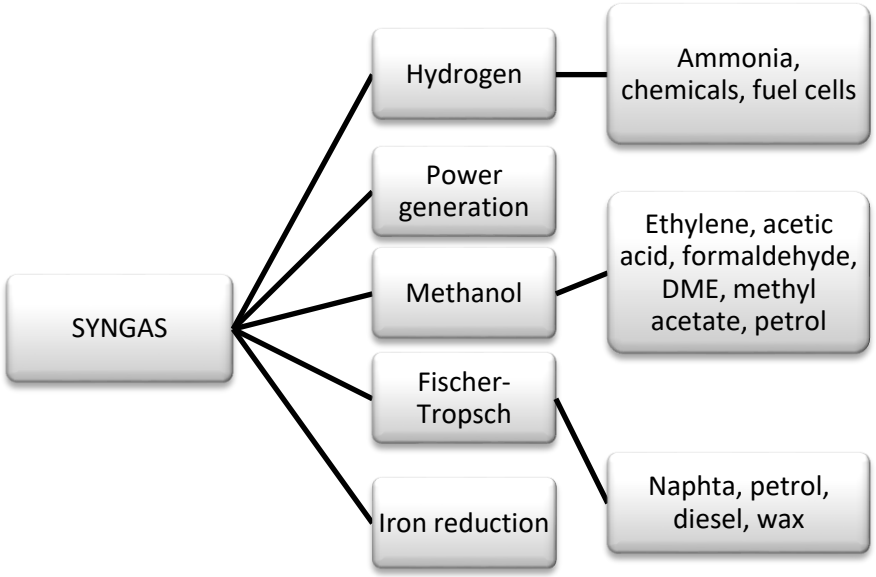

Figure 3.4: Syngas applications

The main application of syngas production is hydrogen generation. In order to understand the importance of these technologies, we can mention that steam reforming of methane with subsequent water-gas shift is responsible for over 90 % of the world hydrogen production.[121] This hydrogen can reach >99.999% purity after purification and it is utilized also for ammonia production or in fuel cells.

However, it is sometimes desirable to convert syngas into the more transportable methanol that can be used as fuel or feedstock for bulk chemicals as shown in Figure 3.4.

Fuel gases derived from coal gasification were used for lighting and heating in many cities after the industrial revolution. Nowadays, syngas is considered a cutting edge technology for a clean and efficient energy production.[122,123]

The Fischer-Tropsch process, known since 1925, employed catalysts based on different metals, like cobalt, iron or nickel. This method is used as an alternative for obtaining liquid hydrocarbons such as gasoline, diesel or other synthetic oils from gas. The process received great attention and experienced incredible development during World War II, when in Germany, particularly in Franz Fischer's laboratories at the Kaiser Wilhelm Institute for Coal Research (currently the Max Plank Institute) at Mülheim, it was employed in order to contrast the lack of foreign oil with German coal stocks.[124]

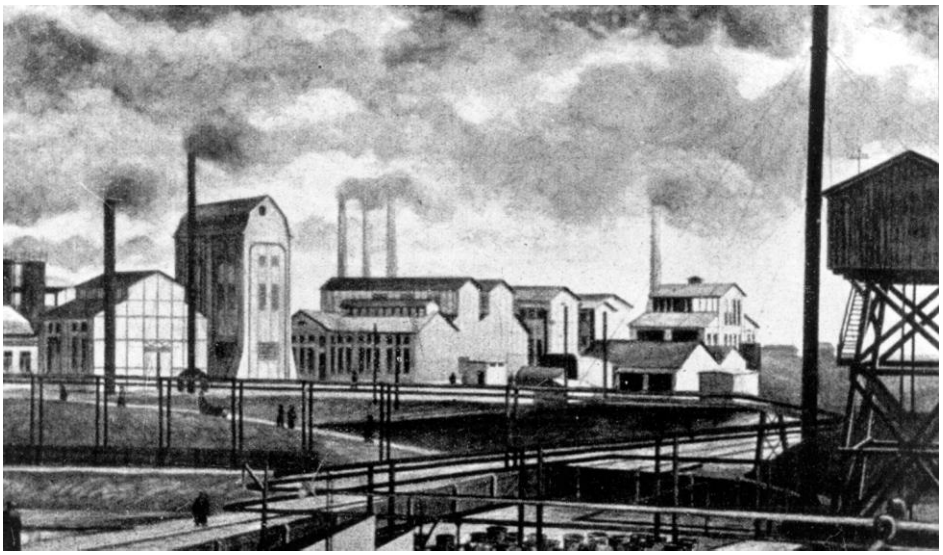

Figure 3.5: Fischer-Tropsch plant in Rheinau, Germany

Syngas is also employed for reducing iron ores in steel manufacturing, acting as a reducing agent in the Direct Reduced Iron ("DRI") process. Iron ores, in fact, are contaminated by different oxides like FeO and Fe_2O_3. The oxygen content is transferred to syngas, that is oxidized into water and CO_2.[125]

Thus, the dehydrogenative decarbonylation is a very helpful reaction, not only for obtaining syngas, but also for cleaving a hydroxyl-methyl group from organic molecules. The drawback, however, is the need for very expensive iridium and rhodium catalysts. As a result, the purpose of the present project is to identify a cheaper catalyst for the dehydrogenative decarbonylation of primary alcohols. As mentioned above, the catalyst should be able to form and release both H_2 and CO which are both good ligands for a variety of metals.

3.2 RESULTS AND DISCUSSIONS

3.2.1 Identification of metal species active towards dehydrogenative decarbonylation reaction

For the study of the reaction of dehydrogenative decarbonylation, a proper pilot system was selected on the basis of the previous studies on the reaction by employing iridium and rhodium.[112,114] Due to its reactivity and low cost, benzyl alcohol (**1**) was a good candidate as a substrate alcohol. On the other end, an aromatic solvent like *p*-xylene was considered in order to ensure solubility of the substrate and to reach a high temperature for promoting the reaction (boiling point 138 °C).

A broad range of metals were tested as catalysts in different oxidation states. It was decided to choose transition metals known to promote dehydrogenation and which could be competitive in cost and performance with iridium and rhodium. Therefore it was opted for ruthenium, iron and copper, which were all added in the amount of 5% with respect to benzyl alcohol.

Air and moisture were excluded from the reaction to avoid a possible oxidation or decomposition reaction that could occur in some cases with oxygen or water. In order to obtain an inert atmosphere, the tubes were oven-dried and evacuated and refilled with nitrogen gas three times prior to the reaction. A positive pressure of nitrogen was applied to keep the inert atmosphere controlled and allow the possible emission of gas through the gas line. *p*-Xylene was dried, degassed and stored under inert atmosphere.

Table 3.1: Preliminary screening of catalysts for the dehydrogenative decarbonylation of benzylalcohol[a]

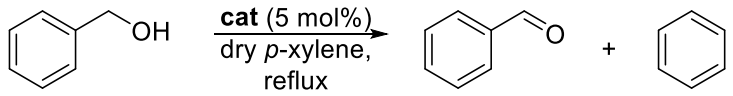

35 **36** **28**

Entry		Catalyst	Unreacted (**35**)%	Yield (**36**)%[b]	Yield (**28**)%[b]
1	Ru(0)	$Ru_3(CO)_{12}$	70	27	-
2		$RuCl_2(CO)_2(PPh_3)_2$	57	3	-
3		$RuH_2(CO)(PPh_3)_3$	36	54	2
4		[(*p*-cymene)$RuCl_2$]$_2$	88	-	-
5	Ru(II)	$RuCl_2(PPh_3)_3$	68	28	1
6		Shvo catalyst (**37**)[c]	9	19	6
7		Grubbs 1st Gen (**38**)	50	42	3
8		I^{i}PrRuCl$_2$(*p*-cymene) (**39**)	42	38	-
9	Ru(III)	$Ru(acac)_3$	15	80	3
10		$RuCl_3 \cdot nH_2O$	-	-	-
11	Fe(II)	$Fe(OAc)_2$[c]	65	14	-
12		[FeCp(CO)$_2$]$_2$ (**40**)	-	-	-
13	Fe(III)	$Fe(acac)_3$[c]	-	14	-

Entry		Catalyst	Unreacted (**35**)%	Yield (**36**)%[b]	Yield (**28**)%[b]
14	Cu(I)	CuI	90	-	-
15	Cu(II)	$Cu(acac)_2$	82	-	-

*[a] Reaction conditions: Benzyl alcohol (1.0 mmol), specified catalyst (5 mol%), p-xylene (2 mL), reflux temperature (138.4 °C) and nitrogen stream. Analyzed after full conversion or prematurely after 16 h. [b] GC yield. [c] Major product **41**. [d] Major product **42**.*

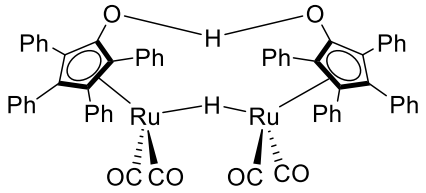

37

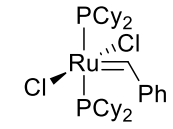

38

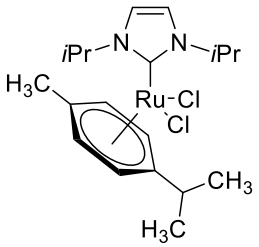

39

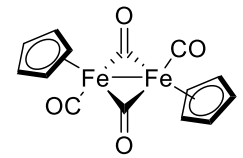

40

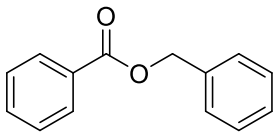

41

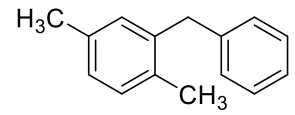

42

Figure 3.6: Some considered catalysts and detected byproducts during the screening of catalysts for the dehydrogenative decarbonylation of benzyl alcohol

The reactions were monitored by a gas chromatography coupled with a mass spectrometer (GC-MS). The yield of benzyl alcohol **35**, benzaldehyde **36** and benzene **28** were found by comparison with the signal of the internal standard *n*-decane. A calibration curve for each of the encountered compounds were measured and then compared to the chosen standard in order to obtain correct yields.

Unfortunately, only in few reactions the aldehyde was obtained in a remarkable amount and all of these involved a ruthenium-based catalyst (entry 1, 3, 5, 7, 8 and 9). In all of these examples the aldehyde production did not exceed 50%, except in the case of $RuH_2(CO)(Ph_3P)_3$ where the aldehyde was obtained in 54% yield and $Ru(acac)_3$ which produced 80% of the aldehyde. Among these reactions, an even lower number also afforded the desired benzene such as $RuH_2(CO)(Ph_3P)_3$(entry 3), $RuCl_2(Ph_3P)_3$ (entry 5) and Grubbs catalyst (**38**) (entry 7). Nonetheless, the decarbonylated product was estimated to be below the catalyst loading and it cannot be excluded that the catalyst was acting as a stoichiometric reagent. It is interesting to note that in these last cases the alcohol showed a poor conversion. This could be due to poisoning of the catalyst with carbon monoxide that is a strong binding ligand and can prevent the catalyst from being recycled.

The formation of side products were also experienced by employing other catalysts. For instance, benzyl benzoate **41** was identified as the main product in entry 6, 11 and 13. The ester is probably obtained from a dehydrogenative coupling between two molecules of alcohol. This was not a completely unexpected reaction since, as discussed in the introduction of this chapter, under dehydrogenative conditions ester formation can occur. A single product, the adduct (**42**) was found using $RuCl_3$ hydrate, that can be described as the Friedel-Crafts adduct between the solvent and the benzylic carbocation derived from **35**. In turn, could be due to coordinated water in the catalyst which may generate hydrochloric acid during the reaction thus promote liberation of the benzylic cation from the alcohol that can react with the solvent.

The preliminary data showed that ruthenium, especially in oxidation state of +2, gave the best outcome although the results did not show the production of the decarbonylated product over the catalyst loading.

The reaction conditions previously applied, did not always show reproducibility. In fact, Table 3.1 includes only the best and most reliable results (in which the mass balance between the starting material and the products of the reaction was reasonably correct). Therefore, it was decided to repeat the most promising reactions, using a bulkier alcohol, 2-naphthyl methanol (**43**), as the substrate. 2-Naphthyl methanol affords a solid hydrocarbon, i.e. naphthalene (**45**), which has the advantage of not lowering the boiling point of the solution and, at the same time, reducing the chance of leaking out of the system.

The reactions that led to the formation of some final compound in the preliminary results were repeated with the new substrate. The reaction with compound **37** was excluded because it was not just slow but it led to undesired products as the major components.

The experiments in Table 3.2 displayed an increasing formation of the desired naphthalene **45**. Despite the encouraging trend the reaction was far from being satisfying. With the proven ability of ruthenium to catalyze the reaction, the next step was to try the effect of ligands that may influence the reactivity of the species. It is well known that in $Ru_3(CO)_{12}$ the carbonyl ligands can be replaced with phosphines in solution, and it was therefore, picked as a possible precursor of ruthenium (0) phosphine catalysts obtained *in situ* by addition of phosphine.[126,127]

Table 3.2: Preliminary screening of catalysts for the dehydrogenative decarbonylation of 2-naphthyl methanol.[a]

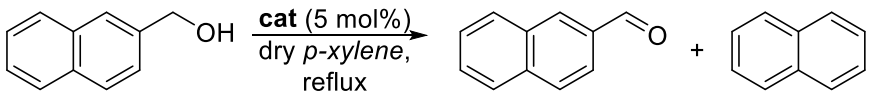

43 **44** **45**

Entry	Catalyst	Conversion (**43**)% [b]	Yield (**44**)%[b]	Yield (**45**)%[b]
1	$Ru_3(CO)_{12}$ (**46**)	4	23	10
2	$RuCl_2(Ph_3P)_3$	17	55	9
3	$RuCl_2(CO)_2(Ph_3P)_3$	29	58	
4	$RuH_2(CO)(Ph_3P)_3$	53	6	12
5	$RuClH(CO)(Ph_3P)_3$	56	3	5
6	$Ru(acac)_3$	47	22	12

[a] Reaction conditions: 2-Naphthyl methanol (1.0 mmol), specified catalyst (5 mol %), p-xylene (2 mL), reflux temperature (138 °C) and nitrogen stream. Analyzed after full conversion or prematurely after 16 h. [b] GC yield.

The precatalysts $RuCl_2$(*p*-cymene)$_2$ and $[Ru(COD)Cl_2]_n$ were selected in order to form phosphine ruthenium (II) complexes similar to $RuCl_2(Ph_3P)_3$ directly in solution. These complexes, when heated in solution with phosphines can form complexes by replacing the neutral ligands *p*-cymene[128–130] and cyclooctadiene (COD), respectively.[131]

In Table 3.3, the reaction with the above mentioned catalytic system is reported with or without adding triphenyl phosphine in a ratio of 2:1 with respect to the catalyst (corresponding to 10 mol %). This was done in order to see the effect of the ligand and set a proper catalytic system for the future screening of different phosphines. In addition, it was decided to increase the boiling point of the solvent to speed up the reaction and achieve a better outcome. Therefore, *p*-xylene was replaced with *p*-cymene that boils at 177 °C.

Table 3.3: Preliminary screening of catalysts for the dehydrogenative decarbonylation of 2-naphthyl methanol.[a]

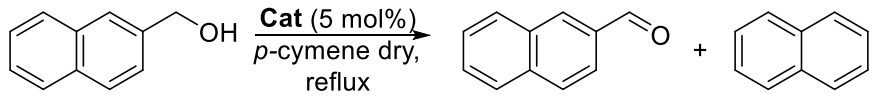

43 **44** **45**

Entry	Catalyst	Conversion (**43**)%[b]	Yield (**44**)%[b]	Yield (**45**)%[b]
1	$Ru_3(CO)_{12}$(**46**)	-	25	26
2	$RuCl_2(Ph_3P)_3$	-	43	20
3	$[RuCl_2(p\text{-cymene})_3]_2$(**47**)	40	9	-
4	$RuCl_2(p\text{-cymene})_3$ + 10% Ph_3P	-	51	14
5	$[Ru(COD)Cl_2]_n$(**48**)	27	14	-

Entry	Catalyst	Conversion (**43**)%[b]	Yield (**44**)%[b]	Yield (**45**)%[b]
6	$[Ru(COD)Cl_2]_n$+ 10% Ph_3P	10	27	38

[a] Reaction conditions: 2-Naphthyl methanol (1.0 mmol), specified catalyst (5 mol %), p-cymene (2 mL), reflux temperature (177 °C) and nitrogen stream. Analyzed after full conversion or prematurely after 16 h. [b] GC yield.

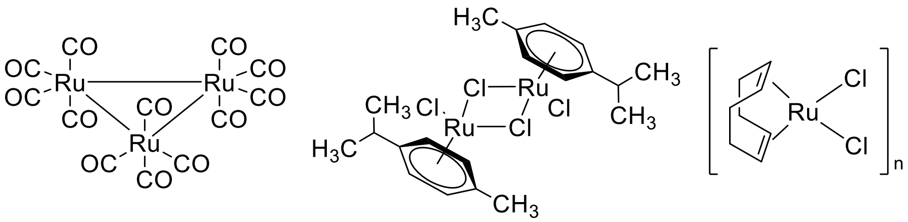

46 **47** **48**

Figure 3.7: Some considered complexes during the screening of catalysts for the dehydrogenative decarbonylation of benzyl alcohol

At the *p*-cymene reflux temperature, the catalysts $RuCl_2(Ph_3P)_3$ and $Ru_3(CO)_{12}$ already showed a better outcome due to the increased temperature. Besides that, the best result was obtained by using $[Ru(COD)Cl_2]_n$ in the presence of 10% Ph_3P (entry 6). Therefore $[Ru(COD)Cl_2]_n$ was chosen as a precatalyst and subsequently tested together with $Ru_3(CO)_{12}$ with a different set of ligands.

3.2.2 Ligand screening

Table 3.4 explores the effect of aromatic phosphines (entries 1-14), alkyl phosphines (entries 15-26), polydentate ligands (entries 27-42), or nitrogen or oxygen-based

ligands (entries 43-46) on the dehydrogenative decarbonylation reaction. Phosphines with different steric hindrance and binding geometries were also considered.

Within the reported cases, aromatic phosphines gave a modest yield, especially those without strongly electron donating or electron withdrawing substituents: in fact, the phosphines that provided the best results were PPh_3 and P(*o*-$MeC_6H_4)_3$. Especially the very hindered P(*o*-$MeC_6H_4)_3$ in combination with precatalyst $[Ru(COD)Cl_2]_n$ (**48**) afforded the decarbonylation product in 61% yield with 9% remaining of the unreacted aldehyde.

Table 3.4: Screening of ligands for the dehydrogenative decarbonylation of 2-Naphthyl methanol.[a]

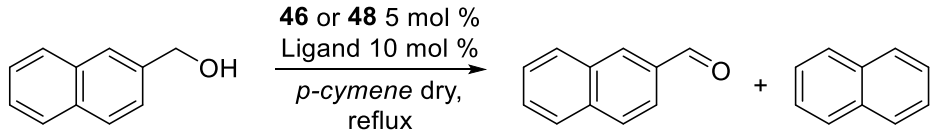

43 **44** **45**

Entry	Catalyst	Ligand	Yield (**44**)%[b]	Yield (**45**)%[b]
1	**46**	PPh_3	50	39
2	**48**	PPh_3	27	38
3[c]	**48**	PPh_3	-[d]	4[d]
4[e]	**48**	PPh_3	40	12
5	**46**	P(*p*-$FC_6H_4)_3$	38	11
6	**48**	P(*p*-$FC_6H_4)_3$	-	21
7	**46**	P(*o*-$MeC_6H_4)_3$	67	32
8	**48**	P(*o*-$MeC_6H_4)_3$	9	61

Entry	Catalyst	Ligand	Yield (**44**)%[b]	Yield (**45**)%[b]
9	**46**	P(*p*-$MeOC_6H_4$)$_3$	50	16
10	**48**	P(*p*-$MeOC_6H_4$)$_3$	50	22
11	**46**	P(*2,6*-$MeOC_6H_3$)$_3$	39	32
12	**48**	P(*2,6*-$MeOC_6H_3$)$_3$	43	10
13	**46**	P(*2*-furyl)$_3$	26	5
14	**48**	P(*2*-furyl)$_3$	27	4
15	**46**	PCy_3	30	49
16	**48**	PCy_3	56	10
17[f]	**48**	PCy_3	25	1
18	**48**	PCy_3 HBF_4	60	11
19	**48**	P(Cyclopentyl)$_3$	51	13
20	**46**	P*n*Bu_3	25	20
21[g]	**46**	P*n*Bu_3	19	4
22	**48**	P*n*Bu_3	81	4
23	**46**	P*t*Bu_3	53	23
24	**48**	P*t*Bu_3	25	6
25	**48**	PCy_2*t*Bu	-	-

Entry	Catalyst	Ligand	Yield (**44**)%[b]	Yield (**45**)%[b]
26	**48**	P(*2*-Biphenyl)^{t}Bu$_2$	60	38
27[b]	**46**	dppe	18	28
28[b]	**48**	dppe	60	18
29[b]	**46**	dppp	22	15
30[b]	**48**	dppp	61	34
31[b]	**46**	dppf	-	-
32[b]	**48**	dppf	59	23
33[b]	**48**	Binap	85	14
34[b]	**46**	DPEPhos	28	13
35[b]	**48**	DPEPhos	27	5
36[b]	**46**	Xantphos	1	0
37[b]	**48**	Xantphos	53	4
38[b]	**46**	BIPHEP	46	37
39[b]	**48**	BIPHEP	59	24
40[b]	**48**	davephos	59	23
41[b]	**48**	$(PPh_2CH_2CH_2)_3P$	29	7
42[b]	**48**	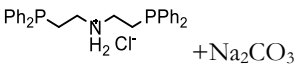 $+Na_2CO_3$	10	2

Entry	Catalyst	Ligand	Yield (**44**)%[b]	Yield (**45**)%[b]
43[b]	**46**	1,10-phenanthroline	16	42
44[b]	**48**	1,10-phenanthroline	6	-
45	**46**	O=P*n*Bu$_3$	46	15
46	**48**	O=P*n*Bu$_3$	62	8

[a] Reaction conditions: 2-Naphthyl methanol (1.0 mmol), catalyst **46** (0.017 mmol) or **48** (0.05 mmol) as specified, specified ligand (10 mol %) unless differently expressed, *p*-cymene (2 mL), reflux temperature (177 °C) and nitrogen stream. Analyzed after full conversion or prematurely after 16 h. [b] GC yield; [c] AgOTf (0.1 mmol); [d] Friedel Crafts adduct obtained as main product; [e] LiCl (0.1 mmol); [f] freshly recrystallized PCy$_3$;. [g] Freshly opened bottle of P^{n}Bu$_3$; [h] Ligand used in 5 mol % compared to the substrate.

The addition of salts to the system with PPh$_3$ was disadvantageous. In fact, it lowered the yields and in case of silver triflate, also favored the formation of a side product, the Friedel-Crafts adduct between naphthyl methanol and *p*-cymene.

Alkyl phosphines seem to react at their best in combination with catalyst **46**. The trend is particularly evident using PCy$_3$, which afforded naphthalene in 49% yield. Alkyl phosphines are difficult to store because they tend to be oxidized in the presence of oxygen. Therefore, PCy$_3$ was utilized freshly recrystallized (entry 17), or in the form of the more stable phosphonium tetrafluoroborate salt[132] and in combination with a base (entry 18). Lastly in case of P(*n*-Bu)$_3$ it was compared with a freshly purchased sample of the reagent. In none of these cases the elimination of possible traces of the phosphine oxide helped the reaction, but it seemed to worsen the outcome. Bidentate and tridentate phosphines were utilized in a ratio of 1:1 as compared to ruthenium. The notable results were obtained only in case of the catalyst **46** in combination with BIPHEP or phenanthroline (entries 38 and 43) and **48** in combination with dppp and

davephos (entries 30 and 40). At last, since the unexpected behavior of alkyl phosphines in the presence of impurities of the corresponding trialkyl-phosphine oxides, pure tributylphosphine oxide was added (entries 45 and 46), however it did not furnish satisfying results.

3.2.3 Optimization of the reaction conditions

Before moving forward with the phosphine screening, the simple catalytic system consisting of $RuCl_2(PPh_3)_3$ was tested in the presence of some oxygen nucleophiles with a strong permanent dipolar moment to evaluate the effect observed in Table 3.4 entries 16, 17 and 20, 21. In fact, phosphine oxides and sulfoxides may facilitate the release of carbon monoxide from a metal in a similar way as amine oxides.[133] The considered compounds are reported in Table 3.5. In all the cases, the addition of the additive did not affect considerably the reaction as we expected.

Table 3.5: Further screening of oxygen nucleophiles in the dehydrogenative decarbonylation of naphthyl methanol[a]

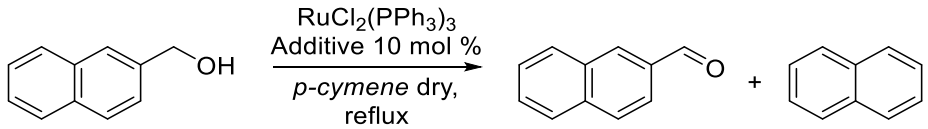

43 **44** **45**

Entry	Additive	Yield (**44**)%[b]	Yield (**45**)%[b]
1	-	46	21
2	$Ph_3P=O$	43	22

Entry	Additive	Yield (**44**)%[b]	Yield (**45**)%[b]
3	DMSO	52	17
4	$Ph_2S=O$	26	15
5	pyridine *N*-oxide	-	-
6	$^{n}Bu_3P=O$	47	20

[a] Reaction conditions: 2-naphthyl methanol (1.0 mmol), $RuCl_2(PPh_3)_3$ (5 mol %), additive (10 mol %), p-cymene (2 mL), reflux temperature (177 °C) and nitrogen stream. Analyzed after full conversion or prematurely after 16 h. [b] GC yield.

In addition, different high boiling solvents were tested. The purpose was to understand the influence other aromatic solvents with lower boiling points, a tertiary alcohol and high boiling ethers. In this case the best results were obtained with the same catalytic system as in Table 3.4, that is the combination of $[Ru(COD)Cl_2]_n$ (**48**) and phosphine **49**.

The reaction was started at room temperature and progressively heated while monitored by GC. The final reflux temperature was kept for an additional 16 hours. In all the reported cases, the product was found in very modest amounts or it was not detected at all.

Table 3.6: Screening of solvent effect in the dehydrogenative decarbonylation of naphthyl methanol[a]

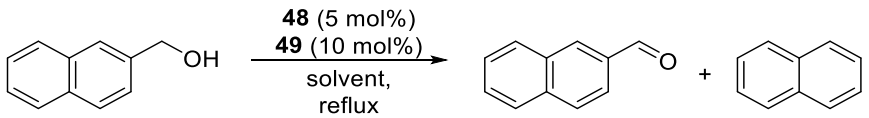

43 **44** **45**

Entry	Solvent	Yield (**44**)%[b]	Yield (**45**)%[b]
1	toluene	26	4
2	mesitylene	22	12
3	*t*-BuOH	7	-
4	monoglyme	9	-
5	diglyme	26	4
6	DMSO	27	-

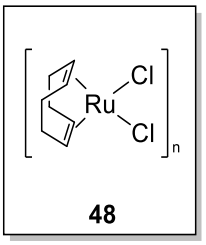

48

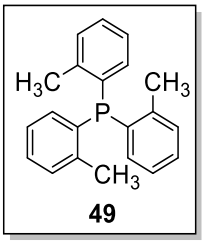

49

*[a] Reaction conditions: 2-naphthyl methanol (1.0 mmol), catalyst **48** (5 mol%), ligand **49** (10 mol %), solvent 2 mL up to reflux and nitrogen stream. Analyzed after full conversion or prematurely after 16 h. [b] GC yield.*

3.2.4 Ligand effect

One of the earliest reactions with P(*o*-MeC_6H_4)$_3$ in combination with catalyst **48** was so far the best result. In addition, the yield increased from 61% after 16 hours to 85% after complete conversion of the alcohol which occurred after 24 hours.

Table 3.7: Effect of phosphine concentration in the dehydrogenative decarbonylation of Naphthyl methanol[a]

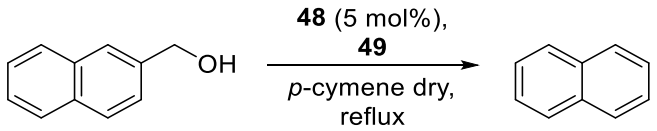

43 **45**

Entry	Phosphine mol %	Concentration [M]	Yield (**45**)%[b]
1	1.25	0.00625	4
2	2.5	0.0125	16
3	5	0.025	31
4	7.5	0.0375	86
5	10	0.05	85
6	12.5	0.0625	91
7	15	0.075	92
8	20	0.1	90

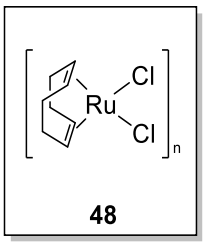

48

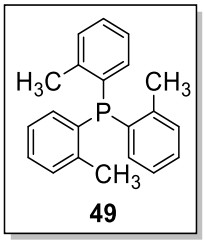

49

*[a] Reaction conditions: 2-Naphthyl methanol (1.0 mmol), catalyst **48** (5 mol %), ligand **49**, p-cymene (2 mL), reflux temperature (177 °C) and nitrogen stream. Analyzed after full conversion. [b] GC yield.*

The use of a 2:1 ratio of the phosphine with respect to the ruthenium source was used in the previous studies, however, as it can be seen from Table 3.7, the loading of the former turned out to show a great influence.

The alcohol conversion increased with the increase in phosphine loading. The best result was achieved by using 15 % of the phosphine in a ratio 3:1 with respect to ruthenium. Higher amounts did not show any improvement. Notably the reaction in entry 1, 2 and 3 contained a thin metallic layer on the surface of the Schlenk tube, while reactions in entry 4 and 5 turned black and reactions in entry 6, 7 and 8 were completely clear at the end of the reaction. The reaction with 15% of phosphine was also faster, probably because the phosphine prevented decomposition and deactivation of the catalyst during the reaction and thus affording complete conversion after 8 hours.

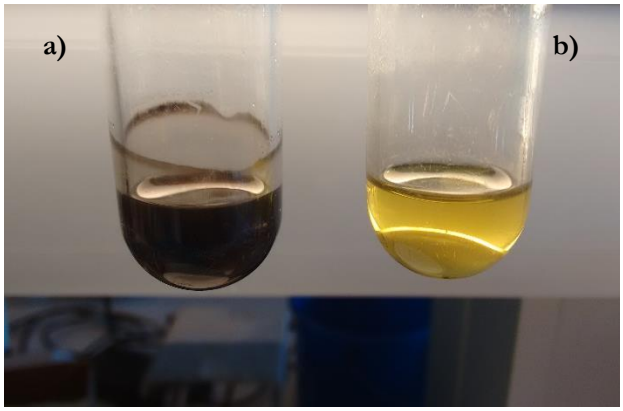

Figure 3.8: *Difference between reactions running with a) 10% of ligand and b) 15 %. The first one show catalyst decomposition responsible for the black color, while the second is clear.*

The reason why tri(*o*-tolyl)phosphine has a huge influence on the reaction might lie in its steric and electronic features. In Figure 3.9, Tolman's map[134] shows the behavior of many phosphines displayed as a function of the increasing cone angle with the metal (from left to right) and increasing electronic parameter (from bottom to top).[134] This last parameter is determined by the CO stretching frequency in different

$Ni(CO)_3L$ complexes (L = phosphorus ligand) and represents the ability of the ligand to draw electron charge from the complex.

Tri(*o*-tolyl)phosphine is located in the bottom-right cones of this scheme suggesting its strong hindrance and pronounced electron releasing effect. These two effects can favor the exchange of ligands on the metal center and thus speed up the reaction.

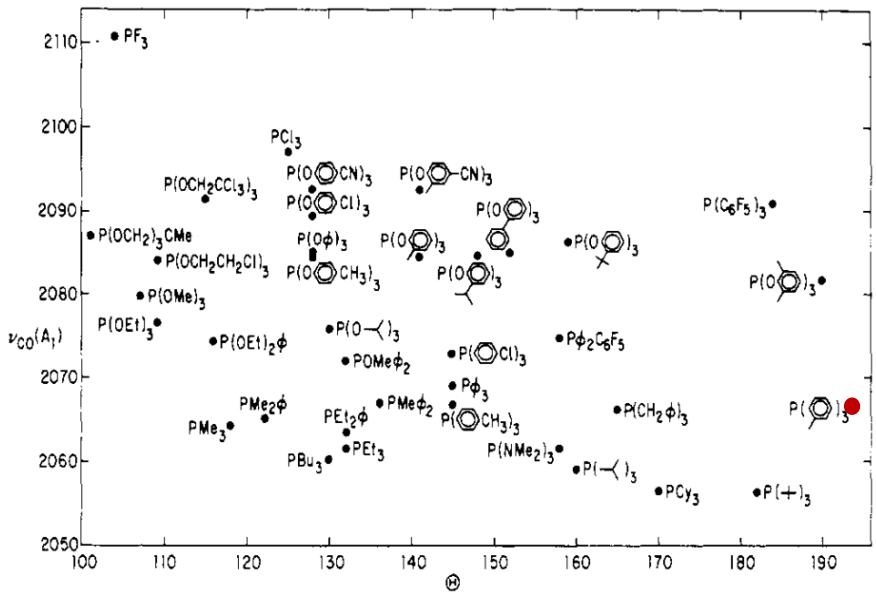

Figure 3.9: stretching frequency for CO in the $Ni(CO)_3L$ complex (ν_{CO}) as a function of ligand cone angle[134]

3.2.5 Effect of air and moisture

So far, the reactions were conducted with anhydrous solvents, deprived of traces of gas by three freeze-pump-thaw cycles and stored under an atmosphere of nitrogen. Moreover, the reactions were all conducted under nitrogen atmosphere to avoid side reactions that could potentially occur with the substrate or the catalyst. These precautions were examined to understand if more ordinary operator-friendly conditions could be employed. The reactions were performed in the presence of air, water or a combination of the two.

Table 3.8: Screening of different reaction conditions for the reaction of dehydrogenative decarbonylation of naphthyl methanol[a]

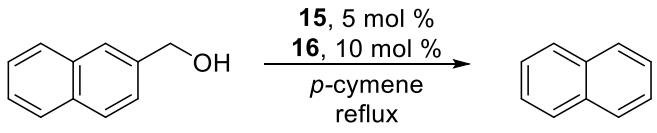

43 **45**

Entry	Water	Air	Yield (**45**)%[b]
1	No	No	92
2	Yes	No	95
3	No	Yes	90
4	Yes	Yes	89
5	No	Only before sealing the tube	95

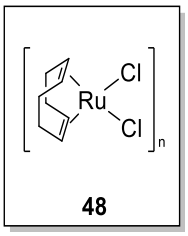

48

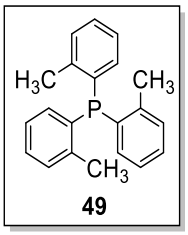

49

*[a] Reaction conditions: 2-Naphthyl methanol (1.5 mmol), catalyst **48** (5 mol %), ligand **49** (10 mol %), p-cymene (2 mL), reflux temperature (177 °C). Analyzed after full conversion. [b] GC yield.*

As shown by the experiments listed in Table 3.8 there is little effect of performing the reaction in the presence of moisture or air. Nevertheless the reaction was still conducted under a nitrogen atmosphere, in order to prevent a possible reaction between the liberated hydrogen and dioxygen, but the solvent was employed with no further purification or dehydration.

3.2.6 Brief note about *p*-cymene as solvent

In the optimization process, it was evident that high temperatures were necessary to promote the reaction in a reasonable time. This is most likely due to the need for releasing the gaseous molecules H_2 and CO. *p*-Cymene was chosen although being considered unusual compared with the other aromatic solvents it guarantees good performance and it is considered less toxic and more environmental friendly.[135]

p-Cymene is a naturally occurring essential oil and its production is still based on petrochemicals. However recent studies open the way to large scale production from renewable sources.[136] In particular it could be obtained by dehydrogenation of limonene.

Recently, it gave very good results as a solvent for the cross-metathesis of estragole with methyl acrylate, especially for preventing double-bond isomerization of the produced olefin.[137]

The major drawback that was particularly evident in dehydrogenative decarbonylation, was due to its high boiling point. In this reaction indeed, the products are molecules that have lost a hydroxymethyl group and therefore are more volatile than the starting alcohol and often also more than the solvent itself. On one side this limited the reaction scope and the possibility of isolating the products after the reaction, allowing, in the great majority of the cases, to determine the reaction yield only by GC-MS.

This may be considered as a problem in most of the applications, although considerations can be done:

-When the reaction aims to isolate syngas, it occurs most likely starting from simple alcohols. In this scenario, recovering the hydrocarbon would not be of interest.

-When instead, the reaction aims to achieve the defunctionalization of a substrate, it is most likely a complex molecule and therefore it would not have problems with volatility.

According to this rationale, the reactions for determining the scope of the dehydrogenative decarbonylation were analyzed mainly by GC-MS with the intention of understanding the process.

3.2.7 Substrate scope and limitations

The reaction conditions studied so far afforded a satisfying protocol for the dehydrogenative decarbonylation of 2-naphthyl methanol. It was then time to extend the method on different benzylic alcohols. The obtained results are reported in Table 3.9. The table includes conversion time in addition to product yields.

As 2-naphthalene methanol (**43**), 1-naphthalene methanol (**50**) also afforded naphthalene in a very good yield. In entries 3 and 4, the reaction of the parent benzyl alcohol **35** and 4-methylbenzyl alcohol **51a** are supposed to produce benzene **28** and toluene **3** as the products, respectively. Unfortunately, no benzene and only a low toluene amount were detected and in both cases no byproducts were observed, although the starting materials were consumed in a short reaction time. A plausible explanation is that these products with a boiling point lower than *p*-cymene are lost by co-evaporation with syngas during the reaction.

Heavier benzyl alcohols (**51 b-f**) bearing electron-donating groups afforded the corresponding products in good yields and reasonable short reaction times. The yields dropped with benzyl alcohols bearing electron withdrawing substituents (alcohols **51 g-j**). 4-(Methylthio)benzyl alcohol was not entirely converted even after 12 hours, leaving a significant amount of the aldehyde and of the unreacted starting material. A plausible explanation is that sulfur can strongly coordinate to ruthenium, causing a poisoning of the catalyst.

Table 3.9: Benzyl alcohols in the of dehydrogenative decarbonylation with ruthenium[a]

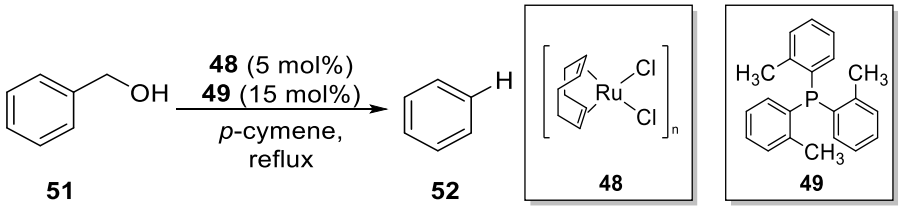

Entry	Substrate		Product		Time (h)	Yield %[b]
1	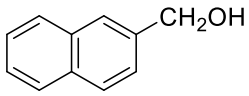	**43**	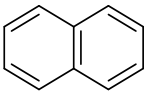	**45**	8	92
2	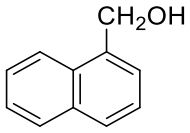	**50**	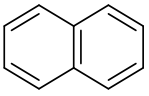	**45**	8	95
3	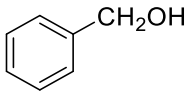	**35**		**28**	5	-

Entry	Substrate		Product		Time (h)	Yield %[b]
4	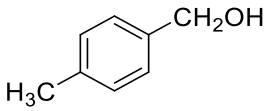	**51a**	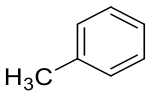	**3**	3	38
5	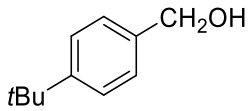	**51b**	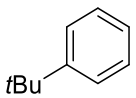	**52b**	6	88
6	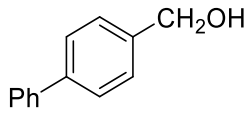	**51c**	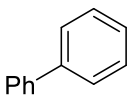	**52c**	5	83
7	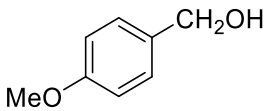	**51d**	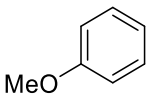	**52d**	3	75
8	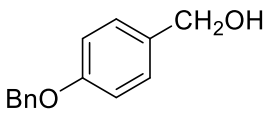	**51e**	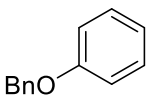	**52e**	6	72[c]
9	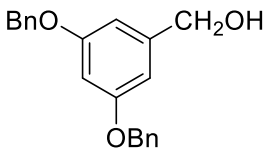	**51f**	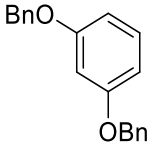	**52f**	6	63[c]
10	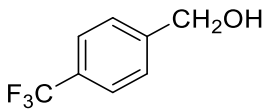	**51g**	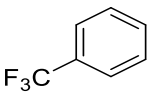	**52g**	12	-
11	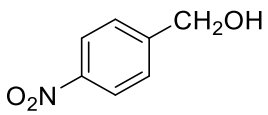	**51h**	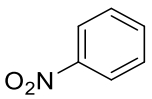	**52h**	12	13

Entry	Substrate		Product		Time (h)	Yield %[b]
12	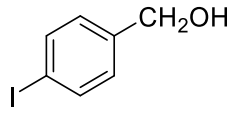	**51i**	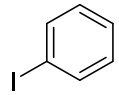	**52i**	12	11
13	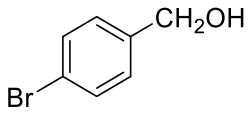	**51j**	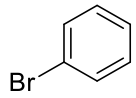	**52j**	12	53
14	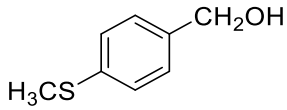	**51k**	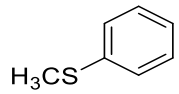	**52k**	12	13

*[a] Reaction conditions: Alcohol (1.0 mmol), catalyst **48** (5 mol %), ligand **49** (15 mol %), p-cymene 2 mL, reflux temperature (177 °C) and nitrogen stream. Analyzed after full conversion. [b] GC yield. [c] Isolated yield.*

In addition, alkyl primary alcohols were tested with the optimized reaction conditions and the results were very diverse (Table 3.10).

Table 3.10: Primary alcohols in the dehydrogenative decarbonylation with ruthenium[a]

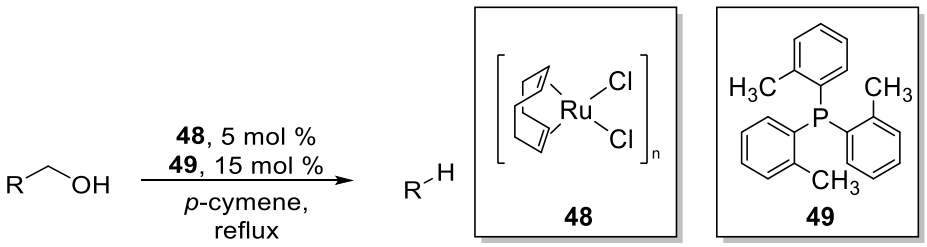

Entry	Substrate		Product		Time (h)	Yield %[b]
1	$CH_3(CH_2)_8CH_2OH$	**53**	$CH_3(CH_2)_7CH_3$	**54**	16	75

Entry	Substrate		Product		Time (h)	Yield %[b]
2	$CH_3(CH_2)_{18}CH_2OH$	**55**	$CH_3(CH_2)_{17}CH_3$	**56**	16	82
3	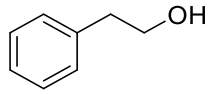	**1**	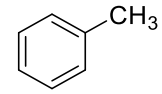	**3**	16	14
4	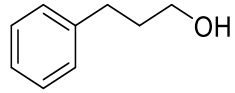	**56**	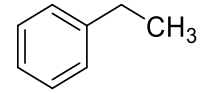	**57**	16	34
5	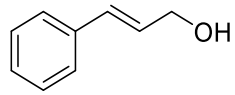	**58**	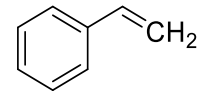	**59**	16	29
6	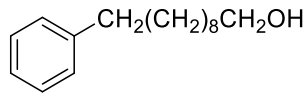	**60**	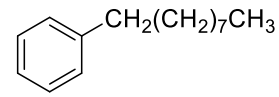	**61**	8	63
7	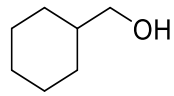	**62**	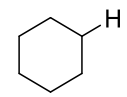	**63**	16	13
8	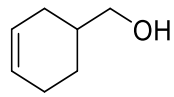	**64**	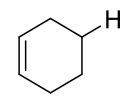	**65**	16	16
9	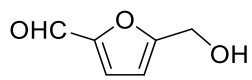	**66**	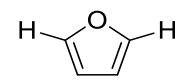	**67**	8	-

*[a] Reaction conditions: Alcohol (1.0 mmol), catalyst **48** (5 mol %), ligand **49** (15 mol %), p-cymene (2 mL), reflux temperature (177 °C) and nitrogen stream. Analyzed after full conversion. [b] GC yield. [c] Isolated yield.*

Long chain hydrocarbons (entries 1, 2 and 3) afforded good yields although with longer reaction times if compared with the benzylic alcohols. In many cases (entries 4, 7 and 8), the picture was complicated by the formation of some of the possible

aldol condensation products. These included the actual aldol, the corresponding enal and the decarbonylation product that can occur on the latter.

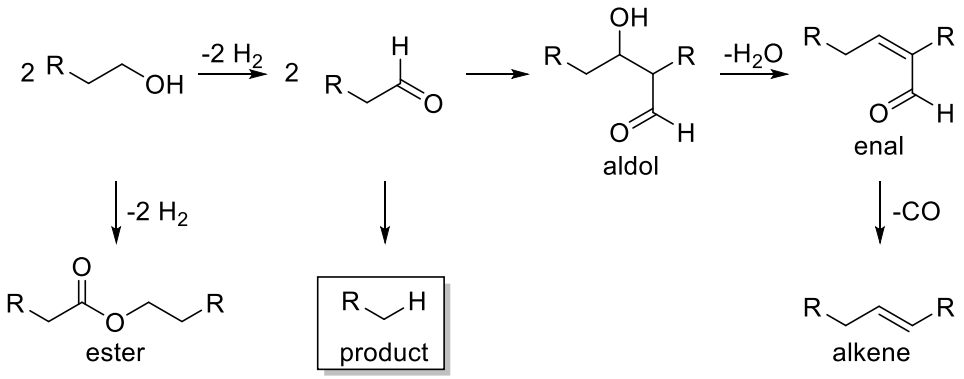

Scheme 3.17: Possible pathways of side products formation

In some other examples, the formation of the ester was observed, like in entry 4. In entries 5 and 8, the saturated product was found as well.

Interestingly, when 5-HMF was used as the starting material (entry 9), the conversion occurred rapidly within 8 hours however, no product was recovered even if intermediates were detected during the reaction. Also in this case, as with benzyl alcohol (Table 3.9 entry 3), the product was extremely volatile (b.p. 31 °C) and may have evaporated from the reaction mixture.

In order to confirm the hypothesis about the reaction with benzyl alcohol and 5-HMF, they were repeated neat, without using a solvent but keeping the reaction temperature at 177 °C below the corresponding reflux temperatures. Results not reported, showed that keeping the temperature to 150 °C and below *p*-cymene reflux temperature, it didn't show any relevant conversion.

The reaction was performed in a distillation apparatus and the product was isolated in a separate flask. The reaction eventually afforded a measurable quantity of the two products, as reported in Table 3.11.

Table 3.11: Reaction under neat condition in distillation apparatus.

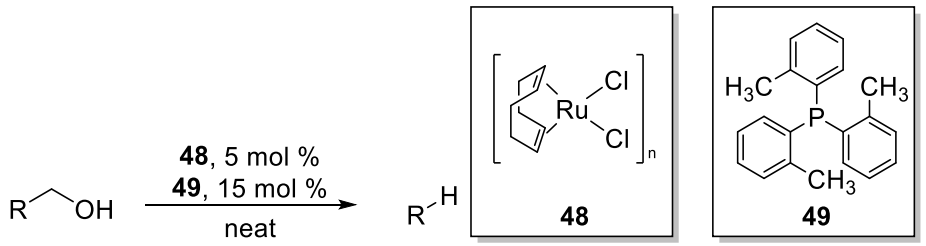

Entry	Substrate	Product	Time (h)	mmol product	TON
1	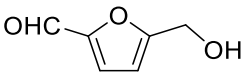	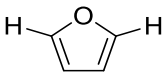	16	0.83	17
2	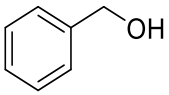	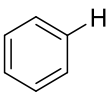	16	0.60	12

*[a] Reaction conditions: Alcohol (2.0 grams as solvent), catalyst **48** (0.05 mmol), ligand **49** (0.15 mmol), 177 °C and nitrogen stream.*

The experiment for determining the reaction conditions and their limitations made us wonder about a possible mechanism of the reaction. Some experiments to elucidate the different aspects of the reaction steps are presented in the next paragraphs.

3.2.8 Identification of the intermediate and gaseous products

The first insight into the reaction pathway came from naphthalene methanol where the intermediate aldehyde was always observed under the reaction conditions and it accumulated in the early stage of the reaction reaching 20 % of the reaction components. This suggested that aldehyde dissociation occurs from the catalyst in a reversible fashion and decarbonylation is not such faster than dehydrogenation.

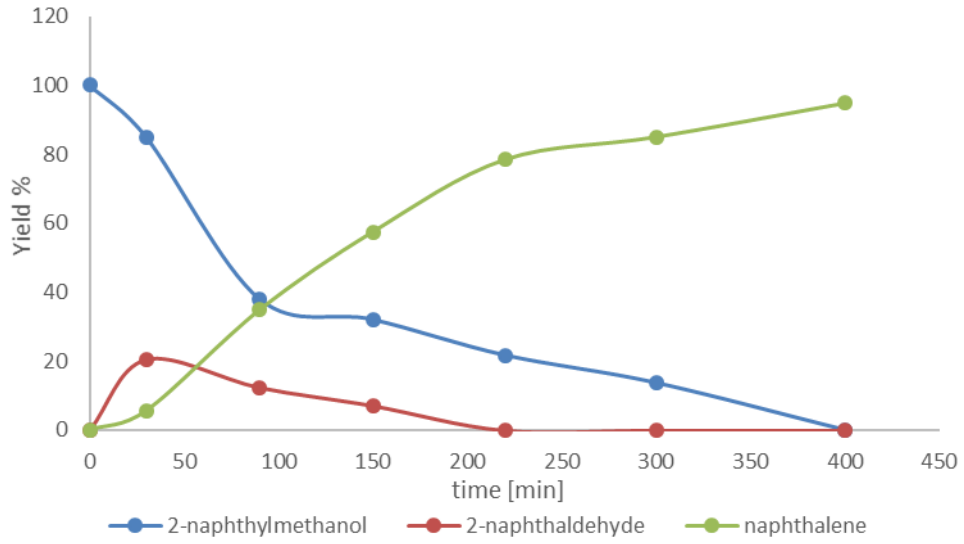

Figure 3.10: Reaction species evolution over time

The reaction proved to be a tandem process in which every step is independent. Furthermore, this result was evident by the fact that the aldehyde also reacted under the same reaction conditions to afford the product.

So far, the reaction was studied only considering the products generated in the solution phase, but as already mentioned, also syngas is expected from the reaction and therefore experiments were run in order to measure and identify the gas mixture.

The volume of the gas developed from the dehydrogenative decarbonylation of naphthyl methanol carried out in a Schlenk tube was measured by connecting the tube to a burette filled with water.

The usual reaction conditions were employed (1.0 mmol of 2-naphthyl methanol) which were supposed to release two equivalent of gas that at 20 °C and at 1 atm occupies a volume of (24.7 mL x 2) = 49.4 mL.

From this experiment, a value of 37.5 mL was obtained, corresponding to 76% of the expected yield of the gas, confirming the formation of two moles of gas for every mole of converted substrate, within the error that needs to be considered such as the possible diffusion of hydrogen gas out of the system.

The nature of the gas was confirmed by utilizing a two-chamber connected vessel (like the one displayed in Figure 3.3). Chamber A was charged with naphthalene methanol, the catalyst **48** and ligand **49**, followed by the addition of an equivalent of diphenyl acetylene as hydrogen scavenger. In chamber B the iridium dimeric complex $[Ir(COD)Cl]_2$ was allowed to react with triphenyl phosphine and carbon monoxide developed from chamber A. The formation of a mixture of *trans* and *cis* stilbene in chamber A and the isolation of Vaska's complex in chamber B confirmed the formation of hydrogen and CO, respectively. It is reported that $[Ir(COD)Cl]_2$ in the presence of triphenyl phosphine and CO can form the yellow complex $Ir(CO)_2(PPh_3)_2Cl$ that precipitates in solution. After evaporation of the solvent under reduce pressure, Vaska's complex was identified although the yield was not determined.[138]

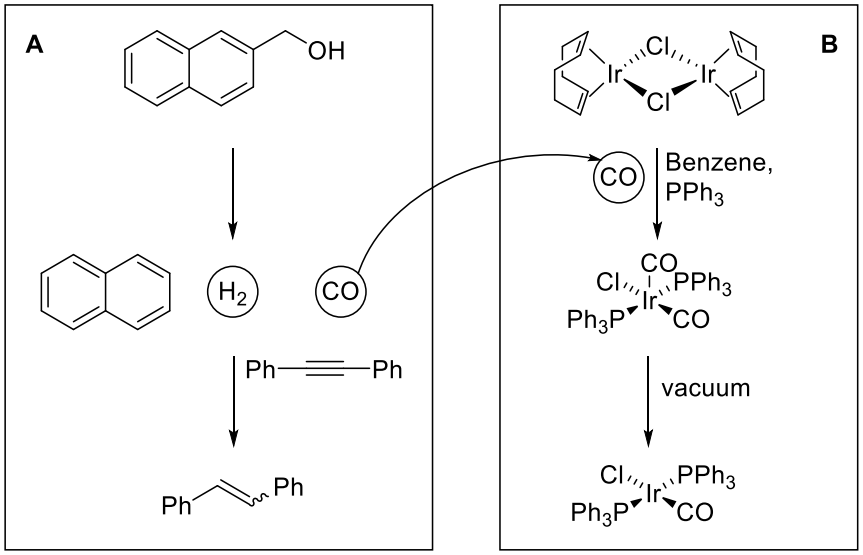

Scheme 3.18: Experiment for the identification of hydrogen in box A and carbon monoxide in box B

3.2.9 Experiments with deuterium labelled substrate

A deeper understanding of the reaction mechanism can arise from the evaluation of some kinetic parameters like the catalyst reaction order and the kinetic isotopic effect (KIE).

Several reactions were run for calculating the catalyst reaction order by keeping constant the concentration of all reagents except for the catalyst-ligand couple that were added in increasing amounts from approximately 0.01 to 0.06 mmol (Figure 3.11).

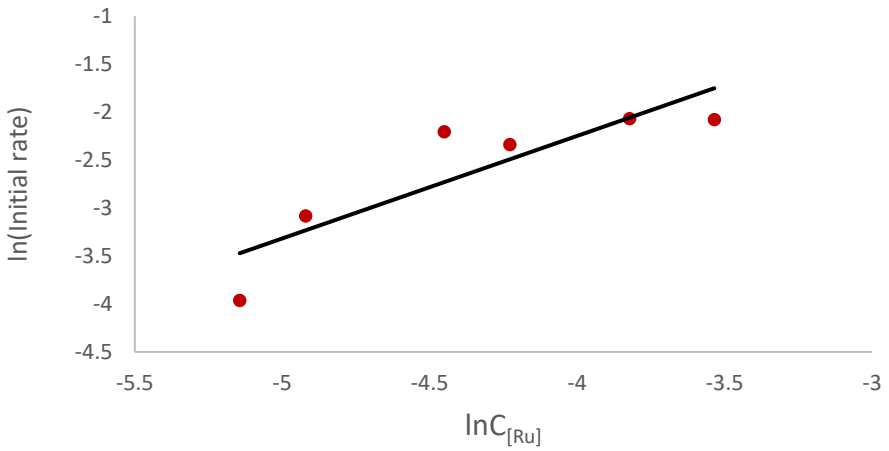

Figure 3.11: Reaction order in ruthenium catalyst.

The plot of the logarithm of the initial rates as a function of the logarithm of the concentration afforded the reaction order as a slope of the resulting line. This resulted in a slope of 1.07 typical of a first order kinetic pathway.

The kinetic isotopic effect was evaluated by measuring naphthalene formation over time when 2-naphthalene methanol or 2-naphtalene methanol-α,α-d_2 were allowed react under the reaction conditions in two non-competitive experiments. The comparison of the initial rates of the two reactions afforded a value k_H/k_D equal to 2.15.

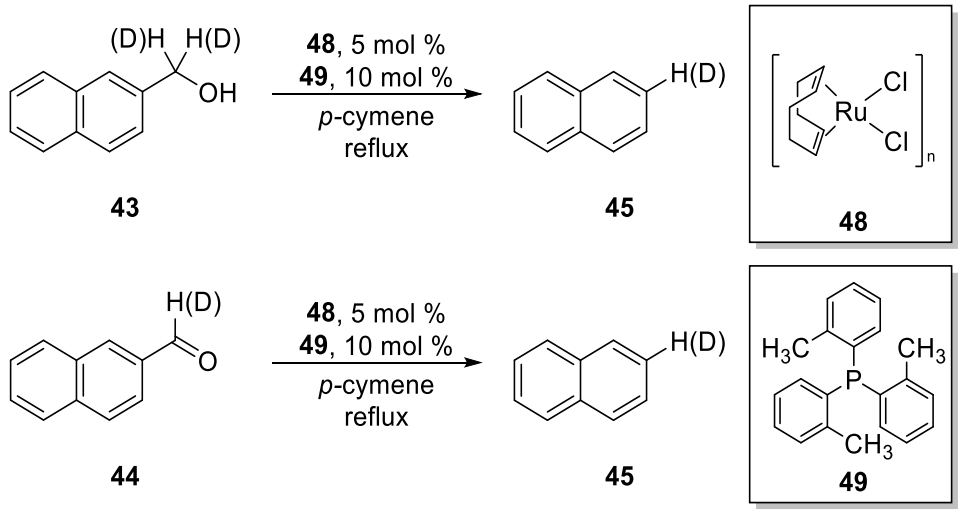

Scheme 3.19: Reaction with deuterium labelled substrates

In the same way when the reaction initial rates for the conversion of 2-naphthaldehyde and its deuterium labeled counterpart were determined, the corresponding a k_H/k_D could be calculated to a value of 1.16.

As we can immediately observe, a small value of KIE of 1.16 for the reaction of the decarbonylation of 2-naphtaldehyde incanted a typical secondary isotope effect. It showed that a breakage of the C-H(D) bond was not affected in the rate-determining step or in a step prior to that. If we assume that the decarbonylation occurs through a sequence of steps involving a C-H insertion of the metal, a migratory extrusion of the carbonyl group we can exclude the C-H insertion as the rate determining step leaving the migratory exclusion as an option. In fact, if we consider typical values of KIE for C-H activation in aromatic compounds they line up with a larger value around 2.5.[139,140]

It follows that the main contribution to the kinetic isotope effect is due to the dehydrogenation step. Although the small value of 2.15, in between a typical primary

and secondary isotope effect, indicates that the early step of β-hydride elimination must be fast and reversible.

3.2.10 Conclusions

In conclusion, a ruthenium-catalyzed protocol for the dehydrogenative decarbonylation of primary alcohols was described, where dihydrogen and carbon monoxide (syngas) were released. The transformation employed 5% of $[Ru(COD)Cl_2]_n$ and 15% of P(*o*-tolyl)$_3$ in refluxing *p*-cymene and could be applied to both benzylic and non-benzylic primary alcohols. The reaction suffered limitations due to the high boiling point of the solvent, however both high boiling hydrocarbons and syngas derived from simpler substrates could be isolated. Considerations about the mechanism were reported suggesting that the two reactions involved (dehydrogenation and decarbonylation) follow two independent catalytic cycles. Moreover, the decarbonylation path seemed more likely to contain the rate-determining step.

3.3 EXPERIMENTAL SECTION

General methods

Reaction solvents were all dried using 3 Å molecular sieves and then degassed by three freeze-pump-thaw cycles. All other solvents were of HPLC grade and were not further purified and all chemicals were purchased from Sigma Aldrich. Column chromatography separations were performed on silica gel (220 - 440 mesh). Thin layer chromatography (TLC) was performed on aluminum sheets precoated with silica gel (Merck 25, 20 × 20 cm, 60 F254). The plates were visualized under UV-light. Reactions were monitored by gas chromatography on a Shimadzu GC-MS-QP2012S instrument equipped with an Equity-5, 30mm × 0.25mm × 0.25μm column. Nonane was used as the internal standard and GC yields were determined with the following equations:

$$y(\%) = k_X \cdot \frac{A_X}{A_0} \cdot \frac{m_X}{MW_0} \cdot \frac{MW_s}{m_s} \cdot 100$$

$$\frac{n_X}{n_0} = k_X \cdot \frac{A_X}{A_0}$$

Where A_X = product peak's area, A_0 = standard peak's area, m_0 = mass (mg) of the internal standard in the reaction mixture, MW_0 = molecular weight of the internal standard, m_s = mass (mg) of the initial substrate, MWs = molecular weight of the initial substrate, k = value extrapolated by the product's calibration curve determined plotting n_X/n_0 as function of A_X/A_0 where n_X and n_0 are number of moles of compound X and standard.

NMR spectra were recorded on a Bruker Ascend 400 spectrometer. Chemical shifts were measured relative to the signals of residual $CHCl_3$ (δ_H = 7.26 ppm) and $CDCl_3$

(δ_C = 77.16 ppm). Multiplicity are reported as s = singlet, d = doublet, t = triplet, q = quartet, dd = double doublet, dt = double triplet, dq = double quartet, ddt = double double triplet, m = multiplet, br. s = broad singlet, while coupling constants are shown in Hz. HRMS measurements were made using ESI with TOF detection.

3.3.1 Procedure for Dehydrogenative Decarbonylation

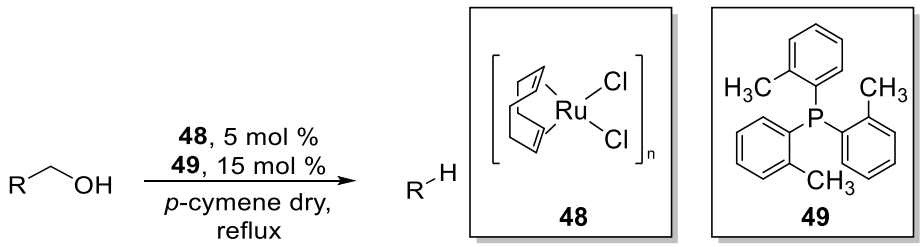

The primary alcohol (1.0 mmol), $Ru(COD)Cl_2$ (14 mg, 0.05 mmol), P(*o*-tolyl)$_3$ (45 mg, 0.15 mmol) and a stir bar were placed in a dry Schlenk tube equipped with a cold finger and connected to the vacuum line. The tube was evacuated and filled with nitrogen three times, followed by addition of decane (50 mg, internal standard) and *p*-cymene (2 mL). The mixture was heated on an oil bath to reflux under a flow of nitrogen and the reaction was monitored by GC-MS. The yield was determined by GC-MS via the internal standard or by evaporation of the solvent and purification of the residue by flash chromatography (pentane/EtOAc, 95:5).

Benzyloxybenzene (**52e**): Isolated as a white solid. ^{1}H NMR (400 MHz, $CDCl_3$) δ = 7.53-7.49 (m, 2H), 7.48-7.43 (m, 2H), 7.41-7.34 (m, 3H), 7.07-7.02 (m, 3H), 5.13 (s, 2H) ppm. ^{13}C NMR (100 MHz, $CDCl_3$) δ = 158.9, 137.2, 129.6, 128.7, 128.0, 127.6, 121.1, 115.0, 70.0 ppm. Spectral data are in accordance with reported data. [141]

1,3-Bis(benzyloxy)benzene (**52f**): Isolated as a white solid. ^{1}H NMR (400 MHz, $CDCl_3$) δ = 7.32-7.27 (m, 5H), 7.37-7.26 (m, 5H), 7.06 (t, J = 8.1 Hz, 1H), 6.52 (t, J = 2.3 Hz, 1H), 6.52 (dd, J = 2.3, 8.1 Hz, 2H), 4.91 (s, 4H) ppm. ^{13}C NMR (100 MHz,

$CDCl_3$) δ = 160.2, 137.1, 130.1, 128.7, 128.1, 127.7, 107.5, 102.4, 70.2 ppm. Spectral data are in accordance with reported data.[142]

3.3.2 Identification of the intermediate and gaseous products

A two chamber setup was employed for determining the nature of the gas mixture developed. Chamber A, the syngas producing chamber, was equipped with a cold finger and was charged with 158 mg of 2-naphthyl methanol (1.0 mmol), 14 mg of $Ru(COD)Cl_2$ (0.05 mmol), 45 mg of P(*o*-tolyl)$_3$ (0.15 mmol), 178 mg of diphenylacetylene (1.0 mmol) and *p*-cymene (2 mL). Chamber B was charged with 67 mg of $[Ir(COD)Cl]_2$ (0.1 mmol, 0.2 equivalents), 105 mg of PPh_3 (0.4 mmols) and 3 mL of benzene as solvent. Chamber A was heated for 8 hours at 177 °C. After this time, a sample of the solution contained in chamber A was analyzed by GC-MS, where *cis* and *trans* stilbene were determined although not quantified. The solid present in chamber B was filtered, washed with hexane and identified as Vaska's complex by IR spectroscopy and ^{31}P NMR.

^{31}P NMR (202 MHz, $CDCl_3$) δ = 29.4. IR: ν (CO) = 1955 cm^{-1}. In accordance with literature data.[138]

3.3.3 Determining reaction order in catalyst

Each reaction was conducted by placing 2-naphthylmethanol (1.0 mmol), decane (50 mg, internal standard) and a stir bar in a dry Schlenk tube equipped with a cold finger and connected to the vacuum line. A standard solution of $Ru(COD)Cl_2$ (700 mg, 2.5 mmol) and P(*o*-tolyl)$_3$ (2.3 g, 7.5 mmol) in 10 mL of *p*-cymene was prepared and added in different aliquots to each reaction tube followed by an additional amount of *p*-cymene to obtain a volume of 2 mL. The tubes were placed in a preheated oil bath at a temperature of 177 °C under a flow of nitrogen and the reactions were monitored by GC-MS. The yields were determined by GC-MS via the internal standard.

3.3.4 Determining kinetic isotope effect with 2-naphthylmethanol

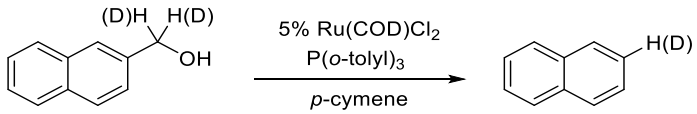

$Ru(COD)Cl_2$ (14 mg, 0.05 mmol), P(*o*-tolyl)$_3$ (45 mg, 0.15 mmol) and a stir bar were placed in two different Schlenck tubes equipped with cold fingers and connected to the vacuum line. Then either 158 mg of 2-naphthylmethanol (1.0 mmol) or 160 mg of α,α-d_2-2-naphthylmethanol (1.0 mmol) were added. The tubes were evacuated and filled with nitrogen three times, followed by addition of decane (50 mg, internal standard) and *p*-cymene (2 mL). The tubes were placed in a preheated oil bath at a temperature of 177 °C under a flow of nitrogen and the reactions were monitored by GC-MS. The yields were determined by GC-MS via the internal standard.

KIE = k_H/k_D = 0.8697/0.4044 = **2.15**

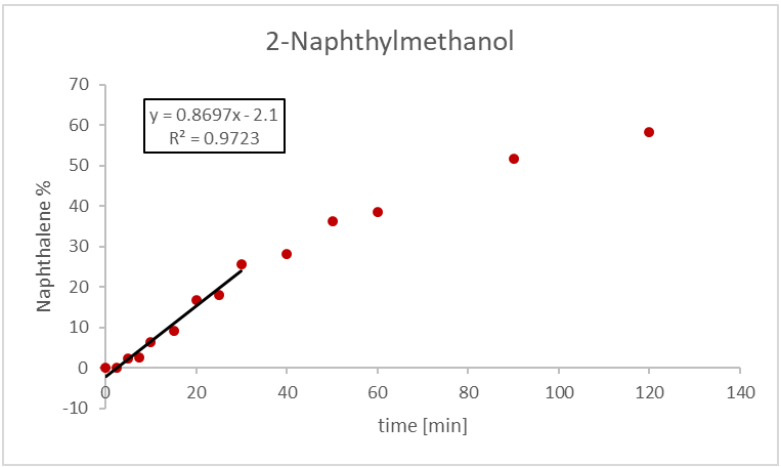

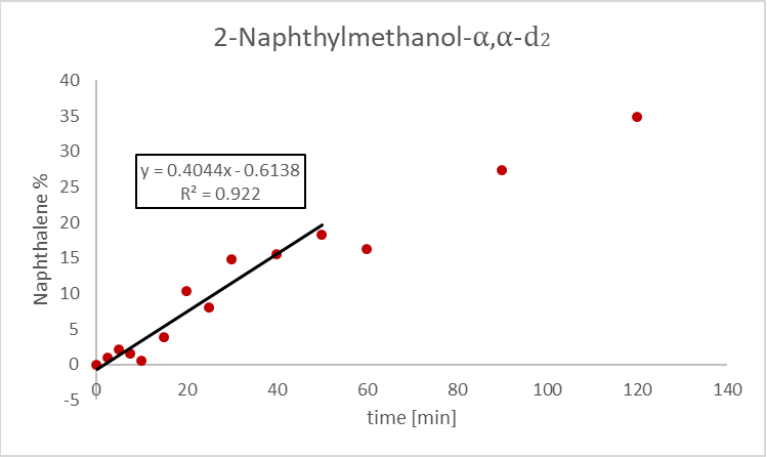

3.3.5 Determining kinetic isotope effect with 2-naphthaldehyde

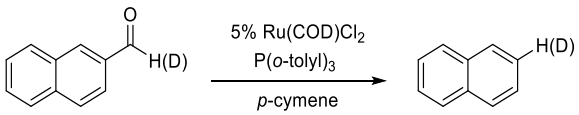

$Ru(COD)Cl_2$ (14 mg, 0.05 mmol), P(*o*-tolyl)$_3$ (45 mg, 0.15 mmol) and a stir bar were placed in two different Schlenck tubes equipped with cold fingers and connected to the vacuum line. Then either 156 mg of 2-naphthaldehyde (1.0 mmol) or 157 mg of α-d-2-naphthaldehyde (1.0 mmol) were added. The tubes were evacuated and filled with nitrogen three times, followed by addition of decane (50 mg, internal standard) and *p*-cymene (2 mL). The tubes were placed in a preheated oil bath at a temperature of 177 °C under a flow of nitrogen and the reactions were monitored by GC-MS. The yields were determined by GC-MS via the internal standard.

KIE = k_H/k_D = 1.2657/1.0884 = **1.16**

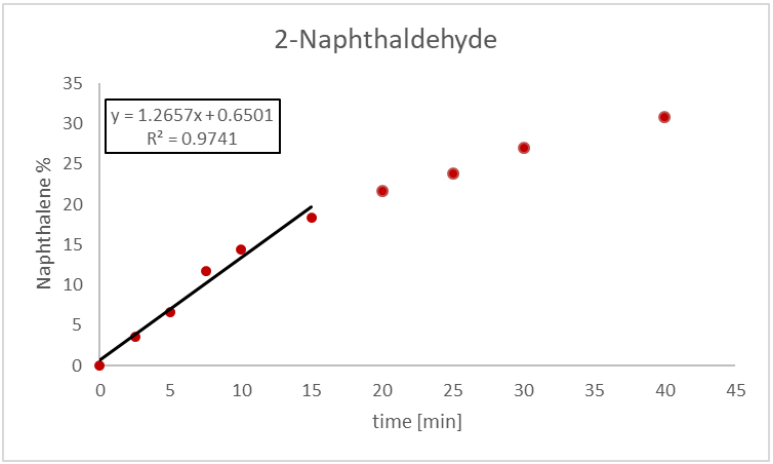
2-Naphthaldehyde
y = 1.2657x + 0.6501
R² = 0.9741
Naphthalene %
time [min]
0
5
10
15
20
25
30
35
40
45

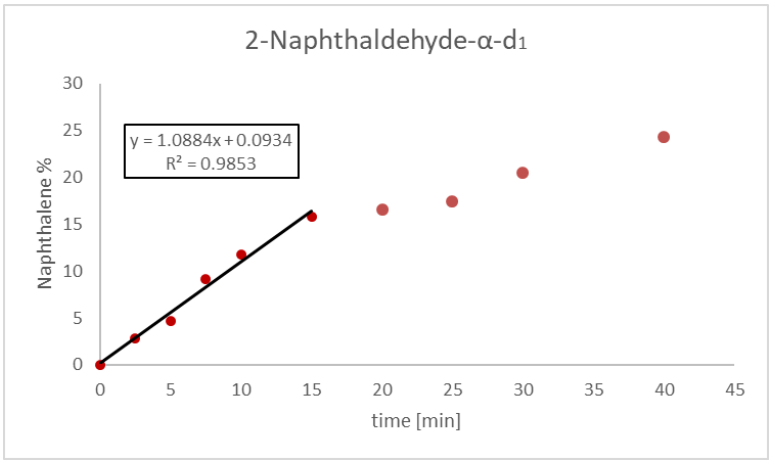
2-Naphthaldehyde-α-d1
y = 1.0884x + 0.0934
R² = 0.9853
Naphthalene %
time [min]
0
5
10
15
20
25
30
35
40
45

4 PUBLICATIONS

The work contained in this thesis yielded two scientific publications in peer-reviewed journals available on journal websites together to the corresponding supplementary information and spectral data:

- "**Synthetic Applications and Mechanistic Studies of the Hydroxide-Mediated Cleavage of Carbon–Carbon Bonds in Ketones**"
  Mazziotta, A.; Makarov, I. S.; Fristrup, P.; Madsen, R. *J. Org. Chem.* **2017**, *82* (11), 5890–5897.

- "**Ruthenium-Catalyzed Dehydrogenative Decarbonylation of Primary Alcohols**"
  Mazziotta, A.; Madsen, R. *European J. Org. Chem.* **2017**, (36), 5417–5420.

5 BIBLIOGRAPHY

(1) Guthrie, J. P.; Cossar, J. *Can. J. Chem.* **1986**, *64* (6), 1250–1266.

(2) Haynes William M. *CRC Handbook of Chemistry and Physics*, 96th illus.; Haynes, W. M., Ed.; CRC Press, 2015.

(3) Masahiro Murakami, N. I. *Cleavage of Carbon-Carbon Single Bonds by Transition Metals*; Murakami, M., Naoto Chatani, Eds.; Wiley-VCH Verlag GmbH & Co. KGaA: Weinheim, Germany, 2015.

(4) Jun, C.-H. *Chem. Soc. Rev.* **2004**, *33* (9), 610–618.

(5) Murakami, M.; Amii, H.; Shigeto, K.; Ito, Y. *J. Am. Chem. Soc.* **1996**, *118* (35), 8285–8290.

(6) Murakami, M.; Itahashi, T.; Ito, Y. *J. Am. Chem. Soc.* **2002**, *124* (47), 13976–13977.

(7) Halcrow, M. A.; Urbanos, F.; Chaudret, B. *Organometallics* **1993**, *12* (3), 955–957.

(8) Murakami, M.; Tsuruta, T.; Ito, Y. *Angew. Chem. Int. Ed.* **2000**, *39* (14), 2484–2486.

(9) Monrad, R. N.; Madsen, R. *J. Org. Chem.* **2007**, *72* (25), 9782–9785.

(10) Zhang, F.; Spring, D. R. *Chem. Soc. Rev.* **2014**, *43* (20), 6906–6919.

(11) Rousseau, G.; Breit, B. *Angew. Chem. Int. Ed.* **2011**, *50* (11), 2450–2494.

(12) Cornella, J.; Righi, M.; Larrosa, I. *Angew. Chem. Int. Ed.* **2011**, *50* (40), 9429–9432.

(13) Luo, J.; Preciado, S.; Larrosa, I. *J. Am. Chem. Soc.* **2014**, *136* (11), 4109–4112.

(14) Bart, S. C.; Chirik, P. J. *J. Am. Chem. Soc.* **2003**, *125* (4), 886–887.

(15) Fessard, T. C.; Andrews, S. P.; Motoyoshi, H.; Carreira, E. M. *Angew. Chem. Int. Ed.* **2007**, *46* (48), 9331–9334.

(16) Paquin, J.-F.; Defieber, C.; Stephenson, C. R. J.; Carreira, E. M. *J. Am. Chem. Soc.* **2005**, *127* (31), 10850–10851.

(17) ten Dam, J.; Hanefeld, U. *ChemSusChem* **2011**, *4* (8), 1017–1034.

(18) Modak, A.; Maiti, D. *Org. Biomol. Chem.* **2016**, *14* (1), 21–35.

(19) Rosatella, A. A.; Simeonov, S. P.; Frade, R. F. M.; Afonso, C. A. M. *Green Chem.* **2011**, *13* (4), 754–793.

(20) Rackemann, D. W.; Doherty, W. O. *Biofuels, Bioprod. Biorefining* **2011**, *5* (2), 198–214.

(21) Huang, Y.-B.; Yang, Z.; Chen, M.-Y.; Dai, J.-J.; Guo, Q.-X.; Fu, Y. *ChemSusChem* **2013**, *6* (8), 1348–1351.

(22) Geilen, F. M. A.; vom Stein, T.; Engendahl, B.; Winterle, S.; Liauw, M. A.; Klankermayer, J.; Leitner, W. *Angew. Chem. Int. Ed.* **2011**, *50* (30), 6831–6834.

(23) Artamkina, G. A.; Beletskaya, I. P. *Russ. Chem. Rev.* **1987**, *56* (10), 983–1001.

(24) Day, J. N. E.; Ingold, C. K. *Trans. Faraday Soc.* **1941**, *37*, 686–707.

(25) Douglas, J. E.; Campbell, G.; Wigfield, D. C. *Can. J. Chem.* **1993**, *71* (11), 1841–1844.

(26) Hills, H. W. J.; Kenyon, J.; Phillips, H. *J. Chem. Soc.* **1936**, 576–583.

(27) Kenyon, J.; Partridge, S. M.; Phillips, H. *J. Chem. Soc.* **1936**, 85–88.

(28) O'Connor, C. *Q. Rev. Chem. Soc.* **1970**, *24* (4), 553–564.

(29) Cannizzaro, S. *Ann. der Chemie und Pharm.* **1853**, *88* (1), 129–130.

(30) Geissman, T. A.; Geissman; A., T. In *Organic Reactions*; John Wiley & Sons, Inc.: Hoboken, NJ, USA, 2011; pp 94–113.

(31) Guthrie, J. P.; Cossar, J. *Can. J. Chem.* **1990**, *68* (9), 1640–1642.

(32) Zucco, C.; Lima, C. F.; Rezende, M. C.; Vianna, J. F.; Nome, F. *J. Org. Chem.* **1987**, *52* (24), 5356–5359.

(33) Symons, E. A.; Clermont, M. J. *J. Am. Chem. Soc.* **1981**, *103* (11), 3127–3130.

(34) Rahil, J.; Pratt, R. F. *J. Am. Chem. Soc.* **1977**, *99* (8), 2661–2665.

(35) Fedor, L. R.; Murty, B. S. R.; De, N. C. *J. Am. Chem. Soc.* **1975**, *97* (15), 4308–4312.

(36) Pearson, R. G.; Mayerle, E. A. *J. Am. Chem. Soc.* **1951**, *73* (3), 926–930.

(37) Pearson, R. G.; Sandy, A. C. *J. Am. Chem. Soc.* **1951**, *73* (3), 931–934.

(38) Jaramillo, P.; Domingo, L. R.; Pérez, P. *Chem. Phys. Lett.* **2006**, *420* (1), 95–99.

(39) Xie, H.-Q.; Truong, N.; Buncel, E.; Purdon, J. G. *Can. J. Chem.* **1994**, *72* (2), 448–453.

(40) Stirling, C. J. M. *Acc. Chem. Res.* **1979**, *12* (6), 198–203.

(41) Lienhard, G. E.; Jencks, W. P. *J. Am. Chem. Soc.* **1965**, *87* (17), 3855–3862.

(42) Hibbert, F.; Satchell, D. P. N. *J. Chem. Soc. B Phys. Org.* **1967**, 653–660.

(43) Hine, J.; Koser, G. F. *J. Org. Chem.* **1971**, *36* (10), 1348–1351.

(44) Stranberg, M.; Anselme, J.-P. *J. Chem. Educ.* **1990**, *67* (7), 616.

(45) Danilov, S. *J. Russ. Phys. Chem.* **1917**, *83*, 282–288.

(46) Forbes, E. J.; Gregory, M. J. *J. Chem. Soc. B Phys. Org.* **1968**, 205–207.

(47) Bunnett, J. F.; Miles, J. H.; Nahabedian, K. V. *J. Am. Chem. Soc.* **1961**, *83* (11), 2512–2516.

(48) Bachmann, W. E. *J. Am. Chem. Soc.* **1935**, *57* (4), 737–738.

(49) Bunnett, J. F.; Connor, D. S.; O'Reilly, K. J. *J. Org. Chem.* **1979**, *44* (23), 4197–4199.

(50) Bunnett, J. F.; Hrutfiord, B. F. *J. Org. Chem.* **1962**, *27* (12), 4152–4156.

(51) Davies, D. G.; Derenberg, M.; Hodge, P. *J. Chem. Soc. C Org.* **1971**, 455–460.

(52) Mehta, G.; Venkateswaran, R. V. *Tetrahedron* **2000**, *56* (11), 1399–1422.

(53) Ishihara, K.; Yano, T. *Org. Lett.* **2004**, *6* (12), 1983–1986.

(54) Asao, T.; Machiguchi, T.; Kitamura, T.; Kitahara, Y. *J. Chem. Soc. D Chem. Commun.* **1970**, *2*, 89–90.

(55) Santilli, C.; Makarov, I. S.; Fristrup, P.; Madsen, R. *J. Org. Chem.* **2016**, *81* (20), 9931–9938.

(56) Mittra, A.; Bhowmik, D. R.; Venkateswaran, R. V. *J. Org. Chem.* **1998**, *63* (25), 9555–9556.

(57) Siegfried R Waldvogel. *Ann. der Chemie und Pharm.* **1849**, *72* (3), 279–282.

(58) Hughes, D. L.; Reamer, R. A.; Bergan, J. J.; Grabowski, E. J. J. *J. Am. Chem.*

Soc. **1988**, *110* (19), 6487–6491.

(59) He, C.; Guo, S.; Huang, L.; Lei, A. *J. Am. Chem. Soc.* **2010**, *132* (24), 8273–8275.

(60) Sifton, W.; Stothers, J. B.; Thomas, S. E. *Can. J. Chem.* **1992**, *70* (5), 1274–1280.

(61) Reichle, M. A.; Breit, B. *Angew. Chem. Int. Ed.* **2012**, *51* (23), 5730–5734.

(62) Haffemayer, B.; Gulias, M.; Gaunt, M. J. *Chem. Sci.* **2011**, *2* (2), 312–315.

(63) Nedenskov, P.; Taub, W.; Ginsburg, D.; Hartiala, K.; Veige, S.; Diczfalusy, E. *Acta Chem. Scand.* **1958**, *12*, 1405–1410.

(64) Kano, T.; Hayashi, Y.; Maruoka, K. *J. Am. Chem. Soc.* **2013**, *135* (19), 7134–7137.

(65) Owen, C. P.; Shahid, I.; Olusanjo, M. S.; Patel, C. H.; Dhanani, S.; Ahmed, S. *J. Steroid Biochem. Mol. Biol.* **2008**, *111* (1–2), 117–127.

(66) Weix, D. J.; Dreher, S. D.; Katz, T. J. *J. Am. Chem. Soc.* **2000**, *122* (41), 10027–10032.

(67) Lim, M.; De Castro, K. A.; Oh, S.; Lee, K.; Chang, Y.-W.; Kim, H.; Rhee, H. *Appl. Organomet. Chem.* **2011**, *25* (1), 1–8.

(68) Hassner, A.; Ruse, M.; Gottlieb, H. E.; Cojocaru, M. *J. Chem. Soc. Perkin Trans. 1* **1988**, *4*, 733–437.

(69) Bochevarov, A. D.; Harder, E.; Hughes, T. F.; Greenwood, J. R.; Braden, D. a.; Philipp, D. M.; Rinaldo, D.; Halls, M. D.; Zhang, J.; Friesner, R. A. *Int. J. Quantum Chem.* **2013**, *113* (18), 2110–2142.

(70) Eisch, J. J. *Organometallics* **2002**, *21* (25), 5439–5463.

(71) Linthorst, J. A. *Found. Chem.* **2010**, *12* (1), 55–68.

(72) Ojima, I.; Tsai, C.-Y.; Tzamarioudaki, M.; Bonafoux, D. In *Organic Reactions*; John Wiley & Sons, Inc.: Hoboken, NJ, USA, 2000; pp 1–354.

(73) Evans, D.; Osborn, J. A.; Jardine, F. H.; Wilkinson, G. *Nature* **1965**, *208* (5016), 1203–1204.

(74) Banks, R. L.; Bailey, G. C. *Ind. Eng. Chem. Prod. Res. Dev.* **1964**, *3* (3), 170–173.

(75) Jean-Louis Hérisson, P.; Chauvin, Y. *Die Makromol. Chemie* **1971**, *141* (1), 161–176.

(76) Astruc, D. *New J. Chem.* **2005**, *29* (1), 42–56.

(77) Negishi, E. *Angew. Chem. Int. Ed.* **2011**, *50* (30), 6738–6764.

(78) Crabtree, R. H. *The organometallic chemistry of the transition metals*; Wiley, 2009.

(79) Hartwig, J. F. *Organotransition metal chemistry: from bonding to catalysis*, 2010 Ed.; University Science Books, 2010.

(80) Gavriluta, A.; Büchel, G. E.; Freitag, L.; Novitchi, G.; Tommasino, J. B.; Jeanneau, E.; Kuhn, P.-S.; González, L.; Arion, V. B.; Luneau, D. *Inorg. Chem.* **2013**, *52* (11), 6260–6272.

(81) Oppenauer, R. V. *Recl. Trav. Chim. Pays-Bas* **1937**, *56* (2), 137–144.

(82) Morton, D.; Cole-Hamilton, D. J. *J. Chem. Soc., Chem. Commun.* **1987**, No. 4, 248–249.

(83) Charman, H. B. *J. Chem. Soc. B* **1970**, 584–587.

(84) Ligthart, G. B. W. L.; Meijer, R. H.; Donners, M. P. J.; Meuldijk, J.; Vekemans, J. A. J. M.; Hulshof, L. A. *Tetrahedron Lett.* **2003**, *44* (7), 1507–1509.

(85) Dobscn, A.; Robinson, S. D. *J. Organomet. Chem.* **1975**, *87* (3), C52–C53.

(86) Zhang, J.; Gandelman, M.; Shimon, L. J. W.; Rozenberg, H.; Milstein, D. *Organometallics* **2004**, *23* (17), 4026–4033.

(87) Zhang, J.; Balaraman, E.; Leitus, G.; Milstein, D. *Organometallics* **2011**, *30* (21), 5716–5724.

(88) Fujita, K.; Tanino, N.; Yamaguchi, R. *Org. Lett.* **2007**, *9* (1), 109–111.

(89) Moran, J.; Preetz, A.; Mesch, R. A.; Krische, M. J. *Nat. Chem.* **2011**, *3* (4), 287–290.

(90) Zhang, G.; Hanson, S. K. *Org. Lett.* **2013**, *15* (3), 650–653.

(91) Chakraborty, S.; Lagaditis, P. O.; Förster, M.; Bielinski, E. A.; Hazari, N.; Holthausen, M. C.; Jones, W. D.; Schneider, S. *ACS Catal.* **2014**, *4* (11), 3994–4003.

(92) Makarov, I. S.; Madsen, R. *J. Org. Chem.* **2013**, *78* (13), 6593–6598.

(93) Sølvhøj, A.; Madsen, R. *Organometallics* **2011**, *30* (21), 6044–6048.

(94) Nordstrøm, L. U.; Vogt, H.; Madsen, R. *J. Am. Chem. Soc.* **2008**, *130* (52), 17672–17673.

(95) Maggi, A.; Madsen, R. *Organometallics* **2012**, *31* (1), 451–455.

(96) Gunanathan, C.; Milstein, D. *Science* **2013**, *341* (6143), 1229712.

(97) Johansson, A. J.; Zuidema, E.; Bolm, C. *Chem. Eur. J.* **2010**, *16* (45), 13487–13499.

(98) Sieffert, N.; Buuhl, M. *J. Am. Chem. Soc.* **2010**, *132* (23), 8056–8070.

(99) Garralda, M. A.; Yamada, T.; Matsuo, T.; Watanabe, K.; Katoh, T.; Liable-Sands, L. M.; Rheingold, A. L.; Braunstein, P.; Coco, S.; Skelton, B. W.; White, A. H. *Dalton Trans.* **2009**, *8* (19), 3635–3645.

(100) Tsuji, J.; Ohno, K. *Tetrahedron Lett.* **1965**, *6* (44), 3969–3971.

(101) Louis M. Pignolet. *Homogeneous Catalysis with Metal Phosphine Complexes*; Pignolet, L. H., Ed.; Springer, Boston, MA: Boston, MA, 1983.

(102) Ding, K.; Xu, S.; Alotaibi, R.; Paudel, K.; Reinheimer, E. W.; Weatherly, J. *J. Org. Chem.* **2017**, *82* (9), 4924–4929.

(103) Beck, C. M.; Rathmill, S. E.; Park, Y. J.; Chen, J.; Crabtree, R. H.; Liable-Sands, L. M.; Rheingold, A. L. *Organometallics* **1999**, *18* (25), 5311–5317.

(104) Kreis, M.; Palmelund, A.; Bunch, L.; Madsen, R. *Adv. Synth. Catal.* **2006**, *348* (15), 2148–2154.

(105) Fristrup, P.; Kreis, M.; Palmelund, A.; Norrby, P.-O.; Madsen, R. *J. Am. Chem. Soc.* **2008**, *130* (15), 5206–5215.

(106) Iwai, T.; Fujihara, T.; Tsuji, Y. *Chem. Commun.* **2008**, *46*, 6215–6217.

(107) Domazetis, G.; Tarpey, B.; Dolphin, D.; James, B. R. *J. Chem. Soc. Chem. Commun.* **1980**, *20*, 939–940.

(108) Rettig, J.; Rettig, J.; Rettig, J.; Belani, R. M.; James, B. R.; Dolphin, D.; Rettig, S. J. *Can. J. Chem.* **1988**, *66* (8), 2072–2078.

(109) Kondo, T.; Akazome, M.; Tsuji, Y.; Watanabe, Y. *J. Org. Chem.* **1990**, *55* (4), 1286–1291.

(110) de Vries, J. G.; Roelfes, G.; Green, R. *Tetrahedron Lett.* **1998**, *39* (45), 8329–8332.

(111) Murahashi, S.; Naota, T.; Ito, K.; Maeda, Y.; Taki, H. *J. Org. Chem.* **1987**, *52* (19), 4319–4327.

(112) Ho, H.-A.; Manna, K.; Sadow, A. D. *Angew. Chem. Int. Ed.* **2012**, *51* (34), 8607–8610.

(113) Obora, Y.; Anno, Y.; Okamoto, R.; Matsu-ura, T.; Ishii, Y. *Angew. Chem. Int. Ed. Engl.* **2011**, *50* (37), 8618–8622.

(114) Olsen, E. P. K.; Madsen, R. *Chem. Eur. J.* **2012**, *18* (50), 16023–16029.

(115) Olsen, E. P. K.; Singh, T.; Harris, P.; Andersson, P. G.; Madsen, R. *J. Am. Chem. Soc.* **2015**, *137* (2), 834–842.

(116) Verendel, J. J.; Nordlund, M.; Andersson, P. G. *ChemSusChem* **2013**, *6* (3), 426–429.

(117) Christensen, S. H.; Olsen, E. P. K.; Rosenbaum, J.; Madsen, R. *Org. Biomol. Chem.* **2015**, *13* (3), 938–945.

(118) Hermange, P.; Lindhardt, A. T.; Taaning, R. H.; Bjerglund, K.; Lupp, D.; Skrydstrup, T. *J. Am. Chem. Soc.* **2011**, *133* (15), 6061–6071.

(119) Rostrup-Nielsen, J. R. *Catal. Today* **1993**, *18* (4), 305–324.

(120) Rostrup-Nielsen, J. R. *Catal. Today* **2000**, *63* (2–4), 159–164.

(121) Ogden, J. M. *Annu. Rev. Energy Environ.* **1999**, *24* (1), 227–279.

(122) Wright, T, I.; Gibbons, T. *Int. J. Hydrogen Energy* **2007**, *32* (16), 3610–3621.

(123) Walton, S. M.; He, X.; Zigler, B. T.; Wooldridge, M. S. *Proc. Combust. Inst.* **2007**, *31* (2), 3147–3154.

(124) Schulz, H. *Appl. Catal. A Gen.* **1999**, *186* (1–2), 3–12.

(125) Guo, D.; Zhu, L.; Guo, S.; Cui, B.; Luo, S.; Laghari, M.; Chen, Z.; Ma, C.; Zhou, Y.; Chen, J.; Xiao, B.; Hu, M.; Luo, S. *Fuel Process. Technol.* **2016**, *148*, 276–281.

(126) Bianchi, M.; Frediani, P.; Matteoli, U.; Menchi, G.; Piacenti, F.; Petrucci, G. *J. Organomet. Chem.* **1983**, *259* (2), 207–214.

(127) Meijer, R. H.; Ligthart, G. B. W. L.; Meuldijk, J.; Vekemans, J. A. J. M.; Hulshof, L. A.; Mills, A. M.; Kooijman, H.; Spek, A. L. *Tetrahedron* **2004**, *60* (5), 1065–1072.

(128) Jafarpour, L.; Huang, J.; Stevens, E. D.; Nolan, S. P. *Organometallics* **1999**, *18* (18), 3760–3763.

(129) Kücükbay, H.; Cetinkaya, B.; Guesmi, S.; Dixneuf, P. H. *Organometallics* **1996**, *15* (10), 2434–2439.

(130) Herrmann, W. A.; Köcher, C.; Gooßen, L. J.; Artus, G. R. J. *Chem. Eur. J.* **1996**, *2* (12), 1627–1636.

(131) Albers, M. O.; Ashworth, T. V.; Oosthuizen, H. E.; Singleton, E.; Merola, J. S.; Kacmarcik, R. T. John Wiley & Sons, Inc.; pp 68–77.

(132) Netherton, M. R.; Fu, G. C. *Org. Lett.* **2001**, *3* (26), 4295–4298.

(133) Albers, M. O.; Coville, N. J. *Coord. Chem. Rev.* **1984**, *53*, 227–259.

(134) Tolman, C. A. *Chem. Rev.* **1977**, *77* (3), 313–348.

(135) Tisserand, R.; Rodney, Y. *Essential Oil Safety*, Second Edi.; Elsevier, 2013.

(136) Martin-Luengo, M. A.; Yates, M.; Rojo, E. S.; Huerta Arribas, D.; Aguilar, D.; Ruiz Hitzky, E. *Appl. Catal. A Gen.* **2010**, *387* (1–2), 141–146.

(137) Granato, A. V.; Santos, A. G.; dos Santos, E. N. *ChemSusChem* **2017**, *10* (8), 1832–1837.

(138) Burk, M. J.; Crabtree, R. H. *Inorg. Chem.* **1986**, *25* (7), 931–932.

(139) Yi, C. S.; Yun, S. Y. *J. Am. Chem. Soc.* **2005**, *127* (48), 17000–17006.

(140) Lail, M.; Bell, C. M.; Conner, D.; Cundari, T. R.; Gunnoe, T. B.; Petersen, J. L. *Organometallics* **2004**, *23* (21), 5007–5020.

(141) Shah, S. T. A.; Khan, K. M.; Hussain, H.; Anwar, M. U.; Fecker, M.; Voelter, W. *Tetrahedron* **2005**, *61* (27), 6652–6656.

(142) Alvarez-Builla, J.; Vaquero, J. J.; Garcia Navio, J. L.; Cabello, J. F.; Sunkel, C.; Fau de Casa-Juana, M.; Dorrego, F.; Santos, L. *Tetrahedron* **1990**, *46* (3), 967–978.